Wilfrid Laurier University

# Scholars Commons @ Laurier

Theses and Dissertations (Comprehensive)

2018

# NEAR-SURFACE PERMAFROST GROUND ICE CHARACTERISTICS AND ECOLOGICAL AND PHYSICAL DRIVERS OF TRANSIENT LAYER ICE CONTENT IN DISCONTINUOUS PERMAFROST

Jason Paul
*Wilfrid Laurier University*, paul0250@mylaurier.ca

# NEAR-SURFACE PERMAFROST GROUND ICE CHARACTERISTICS AND ECOLOGICAL AND PHYSICAL DRIVERS OF TRANSIENT LAYER ICE CONTENT IN DISCONTINUOUS PERMAFROST

by

Jason Paul

(B.Sc. Environmental Sciences, University of British Columbia, 2014)

THESIS
Submitted to the Department of Biology
Faculty of Science
in partial fulfilment of the requirements for the
Master of Science in Integrative Biology
Wilfrid Laurier University

Waterloo, Ontario, Canada, 2018

# Abstract

Accelerated climate warming in northern regions is causing permafrost degradation, leading to the reduction of the areal extent of permafrost. Permafrost is the foundation for many northern ecosystems and communities, so its thaw can have important ecological and societal consequences. Thaw of ice-rich permafrost can cause subsidence of the ground surface proportional to excess ice content. Terrain settlement can cause ponding or damage to infrastructure. Following a surface disturbance that removes much of the vegetation cover, a shift in the ground thermal regime can cause an increase in active layer thickness and rapid thaw of the top portion of permafrost. This upper layer of permafrost is known as the transient layer because it thaws and re-aggrades on multi-decadal to centennial timescales in association with ecosystem disturbance or climate change. Understanding the processes that lead to ice-enrichment of the transient layer can help us better predict ice-rich areas, and identify ecosystems that are at risk of state changes resulting from permafrost thaw.

This research examined the variation of ground ice content of near-surface permafrost, and the factors that influence it in well-drained forests of the discontinuous permafrost zone. The specific objectives of this thesis was to 1) characterize near-surface ground ice content and examine relations between ground-ice, forest type, soil conditions, and permafrost history, and 2) quantify the role of forest characteristics and soil properties as drivers of transient layer ice content, and determine if active layer or ice content are related to ground vegetation communities in this landscape type. Data collection to support these research objectives involved collection of 567 permafrost core samples and completion of soil and vegetation surveys from 10 black spruce and 10 white spruce/birch forests on mineral soils in the North Slave region near Yellowknife, NWT during the summers of 2014 and 2015.

In Chapter 2 I found evidence of a permafrost transient layer in black spruce forests; this was characterized through ground ice profiles that exhibited decreasing ice content with depth into the permafrost as well as horizontal, lenticular cryostructures. In these forests, higher ice content in association with thinner active layers likely relates to transient layer ice enrichment, which occurs as permafrost aggradation slows with forest development. The transient layer was absent from several white spruce/birch sites with thick active layers – it is likely that thaw has truncated formational segregated ice at depth. It is unlikely that permafrost will aggrade upwards in these sites unless change in vegetation cover can modify the soil conditions and microclimate.

In Chapter 3 I demonstrated that soil properties were substantially more important drivers of transient layer ice content than forest characteristics in this landscape type. In addition, no relationship between active layer thickness or transient layer ice content with ground vegetation community composition was found. Our results show that the important drivers of transient layer ice content in the general landscape view (from wetlands to dry, sandy soils) are not necessarily congruent with the important drivers within one landscape type. In this area, prediction of ice content using land cover or surficial site surveys may not be possible without the use of high resolution soils maps; however, stand age may provide a useful approximation of transient layer ice content. This work aids our understanding of how ecosystems in this region may respond to imminent permafrost thaw.

# Acknowledgements

I would like to thank my supervisors Dr. Jenn Baltzer and Dr. Steve Kokelj for their continued support and guidance throughout my program. Both this thesis and I, personally, have greatly benefitted from their critical feedback. I would also like to thank my committee members, Dr. Mike English and Dr. Kevin Stevens for their advice on research design and analysis during the course of my degree. Thank you to Dr. Steve Wolfe and Dr. Peter Morse of the Geological Survey of Canada for their invaluable knowledge and assistance with permafrost data collection. Thank you to everyone at the Northwest Territories Geological Survey for their hospitality and use of their facilities for field staging and sample analysis. Field data collection and sample preparation would not have been possible without the diligent efforts of my field assistants Pierre Berube and Melissa Dergousoff. Thank you to Dr. Nicola Day for the highly informative statistical analysis consultations. Thank you to all of the undergraduate biology students at WLU who volunteered their time while pursuing their own studies to help with tree ring counting.

Many thanks to all of the members of the Baltzer Lab who have always been willing to discuss ideas and work through problems together. Their unwavering support helped to motivate me throughout my studies. I would like to thank my family, friends, and Candice for their patience and encouragement over the past years as I pursued my academic goals. I am deeply grateful to all of you, without whom this thesis would not have been possible.

# Table of Contents

# List of Figures

# List of Tables

# Chapter 1: General introduction

## 1.1 Climate warming in northern Canada

Global air temperatures have been increasing throughout the twentieth century, with pronounced warming occurring in northern high latitude regions (IPCC, 2013). In recent decades, the rate of warming in these regions has been substantially greater than the global mean (ACIA, 2005; IPCC, 2013), with particularly rapid warming occurring in northwestern North America (Serreze *et al*., 2000; Johannessen *et al*., 2004; Riseborough *et al*., 2013; Morse *et al*., 2015). Boreal forest response to rapid warming is uncertain, but increased fire frequency and severity (Soja *et al*., 2007; Flannigan *et al*., 2009), insects and diseases (Dukes *et al*., 2009; Sturrock *et al*., 2011), and extreme weather events (Allen *et al*., 2010) are already affecting these forests (Davis *et al*., 2005; Carcaillet *et al*., 2010; Euskirchen *et al*., 2010). In addition, rising ground temperatures will result in permafrost thaw (altering the stability of the landscape), and change hydrological and soil conditions; together, this can cause major ecosystem changes (Osterkamp *et al*., 2000; Jorgenson *et al*., 2001; Quinton *et al*., 2011).

### 1.1.1 Indications of permafrost thaw

Permafrost is defined as any ground which remains at or below 0°C for two or more years (Mackay, 1972). It is a geological manifestation of climate and underlies about 25% of the land area in the northern hemisphere (Brown, 1997; Zhang *et al*., 2003). Permafrost is divided into continuous (> 90% of the area underlain by permafrost), extensive discontinuous (50 to 90%), sporadic discontinuous (10 to 50%), and isolated zones (< 10%) (Heginbottom *et al*., 1995; Zhang *et al*., 1999). Thin patches of permafrost exist in southern permafrost zones largely because the climate is sufficiently cold to offset the effects of the geothermal heat flux (Mackay and Mathews,

1964), and because seasonal differences in the thermal conductivity of surface organic materials insulate the ground from warming in summer, and promote ground heat loss in winter (Shur and Jorgenson, 2007). Under warming climate conditions, ground surface temperatures increase, and permafrost in the discontinuous zone may be at risk of disappearing completely. This can lead to a northward shift of continuous and discontinuous permafrost zone boundaries (Anisimov and Nelson, 1997; Burn, 1998a; Stendel and Christensen, 2002). It has been estimated that if global mean air temperatures rise by 2 °C above pre-industrial temperatures, at a new equilibrium, permafrost would be reduced by 40% of its current global areal extent (Chadburn *et al*., 2017).

Numerous observations of modern ground warming have been made in northern hemisphere permafrost regions (Osterkamp and Romanovsky, 1999; Harris *et al*., 2003; Osterkamp, 2005; Smith *et al*., 2005; Romanovsky *et al*., 2007, 2010; Smith *et al*., 2010). Minimum ground temperatures at treeline for the top 10 m of permafrost have been observed to have increased by 2 °C since the 1970s (Kokelj *et al*., 2017). Much of the permafrost in the extensive discontinuous zone is warm (> -3 °C); therefore, small changes that alter the surface energy flux, such as rising air temperatures, increasing snow depth, or soil moisture can result in permafrost thaw (Romanovsky *et al*., 2010). When disturbances result in permafrost thaw causing a thicker, saturated active layer, freezeback duration is increased (and thus time for conductive ground cooling during winter is reduced), leading to warmer ground temperatures or thaw (Kokelj *et al*., 2017). However, the high latent heat content of ice-rich permafrost can delay the ground thermal response to surface warming by several decades (Smith and Riseborough, 1993; Smith *et al*., 2008, 2010; Romanovsky *et al*., 2010). Although climate-driven permafrost thaw is generally a very slow process, observations have already been made of permafrost loss and a northward shift of the discontinuous permafrost boundary as a result of high latitude climate warming (Burn, 1998a). Kwong and Gan (1994) found

a northward shift of 120 km in the sporadic discontinuous zone over a 26-year time period (1962 –
1988) near the Mackenzie Highway, south of Great Slave Lake, which was significantly correlated
with climate warming in the area. French and Egorov (1998) observed permafrost degradation and
disappearance at locations in Northern Manitoba in the sporadic discontinuous zone from 1968 –
1976. James *et al.* (2013) observed a loss of permafrost from nearly half of their study sites in
northern British Columbia and southern Yukon between 1964 and 2008, noting a 2°C air
temperature increase in the region and describing the remaining permafrost as patchy, warm, and
ecosystem-protected.

## 1.2 Permafrost thaw consequences

Permafrost provides a critical physical structure for many ecosystems in the north (Zoltai
and Pettapiece, 1973), and as such thaw can have substantial impacts (Turetsky *et al*., 2002;
Yoshikawa and Hinzman, 2003; Epstein *et al*., 2004; Lewkowicz, 2007). For example, surface and
subsurface hydrological regimes may be altered as permafrost thaws (Xue *et al*., 2009; Quinton *et
al*., 2011) with implications for the structure and function of the overlying ecosystem (Baltzer *et al*.,
2014; Helbig *et al*., 2016; Sniderhan *et al*., in review). The potential for land cover change is
determined by the ice content of the permafrost and the rate of thaw (Burn, 1998a; Osterkamp et al.,
2000; Jorgenson et al., 2001). Thawing of ice-rich permafrost often leads to ground surface
subsidence (Washburn, 1979); these depressions can become filled with melt water leading to
ponding. This can result in extreme ecosystem change with forests converting to wetlands
(Osterkamp *et al*., 2009). Alternatively, since permafrost can act to retard groundwater movement
(Mackay, 1983), the thawing of permafrost may increase drainage and convert existing aquatic and
wetland ecosystems into terrestrial ecosystems (Burn, 1998a; Osterkamp *et al*., 2000; Jorgenson *et
al*., 2001; Cheng and Wu, 2007; Osterkamp *et al*., 2009). Thawing permafrost can also alter

adjacent ecosystems. Permafrost loss can cause slumping of soil into adjacent water systems, reducing water quality (Kokelj and Jorgenson, 2013). Similarly, large inputs of dissolved organic carbon from permafrost thaw (Frey and McClelland, 2009) have been shown to reduce productivity of benthic organisms that fuel the food web (Mariash *et al*., 2018). Subsidence also can damage or destroy infrastructure vital to northern communities for transportation, communication, service buildings, and dwellings (White *et al*., 2007; Romanovsky *et al*., 2010). For example, thaw of ice-rich permafrost beneath roads can lead to subsidence and damage to the infrastructure (Hoeve *et al*., 2004; Seto *et al*., 2012). Large landscape changes caused by ice-rich permafrost thaw can also affect access to traditional food sources and harvester safety (White *et al*., 2007).

Soil carbon that has accumulated due to low decomposition rates or that has been frozen in permafrost (Hobbie *et al*., 2000) is at risk of entering the atmosphere as soil temperatures rise (Grulke *et al*., 1990; Ciais *et al*., 1995; Schuur *et al*., 2015). It is estimated that tundra and boreal forest ecosystems currently store approximately one third of the global reactive soil carbon pools (McGuire *et al*., 1995). An increase in active layer thickness could also result in increased decomposition rates by lowering the water table and warming soils – this allows for increased aerobic respiration of carbon dioxide by soil microbes (Oechel and Vourlitis, 1994). It has been estimated that due to climate warming and thawing permafrost, high latitudes will become a net source of carbon dioxide and methane, rather than a carbon sink (Koven *et al*., 2011). Understanding and predicting rates and patterns of permafrost thaw is therefore critical given the potential for this region to act as a positive feedback to global warming (Post *et al*., 1982; Oechel *et al*., 1993; Schuur *et al*., 2015).

## 1.3 Study area landscape

The North Slave study region near Yellowknife, Northwest Territories (NWT) is at the northern extent of the Boreal Ecoclimatic Province. Mean annual air temperature is -4.3°C (1981-2010 climate normal), but the trend indicates an increasing rate of warming (0.85°C per decade between 2002-2017) (Hoeve *et al*., 2004; Wolfe *et al*., 2014; Environment Canada, 2018). It is a dry climate with a mean annual precipitation less than 300 mm (nearly half of which falls as snow) and the high precipitation months occur in the summer (Environment Canada, 2018). The terrain is underlain by the Precambrian Canadian Shield and was scoured by the Laurentide Ice Sheet during the last ice age. Surficial deposits consist of glaciofluvial sands and lacustrine silts and clays deposited by proglacial Lake McConnell. Lithalsas (small hills formed by segregated ice lenses that raise the ground surface) are typically dominated by white birch and white spruce (Wolfe *et al*., 2011, 2014; Morse *et al*., 2015). Plant species are slow-growing with adaptations for low resource conditions. Forests are mainly composed of black spruce (*Picea mariana* (Miller) Britton, Sterns & Poggenburgh) on fine-grained mineral soils and peatlands, and jack pine (*Pinus banksiana* Lambert) on bedrock outcrops and sandy soils, but other species, such as white spruce (*Picea glauca* (Moench) Voss), paper birch (*Betula papyrifera* Marshall and *B. neoalaskana* Sargent), and tamarack (*Larix laricina* (Du Roi) K. Koch) may also be present in abundance.

Lake McConnell was a proglacial lake that reached its maximum extent approximately 10,500 years ago (Smith, 1994) as the Laurentide Ice Sheet retreated northeastward (Dyke *et al*., 2003). The massive lake extended from Great Bear Lake to Great Slave Lake, down to Lake Athabasca and was bounded at the eastern edge by the ice sheet. The water level lowered due to isostatic rebound (slow uplifting of the earth's crust following the disappearance of glacial ice), which was accelerated between 9000 to 8000 years ago due to the incision of new river outlets. Lake McConnell, and earlier extents of Great Slave Lake, deposited glaciolacustrine fine-grained

sediments over the Yellowknife area, preferentially accumulating in lower lying areas of the undulating bedrock (Smith, 1994; Wolfe, 1998). Fine-grained sediments, such as those deposited over the Yellowknife area, are frost susceptible, meaning they provide the substrate for ice growth in the permafrost.

*1.3.1 State of permafrost in North Slave region*

The North Slave region is situated in the zone of discontinuous permafrost (Heginbottom *et al*., 1995).  The mean annual air temperature in the region has been sufficiently cold for establishment of permafrost. Permafrost is found in areas of fine-grained sediments overlain by forests and in areas of organic soil accumulation that form peatlands, but is generally absent from bedrock outcrops, in sandy soils, and under water bodies (Brown, 1973; Zhang *et al*., 2014). The permafrost is thin ($< 50$ m) (Brown 1973) and warm (mean annual ground temperature $> -2°$ C) (Hoeve *et al*., 2004; Morse *et al*., 2015). Active layer thickness can range between less than 0.5 m in peatlands to over 2 m in white birch-dominated forests (Aspler, 1978; Wolfe *et al*., 2011, 2014; Morse *et al*., 2015). Ground ice conditions in fine-grained mineral soils in the area can range from no excess ice (ice that has aggraded beyond saturation of the soil) to high ice content depending on frost susceptibility of the sediments, moisture conditions, and disturbance history (Aspler, 1978; Heginbottom *et al*., 1995; Wolfe *et al*., 2011, 2014; Morse *et al*., 2015).

## 1.4 Controls on permafrost conditions

*1.4.1 Physical factors*

Whether permafrost is present at any particular location depends on a combination of the climate, soil properties, and surface characteristics (Brown, 1965). Factors that result in lower ground surface temperatures can increase the permafrost thickness. Climate ultimately holds the

largest control on permafrost presence and thickness because permafrost generally cannot form in

areas where the mean annual air temperature is above freezing; colder air temperatures and a longer

freezing season promote ground heat loss in the winter months (Kudriavtsev, 1954). Summer rain

increases soil moisture. The moisture that is not lost through evapotranspiration can enhance soil

thermal conductivity thereby increasing the rate of thaw (Hinkel *et al*., 2001), but also can be used

to aggrade ice in the near-surface permafrost at the end of summer when the active layer is fully

thawed (Mackay, 1972). Rain events in the fall experience lower rates of evapotranspiration and

thus are more likely to saturate the soil during freeze-back. If the soil is saturated, it will take longer

to freeze due to latent heat effects (Kokelj *et al*., 2014). In the subarctic, this leads to ground

warming and permafrost thaw. In colder tundra environments, a saturated active layer that has

refrozen has a relatively high thermal conductivity which results in greater winter ground heat flux,

thus lowering ground temperatures (Benninghoff, 1952; Gavriliev, 2004). Winter precipitation

(snow) acts to insulate the ground from the cold air temperatures, lowering the rate of heat loss

from the ground surface (Smith, 1975). Wind patterns, along with vegetation and topography, affect

the distribution of snow on the ground. Forest cover in the subarctic inhibits snow redistribution. In

spring, snow can delay the thawing of the active layer, resulting in lower ground temperatures, and

as snow melts, the water not lost to runoff provides a small input of water to the ground (Mackay

and MacKay, 1974; Zhang *et al*., 1997; Lantz *et al*., 2009).

Soil properties affect the thermal and hydraulic conductivity of the ground (Rieke *et al*.,

1983). Fine-grained sediments (e.g., silt and clay) have higher thermal conductivities than coarse

grained sediments (e.g., gravel and sand; around 1 $W \cdot m^{-1} \cdot K^{-1}$ for dry clays, and 0.2 $W \cdot m^{-1} \cdot K^{-1}$ for

dry sands), and fine-grained sediments have a higher porosity (around 0.5 for clays, and 0.3 for

sands) and lower hydraulic conductivity (around $10^{-7}$ cm/s for clays, and $10^{-2}$ cm/s for sand); thus

fine-grained sediments have a greater potential for water retention (Terzaghi *et al*., 1996; Das, 2008). High porosity sediments have small pore sizes that allow for a portion of the water content to remain unfrozen even under $< 0°C$ temperatures due to pore pressures (Williams and Smith, 1991). As a result, thermal gradients induce a pressure potential in freezing soils enabling unfrozen water to be drawn towards colder soil, supporting development of segregated ice lenses (Williams and Smith, 1991). The unfrozen water content and permeability of frozen fine-grained soils results in these materials to be termed "frost susceptible" (see section 1.4.3).

Topography influences soil moisture conditions and the intensity of solar irradiance, with depressions receiving lower irradiance (cooler ground thermal regime), higher soil moisture, and a thicker snow pack (Lee, 1978; Van Cleve and Viereck, 1981; Woo and Winter, 1993). Localized variation in surface relief, termed "microtopography," caused by frost heave can produce patterned ground, including earth hummocks. In hummocky terrain, the permafrost table is a reflection of the ground surface where the active layer is thickest under the hummock tops, and thinnest under the hummock troughs (Kokelj and Burn, 2003; Kokelj *et al*., 2007). Hummock troughs have higher soil moisture than hummock tops, favouring growth of vegetation and accumulation of organic material (Zoltai and Pettapiece, 1973; Zoltai and Tarnocai, 1974). In summer, ground temperatures under hummock tops are warmer than in the troughs since the thermally conductive fine-grained soils are exposed to warm summer air temperatures and direct solar radiation, in contrast with shaded, organic filled troughs which remain cooler (Tarnocai and Zoltai, 1978).

The active layer thickness above the permafrost table affects both freeze-back duration and the availability of water to the permafrost. Ground with a thick active layer can take a longer time to refreeze in winter. Under very thick active layers a portion of the ground may stay unfrozen above the permafrost table if there is not a sufficient loss of heat from the ground, creating a supra-

permafrost talik (area of year-round unfrozen ground) (Viereck *et al*., 2008). The permafrost table

beneath a thick mineral soil active layer is less likely to be saturated as surface water is often lost

through runoff and evapotranspiration before reaching the permafrost table (Burn, 1998a; Cheng

and Wu, 2007; Morse *et al*., 2015). In contrast, surface water is more likely to infiltrate to the

permafrost table in areas with a shallow, organic-rich active layer (Kokelj and Burn, 2005).

*1.4.2 Biological factors*

The presence of vegetation modifies the physical conditions of the ground compared to a

barren landscape. Under similar climate and substrate conditions, differences in forest structure can

have a large impact on permafrost development over time (Smith, 1975). The canopy, understorey,

and surface vegetation each have controls on the thermodynamic and hydraulic state of the ground.

Surface temperatures have been found to be negatively correlated with vegetation development in a

particular climate zone; barren ground sites are warmest, and treed sites are coldest (Smith, 1975;

Osterkamp *et al*., 2000).

Interception of solar radiation by shrubs and trees decreases the total energy reaching the

ground surface. Treed sites receive less solar radiation at the ground surface than sites with only

shrub cover, leading to cooler ground surface temperatures (Gill, 1971; Smith, 1975). Longwave

radiation energy losses at night are lower when vegetation is present, relative to barren ground.

Additional energy is lost from the phase change (latent heat) associated with the higher rates of

evapotranspiration in treed sites. Other than evaporation of precipitation intercepted by the canopy,

the dominant evaporative loss of water from vegetated surfaces is through transpiration. Stomatal

regulation and the associated rate of water loss by transpiration is influenced by temperature,

relative humidity, soil water, air movement through the canopy, and light levels (Oke, 1997).

Vegetation also acts to capture snow and increase the snow pack during the winter months, leading

to more insulation and higher ground temperatures than barren ground (Nicholson and Granberg, 1973; Smith, 1975). Lower ground temperatures in later successional stages of post-fire boreal forests occur in part due to decreased snow cover on the ground due to spruce tree interception, greater moss growth due to less litter from deciduous species, and the accumulation of the organic layer (Jorgenson *et al*., 1999).

Surface vegetation and organic material such as peat have much lower thermal conductivities than exposed mineral soil, and therefore insulate the ground (Brown, 1965). Experimentally removing 10 cm of surface organic layer to expose predominantly mineral soil resulted in a 3°C increase in mean ground temperature with a five-fold greater range of diurnal temperature, indicating a large increase in ground heat flux (Smith, 1975). The thickness of the organic layer is linked to soil moisture in northern forests because evapotranspirative fluxes are low (Liu *et al*., 2005), permafrost prevents subsurface water flow (Jorgenson et al. 2010), and mosses promote water retention and infiltration (Hinzman *et al*., 1991; Beringer *et al*., 2001; Turetsky *et al*., 2010). If the organic layer is saturated, the thermal conductivity will rise to approximately that of ice during the winter due to the high porosity of organic material, leading to a greater winter upward heat flux (Benninghoff, 1952). Therefore, an organic-rich ground surface has the net effect of having high water content and lower ground temperatures.

Vegetation can reduce active layer thickness by modifying the ground thermal regime. The reduced active layer thickness will also have an effect on vegetation by decreasing the depth to which water is able to drain, essentially raising the water table (Kane, 1997). This will favour a community shift towards vegetation that either require, or can tolerate, higher soil moisture conditions, and is thought to be a main driver of succession in northern environments underlain by permafrost (Walker and Walker, 1996). For example, in parts of the Mackenzie Delta near Inuvik,

NWT, silty soils with an active layer between 90 and 120 cm thick are associated with *Picea/Alnus-Arctastaphylos* forests, succeeded by *Picea/Hylocomium* communities as the active layer thins to 50 – 70 cm and becomes more ice-rich with segregated ice lenses (Gill, 1973, 1975; Smith, 1975; Pearce *et al*., 1988; Kokelj and Burn, 2003). Clayey silt soils in this region with an active layer between 40 and 70 cm thick have ice-rich, near-surface permafrost and support *Picea/Empetrum-Cladina* woodlands characterized by a thick, near-surface organic cover (Pearce *et al*., 1988; Kokelj and Burn, 2003).

*1.4.3 Permafrost cryostructures and water movement*

The movement of water into the top of permafrost along a thermally-induced pressure gradient allows for ice-enrichment of near-surface permafrost (Cheng, 1983; Mackay, 1983). Moisture migration and formation of segregated ice lenses causes ice volume to exceed the void spaces within the soil matrix, leading to the development of excess ice (Konrad and Morgenstern, 1980). In freezing soils, a portion of the water remains unfrozen depending on the grain size of the sediment. The relationship between unfrozen water content and temperature is described by an unfrozen water content characteristic curve, specific to soil type (Williams and Smith, 1991). Coarse sediments (i.e., coarse sands or coarser) have pore sizes that are too large to promote the necessary capillary flow that maintains unfrozen water content in soils near 0 °C. Fine-grained sediments with a high specific surface area are associated with higher unfrozen water content at temperatures below 0°C. Silts have sufficient permeability to promote water flow yet have small enough pores to promote capillary flow, and are therefore frost susceptible (Williams and Smith, 1991). As water freezes in a soil pore, the unfrozen films of water adjacent to the soil particles are maintained at lower pore water pressure. The unfrozen water attracted to the surface of particles by adsorption and capillarity has a low free energy so as to remain in thermodynamic equilibrium with

the ice in the centre of the pore. Freezing water occurring at the top of permafrost, with unfrozen soils in the above active layer, results in a pressure that draws unfrozen water from warmer soil towards the lower pressure at the freezing front (Williams and Smith, 1991). The more finely-grained the sediment, the more unfrozen water migration can occur from the warmer active layer to the colder permafrost table (Burt and Williams, 1976).

The type and thickness of permafrost ice structures depends on sediment grain size, water availability, direction of freezing, and rate of permafrost aggradation. Nine main ice types, or "cryostructures," were identified by Shur and Jorgenson (1998): pore (or structureless), organic-matrix, crustal, vein, lenticular, layered (or bedded), reticulate, ataxitic (or suspended), and solid (Shur and Jorgenson 1998, Table 1). Pore ice permafrost often exists in coarser-grained sediments such as sands, where water in large pore spaces can freeze completely at temperatures near 0°C due to low capillarity. Detrital organic material such as peat will form an organic-matrix cryostructure when frozen at saturation, which becomes nearly the mass and thermal conductivity of ice due to the very high porosity of organic material. Crustal ice may form small excess ice lenses (< 1 mm to > 10 mm in thickness) along the boundary of pebbles or roots in fine-grained mineral permafrost (Mackay, 1984). Vein ice may form as irregularly-oriented excess ice in soil macropores or contraction cracks in the permafrost, as the soil may become compacted as water is drawn out by a thermal gradient (Mackay, 1972). Lenticular ice lenses develop orthogonal to the direction of water migration from the active layer to the permafrost, or during downward aggradation of permafrost into saturated sediments. If there is sufficient water supply, thermal gradient, and the permafrost table is not rising quickly, lenticular ice lenses near the surface may grow large (Smith and Williams, 1990). Layered segregated ice forms as a result of infilling of thermal cracks with ice, and may be accompanied by layers of interchanging sediment grain sizes (Washburn, 1979). Both

lenticular and layered ice lenses can be from < 1 mm to > 100 mm thick. Reticulate cryostructures form a regular or irregular lattice of ice lenses, typically smaller in thickness than layered or lenticular ice lenses. This structure is caused by the infilling of the soil patterns created by the hydraulic contraction of clay-rich sediments (Mackay, 1974). Ataxitic cryostructures contain soil suspended in ice due to ice aggradation in the top of permafrost (Mackay, 1972).

## 1.5 Conceptual model of ground ice aggradation

Several factors can contribute to upward aggradation of the permafrost table, including climate change, sedimentation, and ecological change. Upward aggradation of the permafrost table traps ice lenses that develop at the top of permafrost or at the base of the active layer during refreezing of the active layer (Mackay, 1995). Segregated ice lenses in the bottom of the active layer that do not thaw for two or more summers become incorporated in the top of the permafrost. These ice lenses in the near-surface of the permafrost can further grow by drawing in moisture from the active layer during late summer, which is driven by the thermal gradient from warm active layer to cold permafrost (Cheng and Cheng, 1982; Mackay, 1983; Burn, 1988). As the permafrost table rises, ice becomes incorporated into the aggrading permafrost. The growth of subsurface ice lenses is accompanied by surface heave (Mackay, 1972), uplift of the terrain surface (Kokelj and Burn, 2005), and an increase in hummocky microrelief (Kokelj *et al*., 2007). In forested environments, ecological change following disturbance or fire can cause the active layer to gradually thin. As such, the thermal gradient causing the permafrost table to aggrade decreases, allowing more time for moisture to be drawn into ice lenses at the top of permafrost, leading to large ice lenses in the near-surface permafrost of well-developed forests (Zoltai and Pettapiece, 1973). Eventually, the forest reaches a mature stage with a negligible rate of vegetation change and the thermal controls on

the ground surface stabilize. However, ice lenses may continue to grow as moisture is drawn to the permafrost by a thermal gradient in the summer months (Jorgenson and Osterkamp, 2005).

The process causing permafrost to thaw and re-aggrade, via vegetation controls on ground temperature, is related to surface disturbances. An important surface disturbance in the boreal forest is wildfire (Kasischke and Turetsky, 2006; Nossov *et al*., 2013). Although active fires can reach very high temperatures, the direct impact of heat from the fire on the ground thermal regime is minimal (Viereck and Schandelmeier, 1980; Viereck, 1982). However, fires increase ground temperatures and thaw depth by removing vegetative cover, reducing surface organic layer thickness, changing the albedo of the ground surface, and increasing water storage in the active layer (Burn, 1998b; Yoshikawa and Hinzman, 2003; Nossov *et al*., 2013; Brown *et al*., 2015). The more frequent and/or severe the burn (i.e., higher amounts of organic biomass consumed), the more susceptible the ground becomes to higher heat fluxes (Brown *et al*., 2015). This reduction in canopy radiation shielding, energy losses from evapotranspiration, and lower albedo cause the thaw depth to increase following fire (Rouse, 1976; Tarnocai and Zoltai, 1978; Viereck, 1982; Wein and Bliss, 2009). As the active layer deepens, any ice lenses in the thawing permafrost are eradicated (Kokelj and Burn, 2003). The permafrost table usually begins to stabilize within the first few decades after the fire (Mackay, 1995; Yoshikawa and Hinzman, 2003; Racine *et al*., 2004; Smith *et al*., 2015), but can take longer where severe fire has destroyed substantial vegetation and organic layer (Burn, 1998b; Douglas *et al*., 2008; Viereck *et al*., 2008).

The ground surface will subside proportional to the amount of excess ice in the thawing permafrost (Liu *et al*., 2014). For example, if the permafrost consists of 50% excess ice by volume and one metre of thaw occurs, the ground surface will lower by half a metre (Mackay, 1995). Depending on topography, the resultant water may saturate the active layer, or may leave the site

through groundwater flow (Bird *et al*., 1977; Bense *et al*., 2009). The rate of permafrost thaw slows as the active layer deepens, which provides more time for the ecosystem to recover and cool the ground, preventing further thaw and eventually allowing the permafrost to aggrade upward toward its pre-disturbed depth (Burn, 1998a). This uppermost portion of the permafrost that aggrades and degrades on sub-decadal to multi-centennial timescales, usually as a result of climatic variations or disturbance, is referred to as the transient layer (Shur *et al*., 2005).

## 1.6 Forest ecology

### 1.6.1 Black spruce forests

Black spruce (*P. mariana*) forests compose over 37% of the Boreal Ecoclimatic Province near Yellowknife (Wolfe *et al*., 2011; Olthof *et al*., 2013). Black spruce can grow on well-drained gravels to poorly-drained, fine-grained sediments (Viereck *et al*., 1992), with the majority of stands in this area occurring on the latter (Wolfe *et al*., 2011). Hummocky terrain is common in these stands, and active layers can range in thickness from 30 cm to over 100 cm (Viereck *et al*., 1992; Wolfe *et al*., 2011; Morse *et al*., 2015). Permafrost thickness can exceed 50 m in old growth black spruce forests (Morse *et al*., 2015). Black spruce produces semi-serotinous cones that open through the application of high temperatures that removes their resinous coating; this adaptation allows black spruce to regenerate immediately following a fire (Van Wagner, 1983). However, fast-growing deciduous species (e.g., *Betula* sp.) may also be present in the early stages of black spruce forests (Wang *et al*., 2003; Bond-Lamberty *et al*., 2004). Common tall understory shrubs include *Betula* spp., *Salix* spp., and *Rhododendron groenlandicum*, and common low shrubs include *Vaccinium uliginosum* and *V. vitis-idaea*. The moss layer may be continuous or patchy in well-drained sites, up to 40 cm thick (Morse *et al*., 2015), and dominated by feather moss, but much

thicker accumulations of *Sphagnum* spp. can occur in wetlands. Lichens, including *Cladina* spp. and *Peltigera* spp. are common on drier surfaces such as on the tops and sides of hummocks (Appendix Table A.1). Older stands tend to have a thicker moss layer, fewer shrubs, and a well-developed canopy (Bradley *et al*., 1982).

Earth hummocks are common features in mature black spruce stands. They are formed by freeze-thaw processes within the active layer (Mackay, 1980; Peterson and Krantz, 1998; Peterson *et al*., 2003) and due to the accumulation or degradation of near-surface permafrost ground ice (Mackay, 1995; Kokelj et al., 2007). Vegetation responds to this patterned ground by preferentially growing in and around the wetter depressions of the hummock troughs (Tarnocai and Zoltai, 1978; Kokelj *et al*., 2007). Additionally, black spruce trees growing on the sides of earth hummocks become tilted as microtopography increases. This can be observed in the cross-section at the bases of these trees in the form of reaction wood: greater growth on the downslope side of the tree allows the tree to correct its leaning orientation (Scurfield, 1973; Kokelj and Burn, 2004; Kokelj *et al*., 2007). The growth and thaw of ice-rich permafrost can break roots, split tree trunks, and destabilize trees growing on the sides of hummocks, which grow the majority of their root mass away from the troughs (Mackay, 1974, 2000; Zoltai, 1975).

*1.6.2 White spruce/birch forests*

White birch (*Betula papyrifera* and *B*. *neoalaskana*) and mixed white spruce/birch (*Picea glauca*) stands in this region generally develop on lithalsas (raised mounds due to segregated ice growth in the permafrost up to 8 m high and hundreds of metres wide), leading to better drainage conducive to the growth of these trees. There is usually no hummocky terrain in these forests, and the active layers are generally thinner than 1 m, but can be up to 2 m (Wolfe *et al*., 2011; Morse *et al*., 2015). Mixed white spruce/birch stands typically develop in better drained soils than black

spruce forests, though still moderately moist. Following fire, they typically regenerate as either white birch or white birch and white spruce mixed stands, depending on seed availability or pre-fire stand composition. White birch is relatively fast growing, and when they die out the canopy is replaced by a larger proportion of the slower growing, long-lived white spruce. Mature canopies may be entirely composed of white spruce (Viereck *et al*., 1992). The understorey of a birch-dominated forest is generally less dense than that of black spruce forests, and is dominated by white spruce trees and a *Salix* sp. and *Viburnum edule* shrub layer, an herb layer of *Calamagrostis canadensis*, *Equisetum* spp., and *Rubus acaulis*, and few mosses or lichens due to the annual leaf litter input from the birch canopy (Bradley *et al*., 1982). As the canopy progresses towards a white spruce forest, leaf litter input usually slows, and *Alnus* spp., *Salix* spp., *Vaccinium* spp., *Rhododendron groenlandicum*, and *Empetrum nigrum* can become more common in the shrub layer, and a moss layer of *Hylocomium splendens* may develop (Viereck *et al*., 1992; Appendix Table A.2). Birch forests have a higher albedo and leaf area index than spruce forests (Morse *et al*., 2015), meaning they reflect more incoming radiation that leads to cooler ground temperatures. In addition, birch forests have higher evapotranspiration rates, producing a further microclimate cooling effect (Liu *et al*., 2005). Lower understorey cover in birch forests accumulate a thinner snow pack than black spruce or heterogeneous white spruce forests (Morse *et al*., 2015), thereby allowing for more ground heat loss during the winter (Goodrich, 1982; Jean and Payette, 2014).

## 1.7 Research rationale

Permafrost provides the foundation for many ecosystems and landscapes in the north (Zoltai and Pettapiece, 1973). Therefore, understanding the distribution of ground ice may have research applications in predicting patterns of ecosystem disturbance. Boreal forest state changes in vegetation are occurring as a consequence of factors relating to climate change (Davis *et al*., 2005;

Carcaillet *et al*., 2010; Euskirchen *et al*., 2010); therefore, understanding how plant communities relate to near-surface ice content and active layer thickness in this region will improve our ability to predict community shifts as permafrost degrades. Currently, factors affecting permafrost ice content have chiefly been examined in the context of a large gradient of climate and soil moisture/topographic regimes. Quantitatively assessing factors driving permafrost ice content within part of the landscape will help us better understand how characteristics of these systems affect ice content in the absence of large physical gradients. This could provide characteristics that can be mapped in order to assess ground ice content, which would aid in planning decisions for infrastructure development and forest management. This research is especially relevant for our study region, which is near the most populated area in the Northwest Territories – an area where the need for further research for road planning has been emphasized (Tighe *et al*., 2006; GNWT Department of Transportation, 2011).

## 1.8 Objectives and hypotheses

This thesis is an observational field study designed to examine the relationships between biophysical characteristics and ground ice content of near-surface permafrost in subarctic boreal forests of the North Slave region near Yellowknife, NWT. The specific objectives of this research are: Chapter 2 a) assess the role of forest type on transient layer presence and ground ice content; b) assess how permafrost core sample depth and ground conditions (i.e., microtopography and active layer thickness) relate to variability of ground ice content; and Chapter 3 a) quantitatively model which forest and soil characteristics are important for predicting transient layer ice content; and b) characterize the ground vegetation community in these forests and assess whether ice content or active layer thickness shapes community structure.

Based on this review of the literature, I combine geocryological principles with previously described interactions between vegetation, soil properties, and active layer development. I investigate if near-surface ground ice content in well-drained black spruce and white spruce/birch forests relates to forest characteristics. If so, this gives the potential for utilizing land cover or surficial site surveys to estimate near-surface permafrost characteristics (Jorgenson *et al*. 2001). I also expect that an exploration of near-surface ice profiles and cryostructures will provide insight into the site history and current processes acting on the permafrost (e.g., whether near-surface permafrost is aggrading into the transient layer, or if it has degraded into the deeper formational permafrost). Finally, I expect to be able to relate near-surface ice content and active layer thickness to vegetation communities.

## 1.9 Thesis overview

Chapter 1 has provided some background information pertaining to the research performed within this thesis, focusing on why this research is important in a rapidly changing climate, how permafrost and ice content aggrades, and how surface and ground properties influence permafrost. Chapter 2 is the first data chapter, which focuses on an exploration of the near-surface permafrost ice content within and between both black spruce and white spruce/birch forest types. Ice content was determined by retrieving core samples from multiple boreholes at each site, with ten sites per forest type along a developmental gradient (a stand age gradient for black spruce forests, and a compositional gradient for white spruce/birch forests) in the summers of 2014 and 2015. With this sampling technique, I was able to examine permafrost cryostructures and quantitatively determine ground ice content to address our predictions. There was support for transient layer presence in black spruce forests and most white spruce/birch forests, but in some white spruce/birch forests with thick active layers, deep thaw had eradicated the transient layer. Additionally, while

microtopography was not found to affect local variability in near-surface ice content, it was associated with the presence of a transient layer. Chapter 3 is the second data chapter of the thesis, focused on quantitatively and statistically assessing soil properties and forest characteristics as predictors of near-surface transient layer ice content, and assessing the response of the ground vegetation community to permafrost conditions. In addition to the permafrost samples collected and analyzed in chapter 2, plots were set up to measure forest characteristics at each site. Linear mixed effects models were employed to assess which factors significantly impact ice content of the near-surface permafrost for both forest types. Ground vegetation community was investigated for both forest types using a principal co-ordinates analysis. Physical soil properties were driving transient layer ice content, and active layer thickness and ice content did not influence ground vegetation in this well-drained mineral soil landscape type. Chapter 4 is the final chapter of the thesis and discusses how the findings fit into our current body of knowledge, the integrative nature of the research, and where the future direction of research in this field may take us.

# 1.10 References

ACIA. 2005. Arctic climate impact assessment. *Cambridge University Press*, Cambridge, UK.

Allen CD, Macalady AK, Chenchouni H, Bachelet D, McDowell N, Vennetier M, Kitzberger T, Rigling A et al. 2010. A global overview of drought and heat-induced tree mortality reveals emerging climate change risks for forests. *Forest Ecology and Management*, **259**(4): 660–684. https://doi.org/10.1016/j.foreco.2009.09.001

Anisimov OA, Nelson FE. 1997. Permafrost zonation and climate change in the northern hemisphere: Results from transient general circulation models. *Climatic Change*, **35**: 241–258. https://doi.org/10.1023/A:1005315409698

Aspler LB. 1978. Surficial geology, permafrost and related engineering problems, Yellowknife area, part of 85 J/8. NWT Geoscience office. *EGS Open File 1978*, **8**.

Baltzer JL, Veness T, Chasmer LE, Sniderhan AE, Quinton WL. 2014. Forests on thawing permafrost: Fragmentation, edge effects, and net forest loss. *Global Change Biology*, **20**(3): 824–834. https://doi.org/10.1111/gcb.12349

Benninghoff W. 1952. Interaction of vegetation and soil frost phenomena. *Arctic*, **5**(1): 34–44. Retrieved from http://www.jstor.org/stable/40506520

Bense VF, Ferguson G, Kooi H. 2009. Evolution of shallow groundwater flow systems in areas of degrading permafrost. *Geophysical Research Letters*, **36**(22). https://doi.org/10.1029/2009GL039225

Beringer J, Lynch AH, Chapin III FS, Mack M, Bonan GB. 2001. The representation of arctic soils in the land surface model: the importance of mosses. *Journal of Climate*, **14**: 3324–3335. https://doi.org/10.1175/1520-0442(2001)014<3324:TROASI>2.0.CO;2

Bird CD, Thomson JW, Marsh AH, Scotter GW, Wong PY. 1977. Bryophytes from the area drained by the Peel and Mackenzie rivers, Yukon and Northwest Territories, Canada. *Canadian Journal of Botany*, **55**: 2879–2918. https://doi.org/10.1139/b81-168

Bond-Lamberty B, Wang C, Gower ST. 2004. Net primary production and net ecosystem production of a boreal black spruce wildfire chronosequence. *Global Change Biology*, **10**(4): 473–487. https://doi.org/10.1111/j.1529-8817.2003.0742.x

Bradley SW, Rowe JS, Tarnocai C. 1982. An ecological land survey of the Lockhart River map area, Northwest Territories. *Lands Directorate, Environment Canada*, Ottawa, Ontario.

Brown DRN, Jorgenson MT, Douglas TA, Romanovsky VE, Kielland K, Hiemstra C, Euskirchen ES, Ruess RW. 2015. Interactive effects of wildfire and climate on permafrost degradation in Alaskan lowland forests. *Journal of Geophysical Research: Biogeosciences*, **120**: 1619–1637. https://doi.org/10.1002/2015JG003033

Brown J. 1997. Circum-Arctic map of permafrost and ground-ice conditions. United States Geological Survey.

Brown RJE. 1965. Some observations on the influence of climatic and terrain features on

permafrost at Norman Wells, N.W.T., Canada. *Canadian Journal of Earth Sciences*, **2**: 15–31. https://doi.org/10.1139/e65-003

Brown RJE. 1973. Influence of climatic and terrain factors on ground temperatures at three locations in the permafrost region of Canada. In *Proceedings of the Second International Conference on Permafrost* (pp. 27–34). Yakutsk, USSR: National Academy of Science, Washington, DC.

Burn CR. 1988. The development of near-surface ground ice during the Holocene at sites near Mayo, Yukon Territory, Canada. *Journal of Quaternary Science*, **3**(1): 31–38. https://doi.org/10.1002/jqs.3390030106

Burn CR. 1998a. Field investigations of permafrost and climatic change in northwest North America. In *Proceedings of the Seventh International Conference on Permafrost* (pp. 107–120).

Burn CR. 1998b. The response (1958-1997) of permafrost and near-surface ground temperatures to forest fire, Takhini River valley, southern Yukon Territory. *Canadian Journal of Earth Sciences*, **35**(2): 184–199. https://doi.org/10.1139/e97-105

Burt TP, Williams PJ. 1976. Hydraulic conductivity in frozen soils. *Earth Surface Processes*, **1**(4): 349–360. https://doi.org/10.1002/esp.3290010404

Carcaillet C, Richard PJH, Bergeron Y, Fréchette B, Ali AA. 2010. Resilience of the boreal forest in response to Holocene fire-frequency changes assessed by pollen diversity and population dynamics. *International Journal of Wildland Fire*, **19**(8): 1026–1039. https://doi.org/10.1071/WF09097

Chadburn SE, Burke EJ, Cox PM, Friedlingstein P, Hugelius G, Westermann S. 2017. An observation-based constraint on permafrost loss as a function of global warming. *Nature Climate Change*, **7**(5): 340–344. https://doi.org/10.1038/nclimate3262

Cheng G, Cheng K. 1982. The forming process of thick layered ground ice. *Science in China Series B-Chemistry, Biological, Agricultural, Medical & Earth Sciences*, **25**(7): 777–788. https://doi.org/10.1360/yb1982-25-7-777

Cheng G. 1983. The mechanism of repeated-segregation for the formation of thick layered ground ice. *Cold Regions Science and Technology*, **8**(1): 57–66. https://doi.org/10.1016/0165-232X(83)90017-4

Cheng G, Wu T. 2007. Responses of permafrost to climate change and their environmental significance, Qinghai-Tibet Plateau. *Journal of Geophysical Research*, **112**(April): 1–10. https://doi.org/10.1029/2006JF000631

Ciais P, Tans PP, Trolier M, White JWC, Francey RJ. 1995. A large northern hemisphere terrestrial $CO_2$ sink indicated by the 13C/12C ratio of atmospheric $CO_2$. *Science*, **269**: 1098–1102. https://doi.org/10.1126/science.269.5227.1098

Das G. 2008. Hydrology and soil conservation engineering: including watershed management. *PHI Learning Pvt. Ltd*.

Davis MB, Shaw RG, Etterson JR. 2005. Evolutionary responses to changing climate. *Ecology*,

**86**(7): 1704–1714. https://doi.org/doi:10.1890/03-0788

Douglas TA, Jorgenson MT, Kanevskiy MZ, Romanovsky VE, Shur YL, Yoshikawa K. 2008. Permafrost dynamics at the Fairbanks permafrost experimental station near Fairbanks, Alaska. *Ninth International Conference on Permafrost*, 373–378.

Dukes JS, Pontius J, Orwig D, Garnas JR, Rodgers VL, Brazee N, Cooke B, Theoharides KA et al. 2009. Responses of insect pests, pathogens, and invasive plant species to climate change in the forests of northeastern North America: What can we predict? *Canadian Journal of Forest Research*, **39**(2): 231–248. https://doi.org/10.1139/X08-171

Dyke AS, Moore A, Robertson L. 2003. Degalciation of North America. *Geological Survey of Canada*, Open File 1574.

Environment Canada. 2018. Online climate data. Retrieved May 17, 2018, from http://climate.weather.gc.ca/

Epstein HE, Calef MP, Walker MD, Chapin III FS, Starfields AM. 2004. Detecting changes in arctic tundra plant communities in response to warming over decadal time scales. *Global Change Biology*, **10**(8): 1325–1334. https://doi.org/10.1111/j.1529-8817.2003.00810.x

Euskirchen ES, McGuire AA, Chapin III FS, Rupp TS. 2010. The changing effects of Alaska's boreal forests on the climate system. *Canadian Journal of Forest Research*, **40**(7): 1336–1346. https://doi.org/10.1139/X09-209

Flannigan MDA, Krawchuk MAB, De Groot WJA, Wotton BMA, Gowman LMA. 2009. Implications of changing climate for global wildland fire. *International Journal of Wildland Fire*, **18**(5): 483–507. https://doi.org/10.1071/WF08187

French HM, Egorov IE. 1998. 20th century variations in the southern limit of permafrost near Thompson, Northern Manitoba, Canada. In *Proceedings of the Seventh International Conference on Permafrost*, (55): 297–304.

Frey KE, McClelland JW. 2009. Impacts of permafrost degradation on arctic river biogeochemistry. *Hydrological Processes*, **23**: 169–182. https://doi.org/10.1002/hyp

Gavriliev RI. 2004. Thermal properties of soils and surface covers. In *Thermal Analysis, Construction, and Monitoring Methods for Frozen Ground*. ASCE. https://doi.org/10.1061/9780784407202.ch09

Gill D. 1971. Vegetation and environment in the Mackenzie River Delta, Northwest Territories. *Department of Geography, University of British Columbia*, 694.

Gill D. 1973. Ecological modifications caused by the removal of tree and shrub canopies in the Mackenzie Delta. *Arctic*, **26**(2): 95–111. https://doi.org/10.14430/arctic2904

Gill D. 1975. Influence of white spruce trees on permafrost-table microtopography, Mackenzie River Delta. *Canadian Journal of Earth Sciences*, **12**(2): 263–272. https://doi.org/10.1139/e75-023

GNWT Department Of Transportation. 2011. Highway 3 - climate change vulnerability assessment. *Engineers Canada, Public Infrastructure Engineering Vulnerability Committee*.

Goodrich LE. 1982. The influence of snow cover on the ground thermal regime. *Canadian Geotechnical Journal*, **19**: 421–432. https://doi.org/10.1039/B910216G

Grulke NE, Rieehers GH, Oeehel WC, Hjelm U, Jaeger C. 1990. Carbon balance in tussock tundra under ambient and elevated atmospheric CO2. *Oecologia*, **83**: 485–494. https://doi.org/10.1007/BF00317199

Harris C, Mühll DV, Isaksen K, Haeberli W, Sollid JL, King L, Holmlund P, Dramis F et al. 2003. Warming permafrost in European mountains. *Global and Planetary Change*, **39**(3–4): 215–225. https://doi.org/10.1016/j.gloplacha.2003.04.001

Heginbottom JA, Dubreuil MA, Harker PA. 1995. Canada-permafrost, National Atlas of Canada, National Atlas Information Service. Natural Resources Canada.

Helbig M, Wischnewski K, Kljun N, Chasmer LE, Quinton WL, Detto M, Sonnentag O. 2016. Regional atmospheric cooling and wetting effect of permafrost thaw-induced boreal forest loss. *Global Change Biology*, **22**(12): 4048–4066. https://doi.org/10.1111/gcb.13348

Hinkel KM, Paetzold F, Nelson FE, Bockheim JG. 2001. Patterns of soil temperature and moisture in the active layer and upper permafrost at Barrow, Alaska: 1993-1999. *Global and Planetary Change*, **29**(3–4): 293–309. https://doi.org/10.1016/S0921-8181(01)00096-0

Hinzman LD, Kane DL, Gieck RE, Everett KR. 1991. Hydrologic and thermal properties of the active layer in the Alaskan Arctic. *Cold Regions Science and Technology*, **19**(2): 95–110. https://doi.org/10.1016/0165-232X(91)90001-W

Hobbie SE, Schimel JP, Trumbore SE, Randerson JR. 2000. Controls over carbon storage and turnover in high-latitude soils. *Global Change Biology*, **6**: 196–210. https://doi.org/10.1046/j.1365-2486.2000.06021.x

Hoeve TE, Seto JTC, Hayley D. 2004. Permafrost response following reconstruction of the Yellowknife Highway. In *International Conference on Cold Regions Engineering*. Edmonton, AB.

IPCC. 2013. Climate change 2013: The physical sciences basis. *University Press, Cambridge New York*.

James M, Lewkowicz AG, Smith SL, Miceli CM. 2013. Multi-decadal degradation and persistence of permafrost in the Alaska Highway corridor, northwest Canada. *Environmental Research Letters*, **8**. https://doi.org/10.1088/1748-9326/8/4/045013

Jean M, Payette S. 2014. Effect of vegetation cover on the ground thermal regime of wooded and non-wooded palsas. *Permafrost and Periglacial Processes*, **25**: 281–294. https://doi.org/10.1002/ppp.1817

Johannessen OM, Bengtsson L, Miles MW, Kuzmina SI, Semenov VA, Alekseev GV, Nagurnyi AP, Zakharov VF et al. 2004. Arctic climate change: Observed and modelled temperature and sea-ice variability. *Tellus, Series A: Dynamic Meteorology and Oceanography*, **56**(4): 328–341. https://doi.org/10.1111/j.1600-0870.2004.00060.x

Jorgenson MT, Osterkamp TE. 2005. Response of boreal ecosystems to varying modes of permafrost degradation. *Canadian Journal of Forest Research*, **35**(9): 2100–2111.

https://doi.org/10.1139/x05-153

Jorgenson MT, Racine CH, Walters JC, Osterkamp TE. 2001. Permafrost degradation and ecological changes associated with a warming climate in central Alaska. *Climatic Change*, **48**: 551–579. https://doi.org/10.1023/A:1005667424292

Jorgenson MT, Romanovsky VE, Harden JW, Shur YL, O'Donnell J, Schuur EAG, Kanevskiy MZ, Marchenko S. 2010. Resilience and vulnerability of permafrost to climate change. *Canadian Journal of Forest Research*, **40**(7): 1219–1236. https://doi.org/10.1139/X10-060

Jorgenson MT, Roth JE, Schlentner SF, Pullman ER, Macander M, Racine CH. 1999. An ecological land survey for Fort Wainwright, Alaska. *U.S. Army Corps of Engineers. Cold Regions Research & Engineering Laboratory*.

Kane DL. 1997. The impact of hydrologic perturbations on arctic ecosystems induced by climate change. In *Global Change and Arctic Terrestrial Ecosystems* (pp. 63–81). *Springer New York*, New York, New York. https://doi.org/10.1007/978-1-4612-2240-8_4

Kasischke ES, Turetsky MR. 2006. Recent changes in the fire regime across the North American boreal region - Spatial and temporal patterns of burning across Canada and Alaska. *Geophysical Research Letters*, **33**(9). https://doi.org/10.1029/2006GL025677

Kokelj SV, Burn CR. 2003. Ground ice and soluble cations in near-surface permafrost, Inuvik, Northwest Territories, Canada. *Permafrost and Periglacial Processes*, **14**(3): 275–289. https://doi.org/10.1002/ppp.458

Kokelj SV, Burn CR. 2004. Tilt of spruce trees near ice wedges, Mackenzie Delta, Northwest Territories, Canada. *Arctic, Antarctic, and Alpine Research*, **36**(4): 615–623. https://doi.org/https://doi.org/10.1657/1523-0430(2004)036[0615:TOSTNI]2.0.CO;2

Kokelj SV, Burn CR. 2005. Near-surface ground ice in sediments of the Mackenzie Delta, Northwest Territories, Canada. *Permafrost and Periglacial Processes*, **16**(3): 291–303. https://doi.org/10.1002/ppp.537

Kokelj SV, Burn CR, Tarnocai C. 2007. The structure and dynamics of earth hummocks in the subarctic forest near Inuvik, Northwest Territories, Canada. *Arctic, Antarctic, and Alpine Research*, **39**(1): 99–109. https://doi.org/10.1657/1523-0430(2007)39[99:TSADOE]2.0.CO;2

Kokelj SV, Jorgenson MT. 2013. Advances in thermokarst research. *Permafrost and Periglacial Processes*, **24**(2): 108–119. https://doi.org/10.1002/ppp.1779

Kokelj SV, Lantz TC, Wolfe SA, Kanigan JC, Morse PD, Coutts R, Molina-Giraldo N, Burn CR. 2014. Distribution and activity of ice wedges across the forest-tundra transition, western Arctic Canada. *Journal of Geophysical Research: Earth Surface*, **119**(9): 2032–2047. https://doi.org/10.1002/2014JF003085

Kokelj SV, Palmer MJ, Lantz TJ, Burn CR. 2017. Ground temperatures and permafrost warming from forest to tundra, Tuktoyaktuk Coastlands and Anderson Plain, NWT, Canada. *Permafrost and Periglacial Processes*, **28**(3): 543–551. https://doi.org/10.1002/ppp.1934

Konrad J-M, Morgenstern NR. 1980. A mechanistic theory of ice lens formation in fine-grained soils. *Canadian Geotechnical Journal*, **17**(4): 473–486. https://doi.org/10.1139/t80-056

Koven CD, Ringeval B, Friedlingstein P, Ciais P, Cadule P, Khvorostyanov D, Krinner G, Tarnocai C. 2011. Permafrost carbon-climate feedbacks accelerate global warming. *PNAS*, **108**(36): 14769–14774. https://doi.org/10.1073/pnas.1103910108

Kudriavtsev VA. 1954. The temperature of upper horizons of permafrost in the USSR. *USSR Academy of Sciences: Moscow*.

Kwong Y, Gan T. 1994. Northward migration of permafrost along the Mackenzie Highway and climatic warming. *Climatic Change*, **26**: 399–419. https://doi.org/10.1007/bf01094404

Lantz TC, Kokelj SV, Gergel SE, Henry GHR. 2009. Relative impacts of disturbance and temperature: persistent changes in microenvironment and vegetation in retrogressive thaw slumps. *Global Change Biology*, **15**(7): 1664–1675. https://doi.org/10.1111/j.1365-2486.2009.01917.x

Lee R. 1978. Forest microclimatology. *Columbia University Press*.

Lewkowicz AG. 2007. Dynamics of active-layer detachment failures, Fosheim Peninsula, Ellesmere Island, Nunavut, Canada. *Permafrost and Periglacial Processes*, **18**: 89–103. https://doi.org/10.1002/ppp.578

Liu H, Randerson JT, Lindfors J, Chapin III FS. 2005. Changes in the surface energy budget after fire in boreal ecosystems of interior Alaska: An annual perspective. *Journal of Geophysical Research Atmospheres*, **110**(13): 1–12. https://doi.org/10.1029/2004JD005158

Liu L, Jafarov E, Schaefer K, Jones B, Zebker H, Williams C, Rogan J, Zhang T. 2014. InSAR detects increase in surface subsidence caused by an Arctic tundra fire. *Geophysical Research Letters*, **41**: 3906–3913. https://doi.org/10.1002/2014GL060533.Received

Mackay JR. 1972. The world of underground ice. *Annals of the Association of American Geographers*, **62**(1): 1–22. https://doi.org/10.1111/j.1467-8306.1972.tb00839.x

Mackay JR. 1974. Ice-wedge cracks, Garry Island, Northwest Territories. *Canadian Journal of Earth Sciences*, **11**(10): 1366–1383. https://doi.org/10.1139/e74-133

Mackay JR. 1980. The origin of hummocks, western Arctic coast, Canada. *Canadian Journal of Earth Sciences*, **17**: 996–1006. https://doi.org/10.1139/e80-100

Mackay JR. 1983. Downward water movement into frozen ground, western arctic coast, Canada. *Canadian Journal of Earth Sciences*, **5**. https://doi.org/10.1139/e83-012

Mackay JR. 1984. The frost heave of stones in the active layer above permafrost with downward and upward freezing. *Arctic and Alpine Research*, **16**(4): 439–446. https://doi.org/10.2307/1550906

Mackay JR. 1995. Active layer changes (1968 to 1993) following the forest-tundra fire near Inuvik, N.W.T., Canada. *Arctic and Alpine Research*, **27**(4): 323–336. https://doi.org/10.1657/1523-0430(06-026)

Mackay JR. 2000. Thermally induced movements in ice-wedge polygons, western arctic coast: a long-term study. *Géographie Physique et Quaternaire*, **54**(1): 41. https://doi.org/10.7202/004846ar

Mackay JR, MacKay DK. 1974. Snow cover and ground temperatures, Garry Island, N.W.T. *Arctic*, **27**(4): 287–296. https://doi.org/10.14430/arctic2885

Mackay JR, Mathews WH. 1964. The role of permafrost in ice-thrusting. *The Journal of Geology*, **72**(3): 378–380.

Mariash HL, Cazzanelli M, Rautio M, Hamerlik R, Wooler MJ, Christoffersen KS. 2018. Changes in food web dynamics of low Arctic ponds with varying content of dissolved organic carbon. *Arctic, Antarctic, and Alpine Research*, **5**(1): 1–14. https://doi.org/10.1080/15230430.2017.1414472

McGuire AD, Melillo JM, Kicklighter DW, Joyce L. 1995. Equilibrium responses of soil carbon to climate change empirical and process-based estimates. *Journal of Biogeography*, **22**(4): 785–796.

Morse PD, Wolfe SA, Kokelj SV, Gaanderse AJR. 2015. The occurrence and thermal disequilibrium state of permafrost in forest ecotopes of the Great Slave Region, Northwest Territories, Canada. *Permafrost and Periglacial Processes*, (June). https://doi.org/10.1002/ppp.1858

Nicholson FH, Granberg HB. 1973. Permafrost and snowcover relationships near Schefferville. In *Permafrost: North American Contribution to the Second International Conference* (pp. 151–158). *National Academic Press*, Washington, DC.

Nossov DR, Jorgenson MT, Kielland K, Kanevskiy MZ. 2013. Edaphic and microclimatic controls over permafrost response to fire in interior Alaska. *Environmental Research Letters*, **8**: 035013. https://doi.org/10.1088/1748-9326/8/3/035013

Oechel WC, Hastings SJ, Vourlitis G, Jenkins M, Riechers G, Grulke N. 1993. Recent change of arctic tundra ecosystems from a net carbon-dioxide sink to a source. *Nature*, **361**: 520–523. https://doi.org/10.1038/361520a0

Oechel WC, Vourlitis GL. 1994. The effects of climate charge on land-atmosphere feedbacks in arctic tundra regions. *Trends in Ecology and Evolution*, **9**(9): 324–329. https://doi.org/10.1016/0169-5347(94)90152-X

Oke TR. 1997. Surface climate processes. In *The surface climates of Canada* (pp. 21–43). McGill-Queen's University Press Montreal & Kingston, Canada.

Olthof I, Latifovic R, Pouliot D. 2013. Medium resolution land cover map of Canada from SPOT 4/5 data. In *34th Canadian Symposium on Remote Sensing*. Victoria, BC.

Osterkamp TE. 2005. The recent warming of permafrost in Alaska. *Global and Planetary Change*, **49**(3–4): 187–202. https://doi.org/10.1016/j.gloplacha.2005.09.001

Osterkamp TE, Jorgenson MT, Schuur EAG, Shur YL, Kanevskiy MZ, Vogel JG. 2009. Physical and ecological changes associated with warming permafrost and thermokarst in interior Alaska. *Permafrost and Periglacial Processes*, **256**: 235–256. https://doi.org/10.1002/ppp

Osterkamp TE, Romanovsky VE. 1999. Evidence for warming and thawing of discontinuous permafrost in Alaska. *Permafrost and Periglacial Processes*, **10**(1): 17–37. https://doi.org/10.1002/(SICI)1099-1530(199901/03)10:1<17::AID-PPP303>3.0.CO;2-4

Osterkamp TE, Viereck LA, Shur YL. 2000. Observations of thermokarst and its impact on boreal forests in Alaska, USA. *Arctic, Antarctic, and Alpine Research*, **32**(3): 303–315. https://doi.org/10.1080/15230430.2000.12003368

Pearce C, Mclennan D, Cordes L. 1988. The evolution and maintenance of white spruce woodlands on the Mackenzie Delta, NWT, Canada. *Holarctic Ecology*, **11**(4): 248–258. https://doi.org/10.1111/j.1600-0587.1988.tb00807.x

Peterson R, Krantz W. 1998. A linear stability analysis for the inception of differential frost heave. In *Proceedings of the Seventh International Conference on Permafrost* (pp. 883–889).

Peterson RA, Walker DA, Romanovsky VE, Knudson JA, Raynolds MK, Krantz WB. 2003. A differential frost heave model: cryoturbation-vegetation interactions. *Permafrost*, 885–890.

Post WM, Emanuel WR, Zinke PJ, Stangenberger AG. 1982. Soil carbon pools and world life zones. *Nature*, **298**: 156–159. https://doi.org/10.1038/298156a0

Quinton WL, Hayashi M, Chasmer LE. 2011. Permafrost-thaw-induced land-cover change in the Canadian subarctic: Implications for water resources. *Hydrological Processes*, **25**(May 2010): 152–158. https://doi.org/10.1002/hyp.7894

Racine C, Jandt R, Meyers C, Dennis J. 2004. Tundra fire and vegetation change along a hillslope on the Seward Peninsula, Alaska, USA. *Arctic, Antarctic, and Alpine Research*, **36**(1): 1–10. https://doi.org/10.1657/1523-0430(2004)036[0001:TFAVCA]2.0.CO;2

Rieke R, Vinson TS, Mageau DW. 1983. The role of specific surface area and related index properties in the frost heave susceptibility of soils. In *Proceedings of the Fourth International Conference on Permafrost* (pp. 1066–1071). Fairbanks, Alaska.

Riseborough DW, Wolfe SA, Duchesne C. 2013. Permafrost modelling in northern Great Slave region Northwest Territories, Phase 1 : Climate data evaluation and 1-d sensitivity analysis. *Geological Survey Canada*. https://doi.org/10.4095/292366

Romanovsky VE, Sazonova TS, Balobaev VT, Shender NI, Sergueev DO. 2007. Past and recent changes in air and permafrost temperatures in eastern Siberia. *Global and Planetary Change*, **56**(3–4): 399–413. https://doi.org/10.1016/j.gloplacha.2006.07.022

Romanovsky VE, Smith SL, Christiansen HH. 2010. Permafrost thermal state in the polar northern hemisphere during the international polar year 2007-2009: A synthesis. *Permafrost and Periglacial Processes*, **21**(2): 106–116. https://doi.org/10.1002/ppp.689

Rouse WR. 1976. Microclimatic changes accompanying burning in subarctic lichen woodland. *Arctic and Alpine Research*, **8**(4): 357–376. https://doi.org/10.2307/1550439

Schuur EAG, McGuire AD, Grosse G, Harden JW, Hayes DJ, Hugelius G, Koven CD, Kuhry P. 2015. Climate change and the permafrost carbon feedback. *Nature*, **520**(January 2016): 171–179. https://doi.org/10.1038/nature14338

Scurfield G. 1973. Reaction wood: its structure and function. *Science*, **179**(4074): 647–655.

Serreze MC, Walsh JE, Chapin III FS, Osterkamp TE, Dyurgerov MB, Romanovsky VE, Oechel WC, Morison J et al. 2000. Observational evidence of recent change in the northern high-

latitude environment. *Climatic Change*, **46**: 159–207.
https://doi.org/10.1023/A:1005504031923

Seto JTC, Arenson LU, Cousineau G. 2012. Vulnerability to climate change assessment for a highway constructed on permafrost. In *Proceedings of the International Conference on Cold Regions Engineering* (pp. 515–524). ASCE.

Shur YL, Hinkel KM, Nelson FE. 2005. The transient layer: implications for geocryology and climate-change science. *Permafrost and Periglacial Processes*, **16**(1): 5–17. https://doi.org/10.1002/ppp.518

Shur YL, Jorgenson MT. 1998. Cryostructure development on the floodplain of the Colville River Delta, Northern Alaska. *Proceedings of the Seventh International Conference on Permafrost*, **55**: 993–999.

Shur YL, Jorgenson MT. 2007. Patterns of permafrost formation and degradation in relation to climate and ecosystems. *Permafrost and Periglacial Processes*, **19**: 7–19. https://doi.org/10.1002/ppp

Smith DG. 1994. Glacial Lake McConnell: paleogeography, age, duration, and associated river deltas, Mackenzie River basin, western Canada. *Quaternary Science Reviews*, **13**(1987): 829–843. https://doi.org/10.1016/0277-3791(94)90004-3

Smith MW. 1975. Microclimatic influences on ground temperatures and permafrost distribution, Mackenzie Delta, Northwest Territories. *Canadian Journal of Earth Sciences*, **12**(8): 1421–1438. https://doi.org/10.1139/e75-129

Smith MW, Riseborough DW. 1993. Modelling permafrost response to climate change and climate variability. In *Proceedings, Fourth International Symposium on Thermal Engineering & Science for Cold Regions*. US Army Cold Regions Research and Engineering Laboratory, Special Report.

Smith SL, Burgess MM, Riseborough D, Nixon FM. 2005. Recent trends from Canadian permafrost thermal monitoring network sites. *Permafrost and Periglacial Processes*, **16**(1): 19–30. https://doi.org/10.1002/ppp.511

Smith SL, Burgess MM, Riseborough DW. 2008. Ground temperature and thaw settlement in frozen peatlands along the Norman Wells pipeline corridor, NWT Canada: 22 years of monitoring. In *Proceedings of the Ninth International Conference on Permafrost* (pp. 1665–1670). Fairbanks, Alaska.

Smith SL, Riseborough DW, Bonnaventure P. 2015. Eighteen year record of forest fire effects on ground thermal regimes and permafrost in the central Mackenzie Valley, NWT, Canada. *Permafrost and Periglacial Processes*, (May). https://doi.org/10.1002/ppp.1849

Smith SL, Romanovsky VE, Lewkowicz AG, Burn CR, Allard M, Clow GD, Yoshikawa K, Throop J. 2010. Thermal state of permafrost in North America: a contribution to the international polar year. *Permafrost and Periglacial Processes*, **21**(2): 117–135. https://doi.org/10.1002/ppp.690

Smith SL, Williams PJ. 1990. Ice lense orientation around a chilled buried pipe. In *Proceedings of the Fifth Canadian Permafrost Conference* (pp. 83–87).

Sniderhan AE, Mamet SD, Baltzer JL. In review. Treeline to treeline: non-uniform growth dynamics of a dominant boreal tree species in the face of rapid climate change. Submitted to *Environmental Research Letters*.

Soja AJ, Tchebakova NM, French NHF, Flannigan MD, Shugart HH, Stocks BJ, Sukhinin AI, Parfenova EI et al. 2007. Climate-induced boreal forest change: Predictions versus current observations. *Global and Planetary Change*, **56**(3–4): 274–296. https://doi.org/10.1016/j.gloplacha.2006.07.028

Stendel M, Christensen JH. 2002. Impact of global warming on permafrost conditions in a coupled GCM. *Geophysical Research Letters*, **29**(13): 5–8. https://doi.org/10.1029/2001GL014345

Sturrock RN, Frankel SJ, Brown A V, Hennon PE, Kliejunas JT, Lewis KJ, Worrall JJ, Woods AJ. 2011. Climate change and forest diseases. *Plant Pathology*, **60**(1): 133–149. https://doi.org/10.1111/j.1365-3059.2010.02406.x

Tarnocai C, Zoltai SC. 1978. Earth hummocks of the Canadian Arctic and Subarctic. *Arctic and Alpine Research*, **10**(N): 581–594. https://doi.org/10.1080/00040851.1978.12003997

Terzaghi K, Peck RB, Mesri G. 1996. Soil mechanics in engineering practice. *John Wiley & Sons*.

Tighe SL, Cowe Falls L, Haas R, MacLeod D. 2006. Climate impacts and adaptations on roads in northern Canada. In *Transportation Research Board 85th Annual Meeting*. Washington, DC.

Turetsky MR, Mack MC, Hollingsworth TN, Harden JW. 2010. The role of mosses in ecosystem succession and function in Alaska's boreal forest. *Canadian Journal of Forest Research*, **40**(7): 1237–1264. https://doi.org/10.1139/X10-072

Turetsky MR, Wieder RK, Vitt DH. 2002. Boreal peatland C fluxes under varying permafrost regimes. *Soil Biology and Biochemistry*, **34**(7): 907–912. https://doi.org/10.1016/S0038-0717(02)00022-6

Van Cleve K, Viereck LA. 1981. Forest succession in relation to nutrient cycling in the boreal forest of Alaska. *Forest Succession, Concepts and Application*, 184–211. https://doi.org/10.1007/978-1-4612-5950-3_13

Van Wagner CE. 1983. Fire behaviour in northern conifer forests and shrublands. In, *The role of fire in northern circumpolar ecosystems* (pp. 65–80). *John Wiley & Sons*, Chichester, UK.

Viereck LA. 1982. Effects of fire and firelines on active layer thickness and soil temperatures in interior Alaska. *Permafrost and Soils*, 123–135.

Viereck LA, Dyrness CT, Batten AR. 1992. The Alaska vegetation classification. *USDA General Technial Report*, 142.

Viereck LA, Schandelmeier LA. 1980. Effects of fire in Alaska and adjacent Canada: a literature review. *BLM-Alaska Technical Report*, **6**(February): 1–124.

Viereck LA, Werdin-Pfisterer NR, Adams PC, Yoshikawa K. 2008. Effect of wildfire and fireline construction on the annual depth of thaw in a black spruce permafrost forest in interior Alaska: A 36-year record of recovery. In *Proceedings of the Ninth International Conference on Permafrost*, 1845–1850.

Walker DA, Walker MD. 1996. Terrain and vegetation of the imnavait creek watershed. *Landscape function and disturbance in Arctic tundra. Ecological Studies (Analysis and Synthesis)*, **120** (pp. 73–108). https://doi.org/10.1007/978-3-662-01145-4_4

Wang C, Bond-Lamberty B, Gower ST. 2003. Carbon distribution of a well- and poorly-drained black spruce fire chronosequence. *Global Change Biology*, **9**(7): 1066–1079. https://doi.org/10.1046/j.1365-2486.2003.00645.x

Washburn AL. 1979. Geocryology. *Edward Arnold*, London.

Wein RW, Bliss LC. 2009. Changes in Arctic Eriophorum tussock communities following fire. *Ecology*, **54**(4): 845–852. https://doi.org/10.2307/1935679

White DM, Craig Gerlach S, Loring P, Tidwell AC, Chambers MC. 2007. Food and water security in a changing arctic climate. *Environmental Research Letters*, **2**: 045018. https://doi.org/10.1088/1748-9326/2/4/045018

Williams PJ, Smith MW. 1991. The frozen earth fundamentals of geocryology. *Cambridge University Press*, New York.

Wolfe SA. 1998. Massive ice associated with glaciolacustrine delta sediments, Slave geological province, NWT, Canada. In *Proceedings of the Seventh International Conference on Permafrost* (pp. 1133–1139).

Wolfe SA, Duchesne C, Gaanderse AJR, Houben AJ, D'Onofrio RE, Kokelj SV, Stevens CW. 2011. Report on 2010-11 permafrost investigations in the Yellowknife area, Northwest Territories. *Geological Survey Canada*. https://doi.org/10.4095/289596

Wolfe SA, Stevens CE, Gaanderse AJR, Oldenborger GA. 2014. Lithalsa distribution, morphology and landscape associations in the Great Slave Lowland, Northwest Territories, Canada. *Geomorphology*, **204**: 302–313. https://doi.org/10.1016/j.geomorph.2013.08.014

Woo M-K, Winter TC. 1993. The role of permafrost and seasonal frost in the hydrology of northern wetlands in North America. *Journal of Hydrology*, **141**(1–4): 5–31. https://doi.org/10.1016/0022-1694(93)90043-9

Xue X, Guo J, Han B, Sun Q, Liu L. 2009. The effect of climate warming and permafrost thaw on desertification in the Qing-Tibetan Plateau. *Geomorphology*, **108**(3–4): 182–190. https://doi.org/10.1016/j.geomorph.2009.01.004

Yoshikawa K, Hinzman LD. 2003. Shrinking thermokarst ponds and groundwater dynamics in discontinuous permafrost near Council, Alaska. *Permafrost and Periglacial Processes*, **14**(2): 151–160. https://doi.org/10.1002/ppp.451

Zhang T, Barry RG, Knowles K. 2003. Distribution of seasonally and perennially frozen ground in the Northern Hemisphere. In *Permafrost,* Phillips, Springman & Arenson (pp. 1289–1294).

Zhang T, Barry RG, Knowles K, Heginbottom JA, Brown J. 1999. Statistics and characteristics of permafrost and ground ice distribution in the Northern Hemisphere. *Polar Geography*, **23**(2): 132–154. https://doi.org/10.1080/10889379909377670

Zhang T, Osterkamp TE, Stamnes K. 1997. Effects of climate on the active layer and permafrost on

the north slope of Alaska, U.S.A. *Permafrost and Periglacial Processes*, **8**(1): 45–67. https://doi.org/10.1002/(SICI)1099-1530(199701)8:1<45::AID-PPP240>3.0.CO;2-K

Zhang Y, Olthof I, Fraser RH, Wolfe SA. 2014. A new approach to mapping permafrost and change incorporating uncertainties in ground conditions and climate projections. *Cryosphere*, **8**: 2177–2194. https://doi.org/10.5194/tc-8-2177-2014

Zoltai SC. 1975. Structure of subarctic forests on hummocky permafrost terrain in northwestern Canada. *Canadian Journal of Forest Research*, **5**(1): 1–9. https://doi.org/10.1139/x75-001

Zoltai SC, Pettapiece WW. 1973. Studies of vegetation, landform and permafrost in the Mackenzie Valley: Terrain, vegetation and permafrost relationships in the northern part of the Mackenzie Valley and Northern Yukon, *Environmental-Social Program, Northern Pipelines*.

Zoltai SC, Tarnocai C. 1974. Soil and vegetation of hummocky terrain. *Information Canada*.

# Chapter 2: Near-surface ground ice of boreal forests in discontinuous permafrost

## 2.1 Abstract

Rapid climate warming in the north is leading to increased rates of permafrost thaw. Landscape change can result from the top-down thaw of ice-rich permafrost; therefore, it is important to characterize the ice content of the upper part of the permafrost, which is often ice-rich and will be the first to thaw. Here I characterize structure and variation of near-surface permafrost ice content between two forest types in the North Slave region near Yellowknife, Northwest Territories. At each site, core samples from multiple boreholes were obtained to investigate the top metre of mineral soil permafrost at 20 sites in black spruce and white spruce/birch forests. Cryostructure, soil properties, and volumetric ice content were determined for each core sample, and differences in these characteristics were assessed as a function of forest type, microtopography, active layer thickness, and core sample depth. Black spruce forests were underlain by ground ice that decreased with greater depth below the permafrost table and contained cryostructures characteristic of the transient layer. Permafrost aggradation and ice-enrichment associated with forest development results in higher near-surface ice content in association with thinner active layers in these black spruce forests. Thick active layers in some white spruce/birch sites did not exhibit ground ice conditions associated with transient layer permafrost. Given predicted rates of climate warming in the area, it is likely that the transient layer permafrost will never aggrade in these thick active layer sites unless an ecosystem change imparts thermal controls that further cool the ground surface. There was no effect of microtopography on local variation in ice content, but a transient layer was present in all areas with microtopographic relief. Ecosystem change in this

region as a result of climate warming-induced permafrost thaw will therefore be more predictable in

black spruce forests due to the ubiquitous transient layer presence, which is not consistent in white

spruce/birch forests.

## 2.2 Introduction

High latitudes, and northwestern North America in particular, are experiencing some of the most pronounced climate warming on the planet (IPCC, 2013). This is causing disappearance of thin permafrost and a northward shift of the boundary of discontinuous permafrost (Kwong and Gan, 1994; Burn, 1998). For example, Kwong and Gan (1994) reported a northward shift of the sporadic discontinuous zone by 120 km over a 26-year period in the region south of Great Slave Lake (1962 – 1988). Thawing of permafrost is expected to accelerate as the climate warms, with the rate and impacts of thaw depending on ground ice conditions, terrain type, and ecosystem feedbacks (Shur and Jorgenson, 2007; Baltzer *et al*., 2014; Zhang *et al*., 2014). Permafrost projections modeled for the Great Slave geological province near Yellowknife, Northwest Territories (NWT) show that currently about half of the land area is underlain by permafrost, and by the end of the century permafrost will only exist in isolated patches (Zhang *et al*., 2014). A better understanding of the physical and ecological characteristics of near-surface permafrost terrain will provide a basis for mapping sensitive terrain. This data can be used to define boundary conditions to constrain modeling activities and improve projections of permafrost thaw.

Permafrost thaw can alter the interactions between surface and subsurface hydrology (Xue *et al*., 2009; Quinton *et al*., 2011), lead to terrain subsidence (Mackay, 1972) and instability in sloping terrain (Lewkowicz and Harris, 2005; Lantz and Kokelj, 2008; Kokelj *et al*., 2015), with implications for ecosystem structure, composition, and function (Osterkamp *et al*., 2000; Jorgenson *et al*., 2001; Christensen, 2004). The ice content of near-surface permafrost influences the rate of permafrost thaw and the magnitude of ground subsidence, and dictates the nature of thermokarst development (Kokelj and Jorgenson, 2013). The North Slave region hosts the majority of the population and industrial activity in the Northwest Territories (NWT). Thaw-induced terrain

subsidence can also impact communities by damaging infrastructure, affecting water supply due to changing hydrology, and impacting security of traditional food resources and safety on the land (Romanovsky *et al*., 2010). Characterization of near-surface ground ice conditions is required to assess terrain sensitivity, but many areas, including the North Slave region, lack information on near-surface ground ice conditions (Smith *et al*., 2010).

Several physical and biological controls affect ground ice accumulation in permafrost. Most of the forested landscape develops on fine-grained sediments in the North Slave region. These sediments are characterized by high unfrozen water content – the small pore sizes create pore pressures during freezing that allow for a proportion of the water to remain unfrozen, depending on temperature and salinity. These soils have high frozen hydraulic conductivity making them susceptible to ice-lens development and frost heave as water is drawn towards the freezing front in permafrost from the overlying active layer. Therefore, regional permafrost aggradation into the fine-grained lacustrine sediments resulted in the development of segregated ground ice (Wolfe *et al*., 2014). In forested terrain, surface organic matter content and organic layer thickness may affect both thermal conditions and permeability of the terrain surface. These conditions promote a shallow permafrost table and infiltration of water towards the base of the active layer for ice growth (Van Cleve and Viereck, 1981; Osterkamp and Romanovsky, 1999; Johnstone *et al*., 2010). Microtopographic relief created from frost action may also promote water infiltration through the active layer (Kokelj *et al*., 2007). The development of forest cover and the associated soil organic layer through time can result in upward aggradation of the permafrost table. This sequesters segregated ice lenses that form at the base of the active layer during fall (Shur and Jorgenson, 2007).

The nature of near-surface ground ice conditions is modified throughout time in association with variability in active layer development. Development of the active layer is controlled by climate, and by local or temporal variation in soil properties, organic layer thickness, and vegetation cover. The greatest perturbation to active layer thickness in subarctic boreal forests is associated with fire and post-fire forest recovery (Mackay, 1995; Nossov *et al*., 2013; Smith *et al*., 2015). After a fire, the removal of surface vegetation and the organic layer alters the ground thermal regime causing the thickness of the active layer to increase and underlying permafrost to warm. Under these conditions the top of permafrost thaws, melting ground ice and causing surface subsidence (Mackay, 1995) or thermokarst to develop (Kokelj and Jorgenson, 2013). As the forest vegetation re-establishes, changes to the boundary layer (vegetation, organic layer) alter the ground thermal regime, typically resulting in upward aggradation of the permafrost table as the active layer thins.

These climate or disturbance-driven fluctuations in active layer result in the development of the "transient layer" (Shur *et al*., 2005). An increase in active layer thickness can eradicate ground ice, whereas climate or ecologically driven active layer thinning can lead to formation of aggradational ice. In fine-grained soils, water is drawn along a pressure gradient during soil freezing so that in late summer, available moisture is drawn downward from the active layer into warm permafrost contributing to the growth of segregated ice lenses. The seasonal variation in the thermal gradient and unfrozen water content of the near-surface permafrost leads to a flux divergence – where sufficient moisture is available, this process (in conjunction with a rising permafrost table) can result in the gradual ice-enrichment of near-surface permafrost (Cheng, 1983; Mackay, 1983). Over several successive seasons this can lead to the development of larger segregated ice lenses, with most ice growth near the surface of the permafrost because there is a

moisture source from the active layer (Mackay, 1983; Shur *et al*., 2005). Development of the forest and organic layer will alter the ground thermal regime and cause the permafrost table to aggrade, trapping ice lenses below the freezing front (Mackay, 1972). New ice lenses trapped just below the upward aggrading front gradually lead to a thicker zone of aggradational ice enrichment (Kokelj and Burn, 2003). If upward aggradation is gradual, there is sufficient time for near-surface ice lenses to grow larger; older forests which have not sustained disturbance may be underlain by a thicker zone of near-surface segregated ice than younger forests or disturbed sites (Cheng, 1983; Mackay, 1995; Kokelj and Burn, 2005; Shur *et al*., 2005). Due to this development pathway of the transient layer, excess ice content would be expected to be higher under thinner active layer and decrease with depth into the permafrost if the transient layer is present.

Permafrost history, soil type, and past fluctuation in active layer thickness usually associated with disturbance-related thaw can influence near-surface organic matter profiles and geochemistry. Cryoturbation of thawed substrate can mix surface organics deeper into the soil profile (Tarnocai and Zoltai, 1978) and leaching of soluble materials from thawed soils can lead to geochemical contrasts between active layer, transient layer, and underlying permafrost (Kokelj and Burn, 2003; Lacelle and Vasil'chuk, 2013). Characterizing these parameters can provide information on permafrost history and the potential carbon and geochemical consequences of thaw.

Near-surface ground ice development in boreal forest soils of the Great Slave lowlands can be considered in the context of regional permafrost history, ecosystem disturbance, and subsequent development of the transient layer (Shur *et al*., 2005). Fine-grained lacustrine and fluvial deposits accumulate in lowland terrains in association with terrain uplift and recession of Great Slave Lake, and former glacial Lake McConnell (Smith, 1994; Morse *et al*., 2015). Terrain emergence is associated with permafrost aggradation and ice lens development in fine-grained materials where

moisture supply is sufficient (Wolfe and Morse, 2017; Gaanderse *et al.*, 2018). These processes produce lithalsas, which are common throughout the region. Black spruce (*Picea mariana* (Miller) Britton, Sterns & Poggenburgh) is the most common tree species found on fine-grained mineral soils in this region, and the lithalsas are usually populated with white birch (*Betula papyrifera* Marshall and *B. neoalaskana* Sargent) or white spruce (*Picea glauca* (Moench) Voss) (Wolfe *et al.*, 2011). Due to differences in topography and forest characteristics, white spruce/birch lithalsas in this region can have warmer ground temperatures than in black spruce forests (Morse *et al.*, 2015), potentially leading to differences in permafrost development and thaw.

In this study, our goal is to characterize the variation in ground ice content of the near-surface permafrost in fine-grained mineral soil of black spruce and white spruce/birch forest types near Yellowknife – the dominant forest types in the North Slave region. Specifically, I aim to 1) assess how permafrost core sample depth and ground conditions (i.e., microtopography and active layer thickness) relate to variability of ground ice content; 2) assess the role of forest type on transient layer conditions and ground ice content. I show that in black spruce forests, thin active layers are underlain by higher near-surface ground ice contents that decrease with depth into the permafrost, a pattern indicative of a developed permafrost transient layer. This relationship was not apparent in white spruce/birch sites where the active layers could be thicker (up to 305 cm), sometimes truncating formational ground ice at depth. In conjunction with contrasting soil soluble ion concentrations, these profiles suggest the presence of a transient layer at black spruce sites and the absence of a well-developed transient layer on some lithalsa surfaces. This is especially prevalent where contemporary active layer development truncates ground ice developed in association with downward permafrost aggradation and lithalsa formation. These data provide a more robust understanding of variation in near-surface ground ice conditions, and suggest that an

ice-rich transient layer is not ubiquitous in fine-grained materials through forested areas with warm permafrost, with implications for the persistence of permafrost in the region.

## 2.3 Methods

### 2.3.1 Study area

The North Slave region near Yellowknife is in the zone of extensive discontinuous permafrost (Heginbottom *et al*., 1995) (Appendix Figure A.1). Permafrost typically underlies peatlands and most forested sites, but is absent in bedrock outcrops (Brown, 1973; Zhang *et al*., 2014). The permafrost is believed to be less than 50 m thick (Brown, 1973) and warm (> -2° C) (Hoeve *et al*., 2004; Morse *et al*., 2015). Ground temperature envelopes from the region indicate a narrow range of maximum and minimum temperatures at the top of permafrost, indicative of latent effects in warming permafrost (Morse *et al*., 2015). Temperatures in the Yellowknife area increased at a rate of 0.17° C per decade from 1971-2000 (IPCC, 2013), with an even higher rate of warming since the start of the 21st century (Environment Canada, 2018), indicating that there is significant potential permafrost thaw.

Much of the boreal forest near Yellowknife is underlain by lacustrine sediments deposited by glacial Lake McConnell, which inundated the entire region following the retreat of the Laurentide Ice Sheet (Smith, 1994). Lake Athabasca, Great Slave Lake, and Great Bear Lake represent vestiges of this former larger body of water.  The landscape is a mosaic of bedrock outcrop dominated by jack pine, black spruce, and mixed spruce and deciduous forests, with small areas of white spruce, peatlands, and fens (Appendix Figure A.2; Wolfe *et al*., 2011). Forested terrain is largely underlain by fine-grained sediments; however, little is known about the near-surface ground ice distribution throughout this region of warm permafrost (Heginbottom *et al*.,

1995). Microtopographical relief is often present in forests where frost heave has led to the development of hummocky terrain (Kokelj *et al*., 2007).

*2.3.2 Study design*

To examine biophysical influences on near-surface ground ice content in mineral soil permafrost, twenty study sites were selected within a 30 km radius of Yellowknife spanning a range of black spruce and white spruce/birch forests (Appendix Figure A.1; Appendix Table A.1). To account for potential confounding factors, sites were selected to be well-drained with little to no slope, fine-grained mineral soil, and have uniform forest composition within the site. To assess the influence of stand development on ground ice content, sites were selected to span a range of forest development stages (Appendix Figure A.3). This was evaluated by characterizing dominant tree species, tree size, organic layer thickness, understorey development, and, in the case of black spruce forests, hummock size, to try to capture a successional gradient. Ten sites were chosen for each black spruce and white spruce/birch forest types. The study design was constrained by logistics and site availability and since the study is focused around the Yellowknife area, recently burned forests were uncommon due to rapid fire suppression response time in the area. Therefore, no sites with an early stage of forest development were included in this study (stand ages ranged from 55 to 145 years).

*2.3.3 Permafrost sampling*

Core samples were obtained from the near-surface permafrost to determine ground ice content, sediment grain size, organic carbon content, and pore water chemistry. At each site characterized by hummocky microtopographical relief (10 black spruce, 2 white spruce/birch), four boreholes were drilled using a CRREL (Cold Regions Research and Engineering Laboratory)

permafrost drill. Two of these four boreholes were drilled into hummock tops, and the other two were drilled into the inter-hummock troughs (Appendix Figure A.4) to assess whether microtopography influenced near-surface ground ice content. Hummock width and height measurements were made at borehole locations to characterize microtopography. On each microtopographic location, one borehole was drilled to a depth of 100 cm below the permafrost table and the other drilled to 60 cm below the permafrost table. The depth of 60 cm was chosen because it captures the near-surface permafrost (Shur *et al.*, 2005). The boreholes drilled to 100 cm below the permafrost table were obtained with the goal of capturing the entire transient layer, or in some cases, to capture the interface between the base of the transient layer and underlying permafrost. The sampling design was aimed at detailed assessment of near-surface ground ice variation within and between sites. Logistics, time, and other studies focused on deeper permafrost profiles (Wolfe *et al.*, 2016) contributed to limiting sample collection to top 1 m of permafrost. Core samples were obtained in 10 cm intervals, and cryostructure, visible ice content, and soil characteristics were described. Samples were inferred to be from the transient layer based on the presence and size of uniform, horizontal segregated ice lenses (Shur *et al.*, 2005). Supporting data on transient layer characteristics included assessments of organic matter content and pore water chemistry on representative samples. A similar drilling strategy was employed for the eight white spruce/birch sites that lacked microtopography. However, the terrain was not hummocky, so only three boreholes were drilled to characterize the ice content: two to 100 cm and one to 60 cm depth below the permafrost table (Appendix Figure A.5).

Immediately following the extraction of a core sample, core length, soil type and colour, ice structure, and visible ice content were recorded (Appendix Figure A.6) and a photograph was taken in the field before the sample was sealed in a plastic bag for transport to the lab for analysis. Length

was used to determine the core sample volume, using the equation for the volume of a cylinder (V = $\pi r^2 h$), since the radius of the core barrel was known (r = 3.81 cm). To account for potential errors associated with dimension-based volume calculations, an alternative method for evaluating sample volume was investigated at the outset of the study involving wrapping the core sample in thin plastic, completely submerging it in a full container of water, and then using a balance in the field to measure the mass change of the container, which was equal to the amount of displaced water. Since 1 g of water is equal to 1 cm$^3$, the mass of water that overflowed gave the volume of the submerged sample. Figure 2.1 shows that volume estimates using the two methods were highly comparable for 58 permafrost core samples, so the simpler length method was implemented for subsequent sampling.

*2.3.4 Core sample analysis*

Gravimetric water content was determined by measuring wet and dry weights of the samples. Samples were dried at 105° C for up to 72 hours until completely dry (with an internal visual inspection). Sample gravimetric wet weight was calculated using the equation:

$$\omega = \frac{M_f - M_d}{M_f}$$

Where $M_f$ is the field mass of the sample and $M_d$ is the dry mass (Appendix Figure A.7) of the sample. Water content can then be converted to volumetric ice content by multiplying the mass of water evaporated by the 9% volumetric expansion of water to ice, then dividing by the total field volume to give a proportion of the sample containing ice. Volumetric ice content gives a measure of the total volume of ice in a sample, including pore ice which is not accounted for in estimates of visible or excess ice content of a sample. Volumetric ice content is strongly related to gravimetric water content and visible excess ice measurements (Figure 2.2), and is used in this study to be

synonymous with ground ice content.  Subsamples from each 10 cm core interval from one long

borehole (100 cm into the permafrost) at each site were analyzed for sediment grain size and

organic carbon content. The sediment grain size analysis was performed using a Partica LA-950

Laser Diffraction Particle Size Distribution Analyzer (HORIBA Scientific, Irvine, CA, USA). The

settings for the Partica LA-950 were calibrated for each sample according to the standard operating

procedures (HORIBA Scientific, 2018). Organic carbon content was analyzed using a loss on

ignition test following the methods of Heiri *et al*. (2001)*,* by burning each of the dried subsamples

at 550° C for 4 hours in a muffle furnace then weighing the mass loss. To measure soil pore water

conductivity, dried samples were rehydrated with deionized water to saturation and pore-water was

extracted and measured with an electrical conductivity probe, following Carter and Gregorich

(2007). This analysis was conducted by Exova Canada Inc. (Edmonton, Alberta).

Calculating subsidence risk cannot be done directly from volumetric ice content

measurements, which represent the total ice content of a sample including pore ice, but rather

requires an estimation of excess ice content. To address this, thaw strain of each permafrost sample

was calculated using a modified method of Crory (1973):

$$\gamma = \frac{\rho_{thawed} - \rho_{frozen}}{\rho_{thawed}}$$

Where $\rho_{thawed}$ is the bulk density of representative samples containing no excess ice and

$\rho_{frozen}$ is the sample frozen bulk density of the permafrost sample. This modification was applied

because a chamber to thaw and drain samples for obtaining "thawed bulk density" was not

available. A measure representing thawed bulk density was obtained by estimating mean frozen

bulk densities for samples, typically in the base of the frozen active layer, which did not contain

excess ice. These samples provide a conservative estimate of the bulk density of a sample that

thawed and excess water had drained away freely (i.e., at saturation, but with no excess ice present). An estimate of subsidence from thawing of each sample was then obtained by multiplying its thaw strain by the length of the sample interval (10 cm).

*2.3.5 Statistical analysis*

All statistical tests on the data were performed using R software (version 3.4.4, R Core Team, 2018). Linear models were created to test for relationships between volumetric ice content and hypothesized controls of ground ice accumulation (e.g., sediment grain size or soil organic matter content). To test for differences in site characteristics between forest types (Table 2.1), a two sample t-test was performed on the site-averaged variables. Log transformations were applied to organic layer thickness, silt content, soil organic matter, and active layer thickness data to meet assumptions of normality. The *lme4* package (Bates *et al*., 2017) was used to create linear mixed effects models to determine the influence of microtopography, core sample depth, and active layer thickness (fixed effects) for both black spruce and white spruce/birch forest types on volumetric ice content of the near-surface permafrost. The forest types were analyzed separately because most white spruce/birch forests lacked microtopography, and differences in stand development can lead to changes in environmental conditions that could affect ground ice accumulation. White spruce/birch forests had no microtopographical relief, and so the term was not modeled. To account for the nested sampling design employed in this study (multiple sampling depths within each borehole and multiple boreholes within each site), the random effects term *borehole* nested within *site* was added to the model. Models were selected to test which hypothetical model best explains near-surface permafrost volumetric ice content: hummock top or trough, core sample depth below permafrost table, active layer thickness, or a combination of these factors. In addition, the interaction between core sample depth and active layer thickness was modeled to test whether the

relationship between sample depth and volumetric ice content is altered based on active layer thickness. The corrected Akaike information criterion (AICc) was chosen as the metric for model selection because it is based on variance explained by the model and adjusted for the number of parameters used. The model with the lowest corrected AICc was chosen as the model that best fit the data (Burnham and Anderson, 2002). All possible models of suspected importance were run and evaluated (Tables 2.1, 2.2). In cases where two models had similar AICc values (< 2 difference in AICc value), the most parsimonious model was chosen (i.e., the model with fewest terms). Model-averaged variable estimates for all models were obtained using the "modavg" function of the *AICcmodavg* R package (Mazerolle, 2017). To determine vertical ice trends in both forest types that may be indicative of transient layer presence, the effect of core sample depth by forest type on volumetric ice content was then investigated further by using the "lme" function of the *nlme* package (Pinheiro *et al.*, 2018), using core sample depth and forest type with their interaction as the fixed effects, and *borehole* nested within *site* as the random effects. The same model was used to test for differences in electrical conductivity to evaluate transient layer presence. The standardized major axis function of the *smatr* package (Warton *et al.*, 2018) was used to compare the line of best fit for the two methods of determining sample volume against the line of unity to test for systematic differences between the two methods in slope or intercept of the relationship. If no differences are found from the line of unity with the standardized major axis test, then it shows the two volume methods are consistent in their volume estimates for any size of core sample.

## 2.4 Results

### 2.4.1 Core sample volume

Volumetric ice content is a key parameter that describes permafrost physical characteristics and indicates consequences of thaw. To ensure robust assessment of this parameter, I compared length calculation and water displacement methods for determining volume of permafrost samples. There were highly correlated results ($R^2$ = 0.97; $p < 0.001$) between the two methods of volume estimation for 58 permafrost samples. The slope of 1.09 was significantly greater than a slope of 1 ($p = 0.001$) and the y-intercept of -26 cm$^3$ was significantly less than zero ($p = 0.038$) (Figure 2.1). The best fit model suggests the displacement method yields slightly higher estimates for ice-rich samples; however, the 1:1 line falls within the 95% confidence limit for the volume of samples taken in this study. The similarity in results between the two methods justified continuing further analyses using the more time efficient length calculation estimate for determining ice content.

*2.4.2 Exploring factors associated with ground ice accumulation*

Due to their control over the ground thermal and hydrological regimes, several key factors were analyzed for their relationship with volumetric ice content (VIC). All sites had silty clay or clayey silt, frost susceptible substrate, and the proportion of silt ranged between sites from 13.5 – 75.1% silt (85.4 – 23.7% clay) for black spruce and 9.1 – 59.0% silt (90.4 – 22.4% clay) for white spruce/birch sites (Appendix Figure A.8), with no significant difference in sediment grain size between the two stand types (Figure 2.3; Table 2.1). There were no differences in grain size with depth in black spruce (df = 38, t = 0.08, p = 0.94) or white spruce/birch stands (df = 38, t = -0.99, p = 0.33). Site-averaged grain size was significantly correlated with ice content, with an average decrease of 0.0027 VIC per 1% proportion silt for black spruce stands (df = 8, t = -2.44, p = 0.041). This represents up to a change of 0.17 VIC over the range of proportion silt observed in black spruce sites (Table 2.1). No relationship of volumetric ice content with proportion silt was observed in white spruce/birch stands (df = 8, t = 0.99, p = 0.35). Black spruce forests showed thicker active

layers under hummock tops (mean = 107 cm, SE = 3 cm) than under inter-hummock troughs

(mean = 74 cm, SE = 6 cm; df = 13.6, t = 4.74, p < 0.001; Figure 2.4), but the site-average active

layer thickness was not significantly different from that of white spruce/birch stands. However,

stands in the white spruce forest trajectory had much more variable active layer thicknesses (mean

= 132 cm, SE = 26 cm) than black spruce stands (mean = 90 cm, SE = 4 cm; Table 2.1). Eleven of

thirty-two boreholes in white spruce/birch stands had active layers greater than the thickest

observed in black spruce forests, with three dry mineral soil sites exhibiting thaw depths greater

than 2 m in thickness. In the top metre of permafrost, soil organic matter content was higher in

white spruce/birch stands (mean = 4.1%, SE = 0.5%) than in black spruce stands (mean = 2.1%, SE

= 0.2%; Table 2.1). The soil organic matter content decreased with depth into the permafrost for

black spruce (-0.0095% cm$^{-1}$, t = -2.52, df = 38, p = 0.016), but not white spruce/birch stands (t = -

1.99, df = 40, p = 0.40) (Figure 2.5). Site-averaged soil organic matter content was not significantly

correlated with ice content in black spruce stands (df = 8, t = -0.52, p = 0.62), but it was

significantly correlated with ice content in white spruce/birch stands with an average increase of

0.030 VIC per 1% organic matter (df = 8, t = 2.48, p = 0.038). Black spruce stands exhibited greater

organic layer thickness in inter-hummock troughs (mean = 25 cm) than on hummock tops (mean =

13 cm; t = -3.66, df = 37.3, p < 0.001) (Figure 2.4), but the site-average organic layer thickness was

not significantly different from that of white spruce/birch stands (Table 2.1).

*2.4.3 Stand type comparisons of ground ice*

Forests may hold different magnitudes of control on the ground thermal and hydrological

regimes depending on their composition; therefore, permafrost was compared between the two

forest stand types. There were no significant differences in mean site ice content between forest

types (Table 2.1). However, the thickness of the transient layer, as inferred from cryostructure

(Shur *et al*., 2005), was significantly thicker in black spruce than in white spruce/birch stands (86 cm and 50 cm, respectively; Table 2.1). In this study, the transient layer thickness reported is minimum thickness because the transient layer may have extended beyond the 100 cm below the permafrost table that was sampled (eighteen of thirty-nine 100 cm boreholes had transient layer thicknesses ≥ 100 cm). Lenticular segregated ice was the most common cryostructure in the permafrost samples of both forest types; typically these were observed closer to the surface of the permafrost (Figure 2.6). In black spruce stands, ataxitic cryostructures were observed in 43 of 312 permafrost samples, with 84% of these occurring within the top 40 cm of permafrost. The majority of ataxitic samples (79%) were from ice-rich sites, and the average volumetric ice content for ataxitic samples was 0.76 (SE = 0.011). Reticulate cryostructures were observed in 17 of 312 permafrost samples, with 82% of these occurring deeper than 60 cm below the permafrost table (Figures 2.6, 2.7). All but one occurrence of reticulate cryostructure samples (94%) were observed in ice-poor sites, and the average volumetric ice content for reticulate samples was 0.52 (SE = 0.007). While these cryostructures could also be observed in white spruce/birch stands, chaotic cryostructures were commonly observed in 8 out of the 10 white spruce/birch sites. Chaotic cryostructures often had vertical or sub-vertical ice lenses irregularly intersecting horizontal lenses with ice lenses ranging from 1 to 20 mm in thickness. In total, chaotic or irregular cryostructures occurred in 66 of 255 white spruce/birch permafrost samples, with no apparent relation to depth below the permafrost table in near-surface permafrost. In white spruce/birch sites with thick active layers, irregularly shaped, large ice lenses (up to 100 mm thick) were observed at depths greater than 200 cm below the ground surface in 33 of 85 permafrost samples (Figure 2.8).

Ground subsidence can drastically alter local topography with implications for infrastructure and ecosystem structure and function, so near-surface subsidence potential was determined for both

black spruce and white spruce/birch forests. Ice content dictates the potential subsidence following thaw, but the nature of the substrate (i.e., its thawed bulk density) also influences the behaviour of the materials when they are thawed. There was no difference in ground subsidence potential between stand types (t = -0.50, df = 18, p = 0.62), their variances were equal (F = 0.62, df = 9, p = 0.49), and both stand types exhibit the same decrease at depth (> 60 cm) in the rate of potential ground subsidence (Figure 2.9). All black spruce sites show the same pattern of decreasing rate of subsidence potential with depth, but white spruce/birch sites were more variable in their subsidence potential nearer to the permafrost table. If the top metre of permafrost were to thaw in these sites, the ground surface could subside by 8 – 30 cm in black spruce stands (mean = 14 cm) and 8 – 28 cm in white spruce/birch stands (mean = 16 cm).

*2.4.4 Modeling ground conditions with ice content*

Examining how characteristics change with depth into the permafrost and under different active layer thicknesses helps elucidate thaw response and permafrost history. In black spruce stands, volumetric ice content was affected by the depth at which the sample was taken below the permafrost table and the active layer thickness, but the role of microtopography was not significant (i.e., hummock top vs. inter-hummock trough; Table 2.2). Model-averaged variables highlight the importance of both core sample depth and active layer thickness on volumetric ice content (Table 2.3). At black spruce sites, most ice-rich samples were at the top of permafrost; ice content decreased with core sample depth (Figure 2.10). Similarly, ice content was higher for boreholes with shallower active layers (-0.0011 VIC cm$^{-1}$ active layer thickness; t = -2.10, df = 38, p = 0.042). In white spruce/birch stands, models show that although core sample depth below the permafrost table alone was not effective at explaining ice content, it becomes important when combined with active layer thickness due to the importance of an interaction between active layer thickness and

sample depth (Table 2.4). The interaction shows that sites with thinner active layers have higher ice content at a shallower sample depth below permafrost table (similar to the black spruce results), while those with thicker active layers (> 100 cm) have greater ice content at a greater depth below permafrost table (Table 2.5; Figure 2.4). When the effect of depth of core sample on volumetric ice content was modeled with forest type, it showed a significant decrease in ice content with depth below the permafrost table in black spruce forests, but there was no depth effect in white spruce/birch forests (stand type × core sample depth interaction: t = 2.92, df = 495, p = 0.004). Similar linear mixed effects modeling of electrical conductivity (EC) of pore water showed significantly higher EC in white spruce/birch forests than black spruce forests (t = 3.90, df = 18, p = 0.001), and increasing EC with depth below the permafrost table (t = 2.13, df = 157, p = 0.035), a pattern that was consistent in both forest types (no significant forest type × core sample depth interaction; t = -1.76, df = 157, p = 0.080) (Figure 2.10).

## 2.5 Discussion

### 2.5.1 Near-surface ground ice conditions in the North Slave

In this study, near-surface ground ice stratigraphy was described for fine-grained permafrost-affected soils in the North Slave region. Soil type/texture was an important driver of volumetric ice content in both dominant forest types in this region but in different ways. Specifically, there was a negative association between volumetric ice content and sediment grain size in black spruce forests, and a positive relationship between volumetric ice content and soil organic matter content in white spruce/birch forests. Transient layer cryostructures (ataxitic and lenticular) were observed in all black spruce sites, but were absent in several white spruce/birch sites. The transient layer was inferred based on cryostructure, and was found to generally thicker at sites with thin active layers

(Figure 2.11). Sites without discernable transient layer cryostructures had thicker active layers and more variable ice content in permafrost. Variability of volumetric ice content in black spruce forests was not found to differ as a function of surface microtopography. However, core sample depth below permafrost and active layer thickness were both important predictors of volumetric ice content, with higher ice content occurring near the top of permafrost at sites with thin active layers. These observations are consistent with the model of transient layer development described by Shur *et al*. (2005).

In white spruce/birch forests, active layer thickness mediated the relationship between core sample depth below permafrost table and volumetric ice content such that at sites with shallow active layers, volumetric ice content decreased with sample depth. As with the black spruce forests, this suggests the presence of a transient layer. The opposite was true for white spruce/birch sites with thick active layers, suggesting that active layer development had truncated formational ice associated with the initial establishment of permafrost in these deposits and that the transient layer was absent (Wolfe and Morse, 2017). These results indicate that the thaw response in black spruce forests (with a consistently present transient layer) may be more predictable than in white spruce forests. In some white spruce/birch forests where deep thaw is already occurring and has eroded the entirety of the permafrost transient layer, surface disturbances are unlikely to result in destabilizing ground thaw.

Soil texture influences ice content of the near-surface permafrost; it controls water movement through the active layer and the unfrozen water content of frozen soils. In white spruce/birch forests, a positive relationship with permafrost soil organic matter content and volumetric ice content was found. This suggests that highly porous organic matter allowed for greater infiltration of water to the permafrost table when the permafrost was formerly part of the active layer (Van

Cleve and Viereck, 1981; Osterkamp and Romanovsky, 1999; Johnstone *et al.*, 2010). Soil organic matter content was low in these mineral soil substrate forests, and this relationship with ice content may not have been observed in black spruce forests because soil organic matter content was significantly lower (mean = 2.1% vs. mean = 4.1%; Table 2.1). Finer-grained sediments are associated with higher unfrozen water content characteristics making them more susceptible to ice lensing and frost heave (Anderson *et al.*, 2003). While sediment grain size was negatively correlated with volumetric ice content in black spruce forests, there was no significant relationship in white spruce/birch forests. Both forest types had similar sediment grain sizes (Table 2.1), so this could indicate that for frost susceptible soils like those in our study region, other factors such as soil organic matter might be a better predictor of volumetric ice content.

Organic layer thickness is an important control on the ground thermal regime, with implications for active layer thickness and subsequently near-surface permafrost ice enrichment (Shur and Jorgenson, 2007). A thick organic layer created by peat-forming mosses alters soil thermal properties – the organic layer can insulate the ground surface from warm summer temperatures and increase soil moisture retention (Mackay, 1972). Despite the fact that our sites captured a broad range of organic layer thicknesses (10.8 – 33.8 cm for black spruce; 6.7 – 63.7 cm for white spruce/birch), there was no relationship with volumetric ice content (Table 2.1). This could be somewhat unique to the study area, which receives rapid fire suppression due to its proximity to human population. This can cause an incongruity of vegetation development between trees and the organic layer at some study sites.

*2.5.2 Black spruce forests*

The results from the black spruce stand type appear to support that near-surface ground ice distribution is related to transient layer development. Active layer thickness was inversely related to

volumetric ice content in black spruce forests (Table 2.2) likely because infiltration of water through a thicker active layer is more difficult, thereby limiting the availability of water for ice growth at the freezing front of the permafrost (Hinkel *et al*., 2001). Morse *et al*. (2015) did not identify differences in ice content with depth in the top metre of permafrost for unburned black spruce, white birch, and peatland systems. However, our analyses based on a significantly larger dataset showed that core sample depth below the permafrost table is an important predictor of ice content in black spruce stands (Tables 2.2, 2.3). This provides evidence that ice lenses grow larger as permafrost aggrades with a thinning active layer, a pattern commonly associated with mature forest development. However, ice content was not significantly correlated with stand age, suggesting that other forest characteristics and site-specific conditions may influence the physical conditions of the ground. The lack of stand age's influence on ice content may be due to large local variation in these characteristics; not all sites develop in the same way due to differences in site location, ecological history, and soil properties. Logging activity or light fires, influenced by fire suppression activity around the populated area of Yellowknife, can result in asynchronous development of vegetation.

From this investigation, no effect of microtopography on permafrost ice content was observed in black spruce forests. Moisture content has been found to be higher in the inter-hummock troughs (Tarnocai and Zoltai, 1978), but it is possible this moisture is also available to aggrade ice under hummock tops as the moisture may flow down along the bowl-shaped depression at the bottom of the active layer (Mackay, 1980). Although volumetric ice content may not significantly differ between hummock tops and troughs, microtopography will likely play an important role in the response to permafrost thaw by allowing water released from the thawed permafrost to settle rather than drain away (Jorgenson *et al*., 2010).

*2.5.3 White spruce/birch forests*

Several of the white spruce/birch forest sites did not exhibit ice growth indicative of a transient layer. At sites with thick active layers ($\geq$ 213 cm; three white spruce/birch sites) there was no evidence of transient layer cryostructures. At these sites, thick active layers have either eradicated or prevented development of the transient layer and the deep permafrost table appears to be truncating underlying formational ice (characterized by large, segregated ice lenses) (Wolfe and Morse, 2017). The significant interaction between core sample depth and active layer thickness for white spruce/birch sites indicates an increase in ice content with core sample depth into the permafrost. This is opposite to observations from black spruce forests in this study and the transient layer model of near-surface segregated ice development (Shur *et al*., 2005). In addition, pore water EC of permafrost samples was significantly higher in white spruce/birch forests (Figure 2.10), suggesting permafrost that has not been subjected to repetitive leaching in the thawed state. In contrast, the lower EC measured in near-surface permafrost of black spruce sites which increases with depth is indicative of leaching during periods of past thaw – characteristic of transient layer conditions (Kokelj and Burn, 2003; Lacelle and Vasil'chuk, 2013). Eleven of the thirty-two boreholes in the white spruce/birch forest trajectory had active layer thicknesses greater than the thickest active layer in a black spruce site (130 cm). The permafrost samples from below these thicker active layers did not exhibit cryostructures commonly associated with near-surface aggradational ice (Figure 2.6) (Cheng, 1983; Mackay, 1983; Kokelj and Burn, 2003). Our data suggest that under thick active layers characteristic of several white spruce/birch forest sites, the transient layer has been eradicated by deep thaw, or has never developed. At these sites, near-surface permafrost encountered more than 150 cm below the terrain surface was comprised of older segregated ice (irregular, sometimes very thick ice lenses). This is ice that would have developed

during downward aggradation of permafrost and the development of the lithalsas, on which stands in the white spruce trajectory typically grow (Wolfe *et al*., 2014; Morse *et al*., 2015). Lithalsas typically develop from uplifted shallow water lacustrine deposits with high organic matter content throughout the soil profile (Seppälä, 1986; Wolfe *et al*., 2014), which explains the higher soil organic matter content in permafrost beneath white spruce/birch stands compared to black spruce stands (Table 2.1). In the thick active layer sites that lack a transient layer, projected climate warming will further degrade permafrost on decadal time scales. However, ecosystem change involving further development of surface vegetation cover could modify ground thermal properties, cause the active layer to thin and near-surface permafrost to aggrade, potentially resulting in the development of a permafrost transient layer and near-surface aggradational ice. If this occurs, permafrost degradation from climate warming will be delayed.

The hypothesis that development of the transient layer and near-surface ice is a function of stand age was not supported by data from the white spruce/birch forests. There was a poor gradient of stand age in the study sites, with nine of the ten sites clustering around 65 years old, even though there was an apparent gradient in stand composition and structure indicative of succession. This highlights the importance of local differences in sites, even among the same stand age and stand composition. A white spruce forest will recover post-disturbance as either white birch or mixed white birch and white spruce depending on fire severity and seed availability (Viereck *et al*., 1992). The development of these stands and thus the biophysical controls on the ground thermal regime at a site is dependent on the local growing conditions, influenced in part by site history and drainage. These reasons explain why it is difficult to accurately predict near-surface ice content based on stand structure or composition. However, taking a general landscape view of the area, the black spruce results may be more important for characterizing ice content and predicting thaw rates

because black spruce forests comprise 57% of the landscape around Yellowknife underlain by permafrost, while mixed spruce and birch forests comprise 38% and white birch forests less than 2% (Olthof *et al*., 2013; Morse *et al*., 2015).

*2.5.4 Implications of thawing permafrost*

The results show that among moderately- to well-developed black spruce and white spruce/birch stands there was no overall difference in subsidence potential in the top metre of permafrost (Figure 2.9). For white spruce/birch sites, thawing permafrost may result in uneven ground subsidence over distances of only a few metres in some cases, as evidenced by the high variation in potential subsidence seen between boreholes within the same site. This may also highlight the need to sample multiple points within a site to properly assess the spatial variability in permafrost ground ice conditions since one borehole may provide an inaccurate representation due to potential for high local variability. However, in some stands of white spruce/birch forests, an increase in active layer thickness as a result of disturbance is unlikely because there is little organic material to disturb. Warm permafrost at these sites is likely to degrade with future warming unless ecosystem change can offer protection of the permafrost by influencing surface ground thermal conditions. Although active layer thickness was more variable in white spruce/birch sites, it was not significantly different from that of black spruce sites (Table 2.1). Since ice content was highest at the top of permafrost in black spruce sites where the active layer was not very thick, surface disturbance can lead to relatively rapid thaw and ground subsidence. However, in white spruce/birch sites, some active layers were very thick (> 200 cm) and will take much longer for permafrost to thaw following a surface disturbance. Therefore, these sites may be more resilient to ground subsidence following a surface disturbance. Furthermore, it is important to properly assess

topography and substrate for site management purposes because even small differences in terrain, soil, or forest conditions may be indicative of large differences in permafrost ground ice content.

## 2.6 Conclusions

Ground ice profiles in black spruce forests showed decreasing ice content with depth into the permafrost and horizontal, lenticular cryostructures consistent with the transient layer of permafrost. In these forests, higher near-surface ice content in association with thinner active layers results from permafrost aggradation and ice-enrichment associated with forest development. Evidence of a transient layer was absent from white spruce/birch forests at sites where thick active layers ($\geq 213$ cm) truncated formational ice at depth. Under current climate warming projections, upward aggradation of the permafrost table and transient layer development is unlikely unless ecosystem change increases organic layer thicknesses, allowing upward aggradation of the permafrost table. Our improved understanding of the distribution of near-surface ground ice content in the region will help to characterize the potential landscape change under a warming climate, and will assist in planning for infrastructure expansion.

## 2.7 References

Anderson R, Llamedo M, Tohidi B, Burgass RW. 2003. Experimental measurement of methane and carbon dioxide clathrate hydrate equilibria in mesoporous silica. *The Journal of Physical Chemistry B*, **107**(15): 3507–3514. https://doi.org/10.1021/jp0263370

Baltzer JL, Veness T, Chasmer LE, Sniderhan AE, Quinton WL. 2014. Forests on thawing permafrost: Fragmentation, edge effects, and net forest loss. *Global Change Biology*, **20**(3): 824–834. https://doi.org/10.1111/gcb.12349

Barton K. 2018. MuMIn: Multi-model inference. https://cran.r-project.org/package=MuMIn

Bates D, Maechler M, Bolker B, Walker S. 2017. lme4: Linear mixed-effects models using "eigen" and S4. https://cran.r-project.org/package=lme4

Brown RJE. 1973. Influence of climatic and terrain factors on ground temperatures at three locations in the permafrost region of Canada. In *Proceedings of the Second International Conference on Permafrost* (27–34). Yakutsk, USSR: National Academy of Science, Washington, DC.

Burn CR. 1998. Field investigations of permafrost and climatic change in northwest North America. In *Proceedings of the Seventh International Conference on Permafrost* (pp. 107–120).

Burnham KP, Anderson DR. 2002. Model selection and multimodel inference. A practical information-theoretic approach (2nd edn). *Springer-Verlag*, New York.

Carter MR, Gregorich E. 2007. Soil sampling and methods of analysis. *Canadian Society of Soil Science*. https://doi.org/10.1017/S0014479708006546

Cheng G. 1983. The mechanism of repeated-segregation for the formation of thick layered ground ice. *Cold Regions Science and Technology*, **8**(1): 57–66. https://doi.org/10.1016/0165-232X(83)90017-4

Christensen TR. 2004. Thawing sub-arctic permafrost: Effects on vegetation and methane emissions. *Geophysical Research Letters*, **31**(4): L04501. https://doi.org/10.1029/2003GL018680

Crory FE. 1973. Settlement associated with the thawing of permafrost. *In Permafrost: The North American Contribution to the Second International Conference* (pp. 599–607). Yakutsk, USSR: National Academy of Science, Washington, DC.

Environment Canada. 2018. Online climate data. Retrieved May 17, 2018, from http://climate.weather.gc.ca/

Gaanderse AJR, Wolfe SA, Burn CR. 2018. Composition and origin of a lithalsa related to lake-level recession and Holocene terrestrial emergence, Northwest Territories, Canada. *Earth Surface Processes and Landforms*, **43**(5): 1032–1043. https://doi.org/10.1002/esp.4302

Heginbottom JA, Dubreuil MA, Harker PA. 1995. Canada-permafrost, National Atlas of Canada, National Atlas Information Service. *Natural Resources Canada*, MCR, 4177.

Heiri O, Lotter AF, Lemcke G. 2001. Loss on ignition as a method for estimating organic and carbonate content in sediments: reproducibility and comparability of results. *Journal of Paleolimnology*, **25**: 101–110. https://doi.org/10.1017/CBO9781107415324.004

Hinkel KM, Paetzold F, Nelson FE, Bockheim JG. 2001. Patterns of soil temperature and moisture in the active layer and upper permafrost at Barrow, Alaska: 1993-1999. *Global and Planetary Change*, **29**(3–4): 293–309. https://doi.org/10.1016/S0921-8181(01)00096-0

Hoeve TE, Seto JTC, Hayley D. 2004. Permafrost response following reconstruction of the Yellowknife Highway. In *International Conference on Cold Regions Engineering*. Edmonton, AB.

HORIBA Scientific. 2018. Introducing the Method Expert. Doc# WP005. Retrieved from: http://www.horiba.com/scientific/products/particle-characterization/download-center/white-papers/

IPCC. 2013. Climate change 2013: The physical sciences basis. *University Press, Cambridge New York*.

Johnstone JF, Chapin III FS, Hollingsworth TN, Mack MC, Romanovsky VE, Turetsky MR. 2010. Fire, climate change, and forest resilience in interior Alaska. *Canadian Journal of Forest Research*, **40**(7): 1302–1312. https://doi.org/10.1139/X10-061

Jorgenson MT, Racine CH, Walters JC, Osterkamp TE. 2001. Permafrost degradation and ecological changes associated with a warming climate in central Alaska. *Climatic Change*, **48**: 551–579. https://doi.org/10.1023/A:1005667424292

Jorgenson MT, Romanovsky VE, Harden JW, Shur YL, O'Donnell J, Schuur EAG, Kanevskiy MZ, Marchenko S. 2010. Resilience and vulnerability of permafrost to climate change. *Canadian Journal of Forest Research*, **40**(7): 1219–1236. https://doi.org/10.1139/X10-060

Kokelj SV, Burn CR. 2003. Ground ice and soluble cations in near-surface permafrost, Inuvik, Northwest Territories, Canada. *Permafrost and Periglacial Processes*, **14**(3): 275–289. https://doi.org/10.1002/ppp.458

Kokelj SV, Burn CR. 2005. Near-surface ground ice in sediments of the Mackenzie Delta, Northwest Territories, Canada. *Permafrost and Periglacial Processes*, **16**(3): 291–303. https://doi.org/10.1002/ppp.537

Kokelj SV, Burn CR, Tarnocai C. 2007. The structure and dynamics of earth hummocks in the subarctic forest near Inuvik, Northwest Territories, Canada. *Arctic, Antarctic, and Alpine Research*, **39**(1): 99–109. https://doi.org/10.1657/1523-0430(2007)39[99:TSADOE]2.0.CO;2

Kokelj SV, Jorgenson MT. 2013. Advances in thermokarst research. *Permafrost and Periglacial Processes*, **24**(2): 108–119. https://doi.org/10.1002/ppp.1779

Kokelj SV, Tunnicliffe J, Lacelle D, Lantz TC, Fraser RH. 2015. Retrogressive thaw slumps: From slope process to the landscape sensitivity of northwestern Canada. *Geo-Québec 2015*.

Kwong Y, Gan T. 1994. Northward migration of permafrost along the Mackenzie Highway and climatic warming. *Climatic Change*, **26**: 399–419. https://doi.org/10.1007/bf01094404

Lacelle D, Vasil'chuk YK. 2013. Recent progress (2007-2012) in permafrost isotope geochemistry. *Permafrost and Periglacial Processes*, **24**(2): 138–145. https://doi.org/10.1002/ppp.1768

Lantz TC, Kokelj SV. 2008. Increasing rates of retrogressive thaw slump activity in the Mackenzie Delta region, N.W.T., Canada. *Geophysical Research Letters*, **35**(6): 1–5. https://doi.org/10.1029/2007GL032433

Lewkowicz AG, Harris C. 2005. Morphology and geotechnique of active-layer detachment failures in discontinuous and continuous permafrost, northern Canada. *Geomorphology*, **69**(1–4): 275–297. https://doi.org/10.1016/j.geomorph.2005.01.011

Mackay JR. 1972. The world of underground ice. *Annals of the Association of American Geographers*, **62**(1): 1–22. https://doi.org/10.1111/j.1467-8306.1972.tb00839.x

Mackay JR. 1980. The origin of hummocks, western Arctic coast, Canada. *Canadian Journal of Earth Sciences*, **17**: 996–1006. https://doi.org/10.1139/e80-100

Mackay JR. 1983. Downward water movement into frozen ground, western arctic coast, Canada. *Canadian Journal of Earth Sciences*, **5**. https://doi.org/10.1139/e83-012

Mackay JR. 1995. Active layer changes (1968 to 1993) following the forest-tundra fire near Inuvik, N.W.T., Canada. *Arctic and Alpine Research*, **27**(4): 323–336. https://doi.org/10.1657/1523-0430(06-026)

Mazerolle M. 2017. AICcmodavg: Model selection and multimodel inference based on (Q)AIC(c). https://cran.r-project.org/package=AICcmodavg

Morse PD, Wolfe SA, Kokelj SV, Gaanderse AJR. 2015. The occurrence and thermal disequilibrium state of permafrost in forest ecotopes of the Great Slave region, Northwest Territories, Canada. *Permafrost and Periglacial Processes*, (June). https://doi.org/10.1002/ppp.1858

Nossov DR, Jorgenson MT, Kielland K, Kanevskiy MZ. 2013. Edaphic and microclimatic controls over permafrost response to fire in interior Alaska. *Environmental Research Letters*, **8**: 035013. https://doi.org/10.1088/1748-9326/8/3/035013

Olthof I, Latifovic R, Pouliot D. 2013. Medium resolution land cover map of Canada from SPOT 4/5 data. In *34th Canadian Symposium on Remote Sensing*. Victoria, BC.

Osterkamp TE, Romanovsky VE. 1999. Evidence for warming and thawing of discontinuous permafrost in Alaska. *Permafrost and Periglacial Processes*, **10**(1): 17–37. https://doi.org/10.1002/(SICI)1099-1530(199901/03)10:1<17::AID-PPP303>3.0.CO;2-4

Osterkamp TE, Viereck LA, Shur YL. 2000. Observations of thermokarst and its impact on boreal forests in Alaska, USA. *Arctic, Antarctic, and Alpine Research*, **32**(3): 303–315. https://doi.org/10.1080/15230430.2000.12003368

Pinheiro J, Bates D, R-core. 2018. nlme: Linear and nonlinear mixed effects models. https://cran.r-project.org/package=nlme

Quinton WL, Hayashi M, Chasmer LE. 2011. Permafrost-thaw-induced land-cover change in the Canadian subarctic: Implications for water resources. *Hydrological Processes*, **25**(May 2010):

152–158. https://doi.org/10.1002/hyp.7894

R Core Team. 2018. R: A language and environment for statistical computing. Vienna, Austria. http://www.R-project.org/

Romanovsky VE, Smith SL, Christiansen HH. 2010. Permafrost thermal state in the polar northern hemisphere during the international polar year 2007-2009: A synthesis. *Permafrost and Periglacial Processes*, **21**(2): 106–116. https://doi.org/10.1002/ppp.689

Seppälä M. 1986. The origin of palsas. *Geografiska Annaler: Series A, Physical Geography*, **68**(3): 141–147. https://doi.org/10.1080/04353676.1986.11880167

Shur YL, Hinkel KM, Nelson FE. 2005. The transient layer: implications for geocryology and climate-change science. *Permafrost and Periglacial Processes*, **16**(1): 5–17. https://doi.org/10.1002/ppp.518

Shur YL, Jorgenson MT. 2007. Patterns of permafrost formation and degradation in relation to climate and ecosystems. *Permafrost and Periglacial Processes*, **19**: 7–19. https://doi.org/10.1002/ppp

Smith DG. 1994. Glacial Lake McConnell: paleogeography, age, duration, and associated river deltas, Mackenzie River basin, western Canada. *Quaternary Science Reviews*, **13**(1987): 829–843. https://doi.org/10.1016/0277-3791(94)90004-3

Smith SL, Riseborough DW, Bonnaventure P. 2015. Eighteen year record of forest fire effects on ground thermal regimes and permafrost in the central Mackenzie Valley, NWT, Canada. *Permafrost and Periglacial Processes*, (May). https://doi.org/10.1002/ppp.1849

Smith SL, Romanovsky VE, Lewkowicz AG, Burn CR, Allard M, Clow GD, Yoshikawa K, Throop J. 2010. Thermal state of permafrost in North America: a contribution to the international polar year. *Permafrost and Periglacial Processes*, **21**(2): 117–135. https://doi.org/10.1002/ppp.690

Tarnocai C, Zoltai SC. 1978. Earth hummocks of the Canadian Arctic and Subarctic. *Arctic and Alpine Research*, **10**(N): 581–594. https://doi.org/10.1080/00040851.1978.12003997

Van Cleve K, Viereck LA. 1981. Forest succession in relation to nutrient cycling in the boreal forest of Alaska. *Forest Succession, Concepts and Application*, 184–211. https://doi.org/10.1007/978-1-4612-5950-3_13

Viereck LA, Dyrness CT, Batten AR. 1992. The Alaska vegetation classification. *USDA General Technial Report*, 142.

Warton D, Duursma R, Falster D, Taskinen S. 2018. smatr: (Standardised) major axis estimation and testing routines. https://cran.r-project.org/package=smatr

Wolfe SA, Duchesne C, Gaanderse AJR, Houben AJ, D'Onofrio RE, Kokelj SV, Stevens CW. 2011. Report on 2010-11 permafrost investigations in the Yellowknife area, Northwest Territories. *Geological Survey Canada*. https://doi.org/10.4095/289596

Wolfe SA, Stevens CE, Gaanderse AJR, Oldenborger GA. 2014. Lithalsa distribution, morphology and landscape associations in the Great Slave Lowland, Northwest Territories, Canada.

*Geomorphology*, **204**: 302–313. https://doi.org/10.1016/j.geomorph.2013.08.014

Wolfe SA, Morse PD, Kokelj S V. 2016. Great Slave Lowland: The legacy of glacial Lake McConnell. *Landscapes and Landforms of Western Canada*, 87. Springer International Publishing, Switzerland.

Wolfe SA, Morse PD. 2017. Lithalsa formation and Holocene lake-level recession, Great Slave Lowland, Northwest Territories. *Permafrost and Periglacial Processes*, **28**(3): 573–579. https://doi.org/10.1002/ppp.1901

Xue X, Guo J, Han B, Sun Q, Liu L. 2009. The effect of climate warming and permafrost thaw on desertification in the Qing-Tibetan Plateau. *Geomorphology*, **108**(3–4): 182–190. https://doi.org/10.1016/j.geomorph.2009.01.004

Zhang Y, Olthof I, Fraser RH, Wolfe SA. 2014. A new approach to mapping permafrost and change incorporating uncertainties in ground conditions and climate projections. *Cryosphere*, **8**: 2177–2194. https://doi.org/10.5194/tc-8-2177-2014

## 2.8 List of Figures
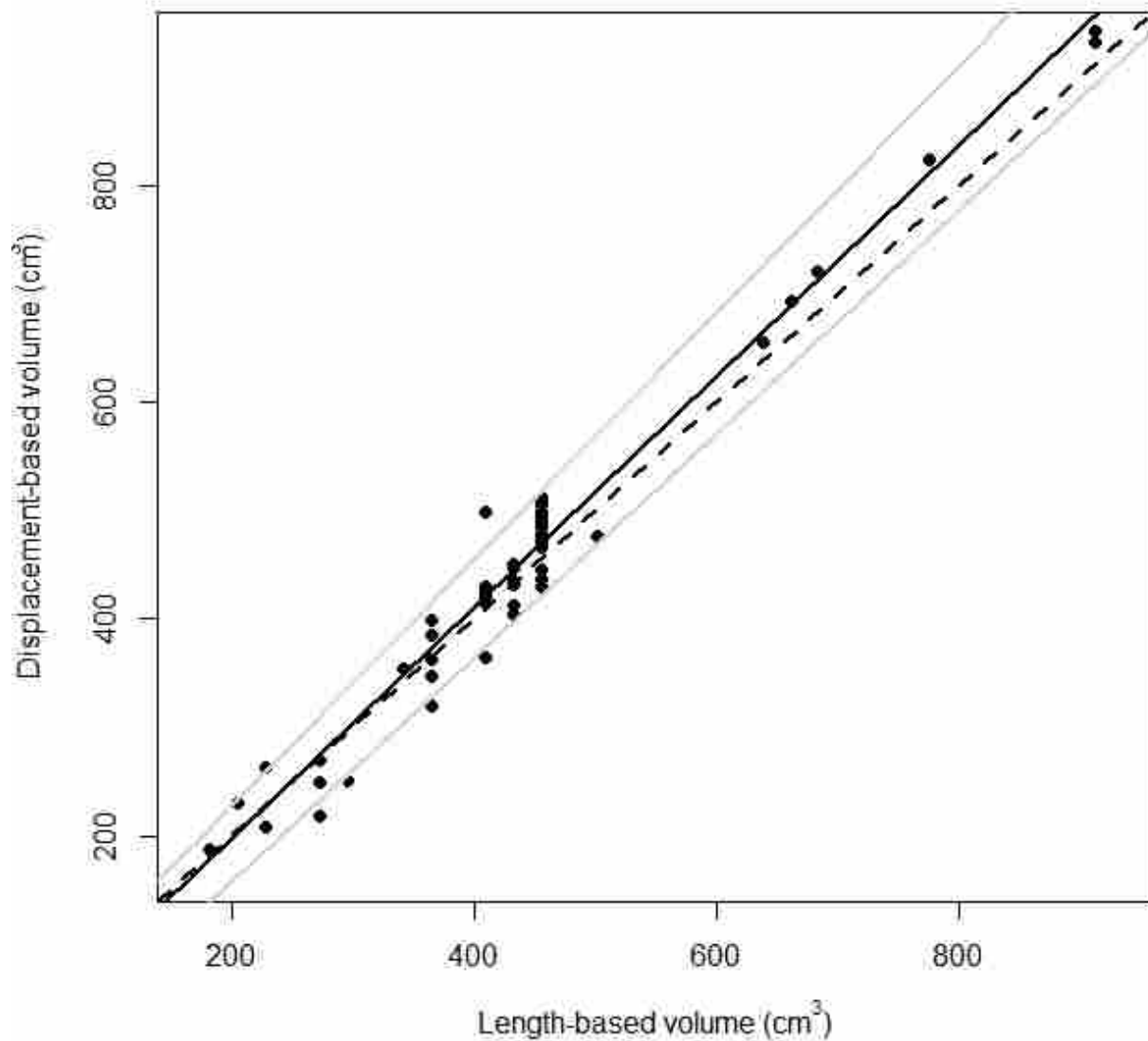


Figure 2.1. Comparing the two methods for determining core sample volume; the water displacement method by the length of the sample volume of a cylinder method for permafrost samples of sites 1 and 2 (n = 58). Solid black line is the model fit (slope = 1.09; intercept = -25.8), and grey lines are the 95% confidence lower limit (slope = 1.04; intercept = -50.0) and upper limit (slope = 1.14; intercept = -1.5). Black dashed line is the line of unity, of slope = 1 and intercept = 0. Data are correlated with $R^2$ = 0.97 and p < 0.001.
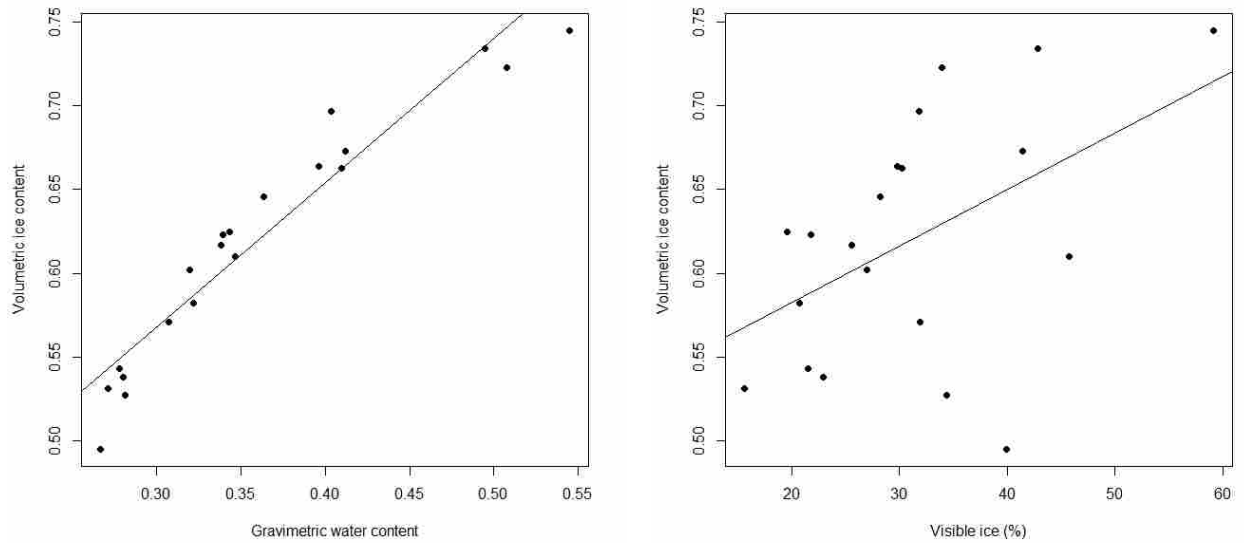
Figure 2.2. Left: Volumetric ice content plotted against gravimetric water content (fraction of water mass to field mass) for near-surface permafrost site averages of all twenty sites. These two estimations of site ice content are correlated with an adjusted $R^2 = 0.91$ (slope = 0.86, t = 14.07, p < 0.001). Right: Volumetric ice content plotted against percent visible ice (determined by manual core sample observation in field) for near-surface permafrost site averages of all twenty sites. These two estimations of ice content are correlated with an adjusted $R^2 = 0.19$ (slope = 0.0034, t = 2.37, p = 0.029).
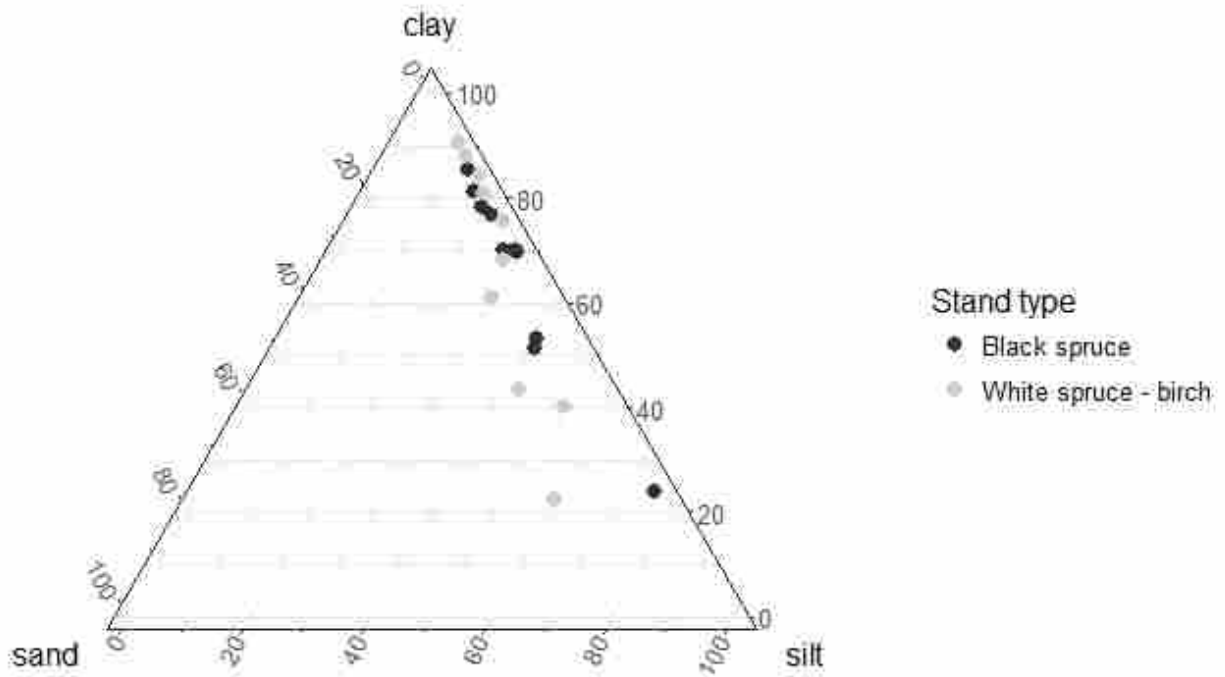
Figure 2.3. Ternary plot of mean sediment grain size at each site for black spruce and white spruce/birch forests. Grain size analyzed at -10, 10, 50, and 90 cm below permafrost table at one borehole per site.
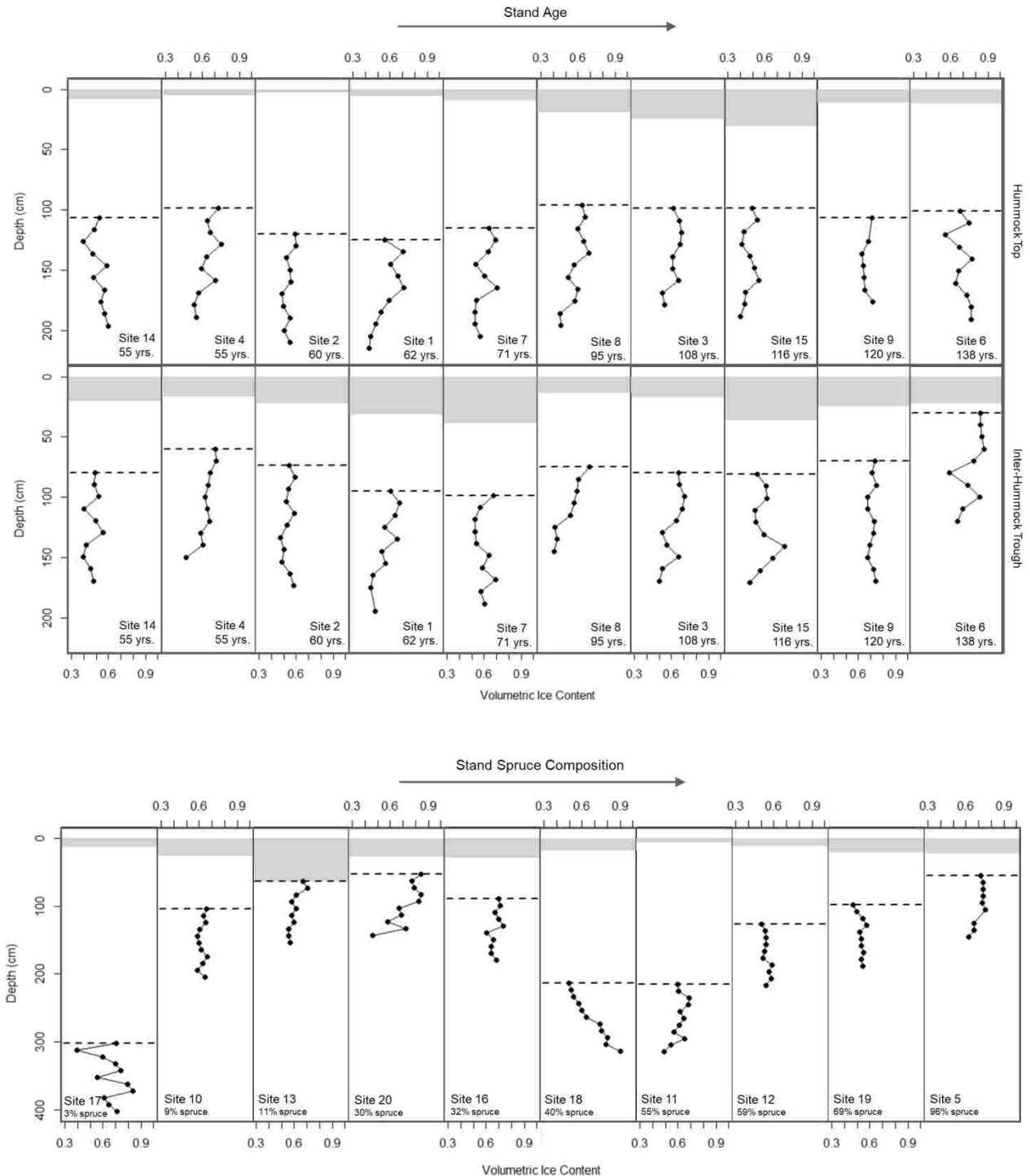
Figure 2.4. Top: Average volumetric ice content of the near-surface permafrost plotted against depth below the ground surface for black spruce sites. Both boreholes from a hummock top (top row) and both boreholes at an inter-hummock trough (bottom row) are plotted for each site. Sites are arranged as an age gradient with younger stands on the left and older stands on the right. For the first 6 points below the dashed line, n = 2, then for the remaining 4 points, n = 1. Bottom: Average volumetric ice content from all boreholes at each site plotted against depth below ground surface

for permafrost core samples of sites in the white spruce forest trajectory. Due to mostly even ages between sites, they are arranged as a gradient with low white spruce/high birch composition on the left and high white spruce/low birch composition on the right. For the first 6 points below the dashed line, n = 3, then for the remaining 4 points, n = 2 (exceptions are sites 5 and 20, where n = 4 for the first 6 points, followed by n = 2 for the remaining 4 points, and sites 17 and 18, where n = 2 for all points). Shaded area shows thickness of organic layer; dashed line represents the top of the permafrost table.
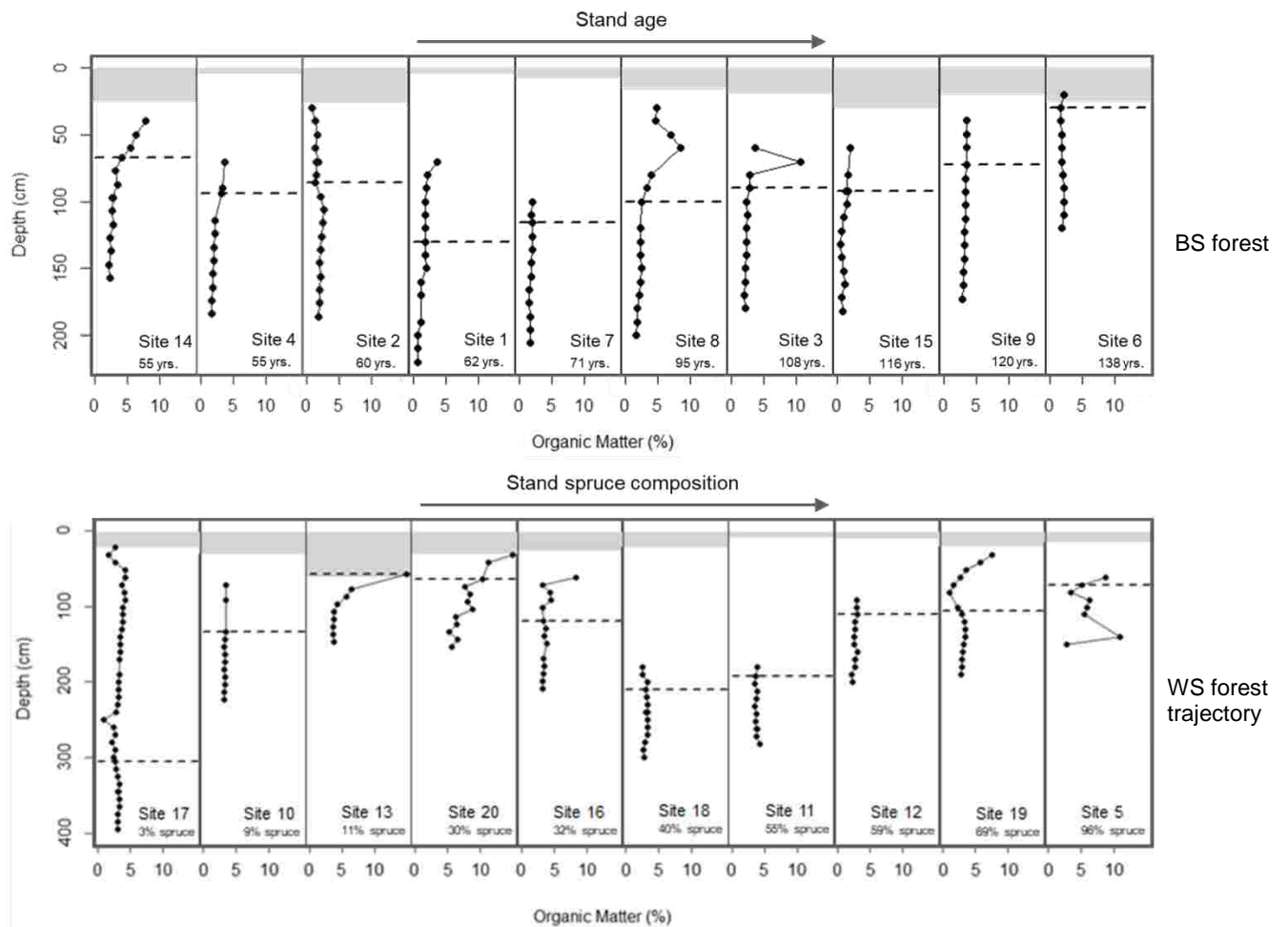
Figure 2.5. Soil organic matter content (% mass of the core sub-sample) plotted against depth below ground surface at each site of black spruce forests (top) and the white spruce forest trajectory (bottom). Black spruce sites are arranged as an age gradient with younger stands on the left and older stands on the right; white spruce/birch sites are arranged by stand composition, with low white spruce/high birch on the left, and high white spruce/low birch on the right. Shaded area shows thickness of organic layer; dashed line represents the top of the permafrost table.
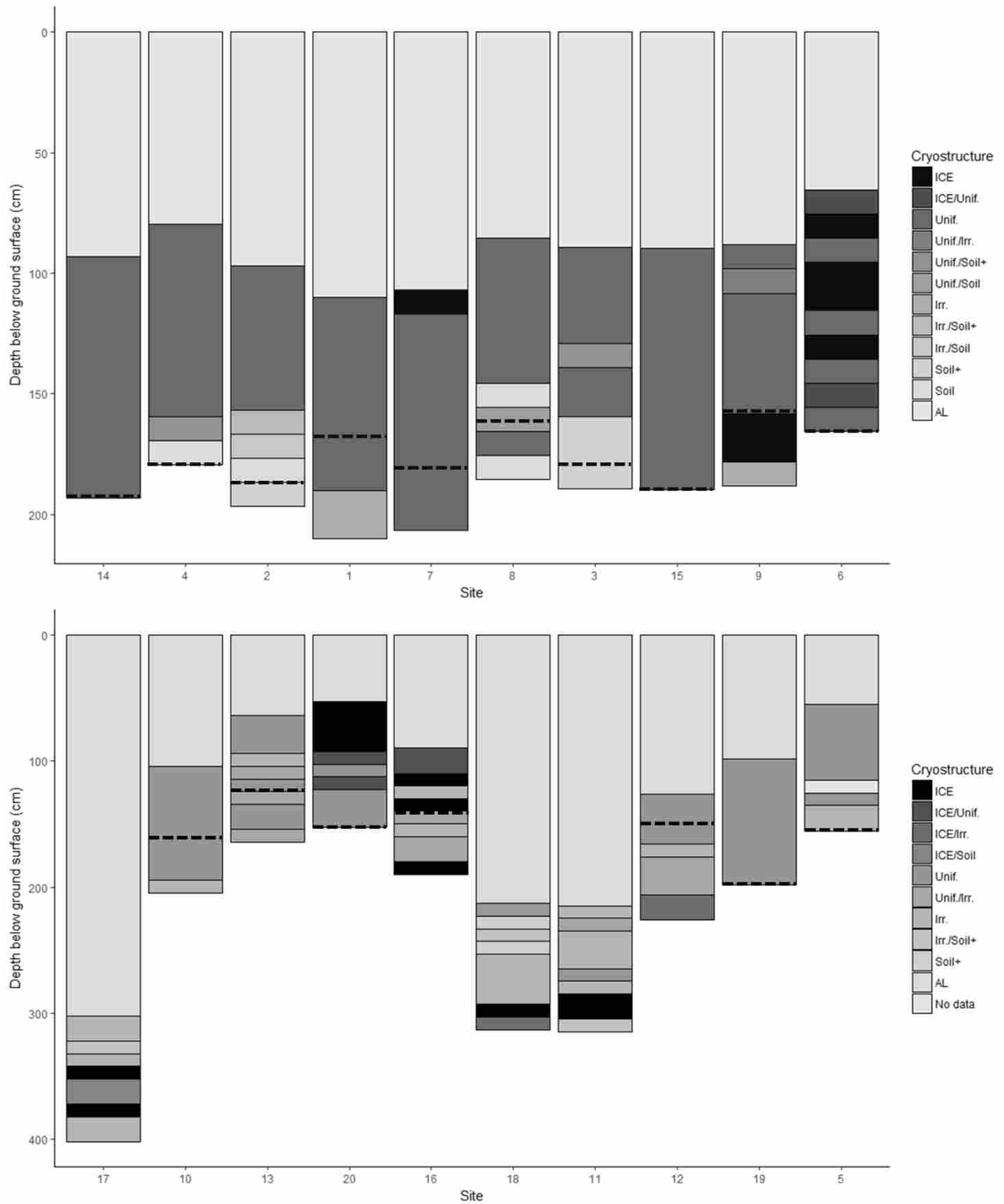
Figure 2.6. Top: The most common cryostructure observed at every 10 cm depth interval for each black spruce site, ordered by increasing stand age. Bottom: The most common cryostructure observed at every 10 cm depth interval for each white spruce/birch site, ordered by increasing composition spruce. Dashed black line indicates the (minimum) average depth of the transient

layer, determined by visual observation according to Shur *et al*. (2015) at each 1 metre borehole at each site. No dashed line indicates that no transient layer was observed in the permafrost of that site. Cryostructures were determined in the field for each core sample by a visual examination of the amount and shape of excess visible ice. Cryostructure codes: ICE = > 50% of the core sample is excess ice, by volume ("ataxitic"); Unif. = uniformly stratified or distinctly oriented ice formations (often lenticular ice lenses); Irr. = random or irregularly oriented ice formations (chaotic ice lenses); Soil+ = low excess ice (< 2%), well-bonded soil; Soil = no excess ice, well-bonded soil; AL = Active layer (only occurs at the top portion of the borehole; its thickness corresponds to the site-average active layer thickness); No data occurred once, as a permafrost sample was not successfully retrieved from the interval 60 – 70 cm below the permafrost table in site 5. Generally, Unif. and ICE codes correspond well to transient layer cryostructures.
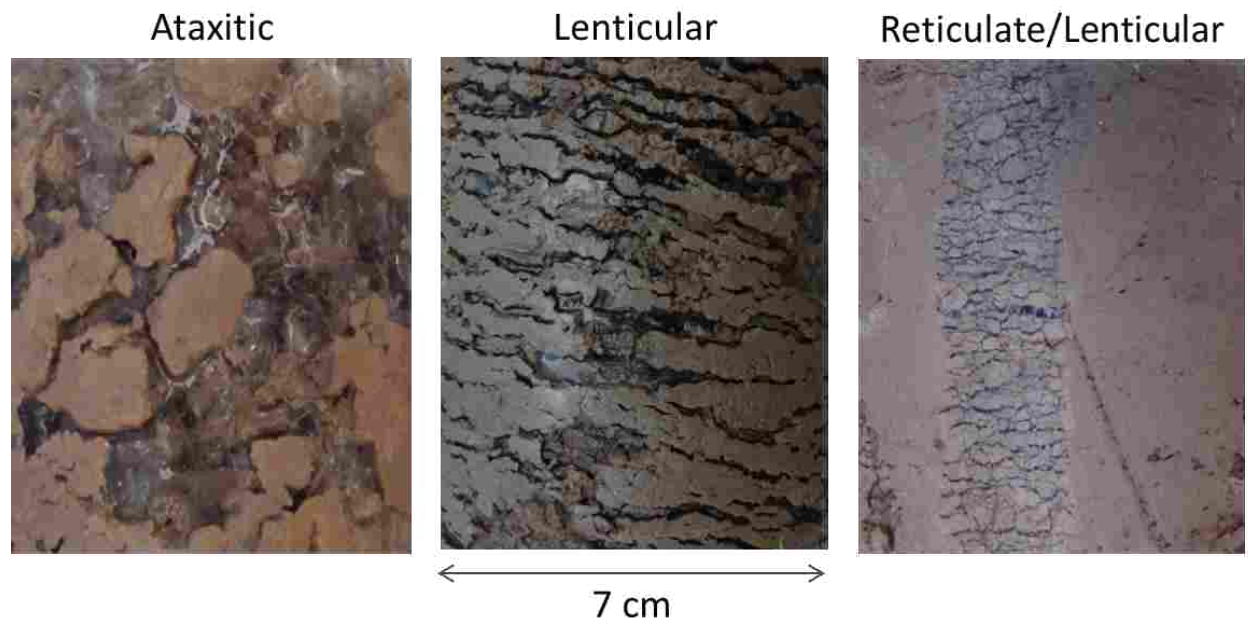
Figure 2.7. Commonly observed permafrost cryostructures. Ataxitic is typically seen at the top of permafrost in ice-rich sites – note it is mostly excess ice with soil inclusions. Lenticular can be observed at any depth in the top metre of permafrost – note the regularly oriented horizontal ice lenses of similar thicknesses. Reticulate is typically only seen in the bottom half of the top metre of permafrost in ice-poor sites – note the regularly oriented thin ice lenses (typically < 1 mm) of both horizontal and vertical direction (in this photo the soil smeared on the surface of the sample was scraped away so the cryostructure may be viewed).
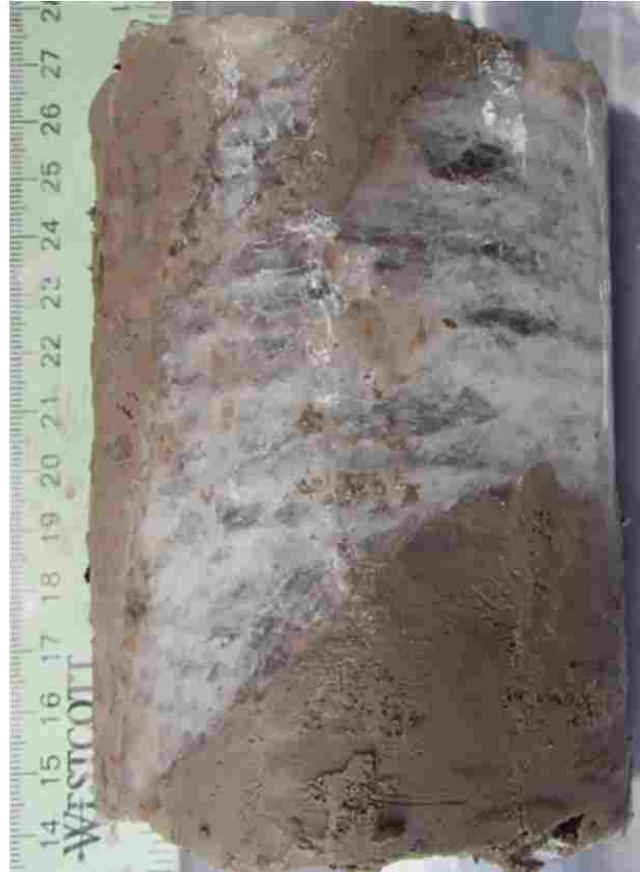
Figure 2.8. Less commonly observed permafrost cryostructures. Chaotic, irregularly-oriented ice lenses (left) may be observed in the permafrost in white spruce/birch stands.  Large, irregular ice lenses of suspected lithalsa origin (right) may be observed in the permafrost under thick active layers in white birch - spruce stands.
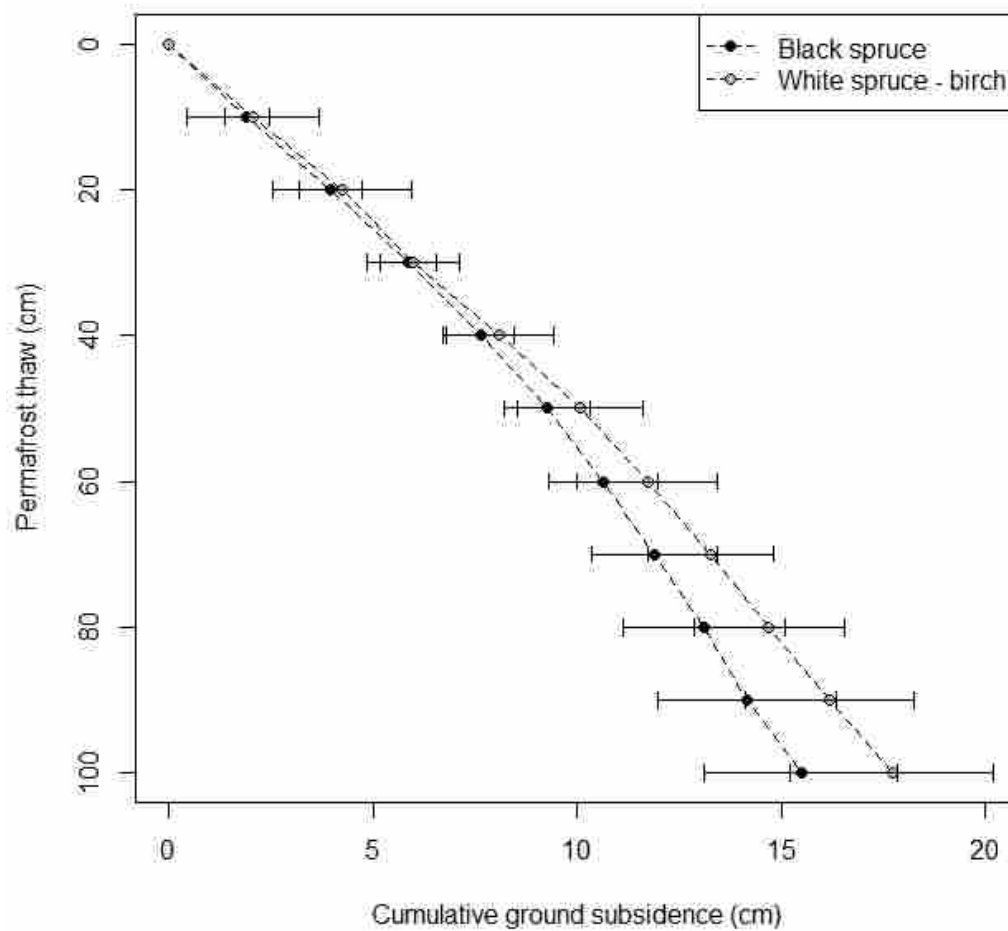
Figure 2.9. Mean cumulative ground subsidence potential calculated from sample thaw strain (Crory, 1973) for all black spruce sites and all white spruce/birch sites plotted against associated permafrost thaw. Error bars represent the standard error of subsidence for samples at each depth into the permafrost.
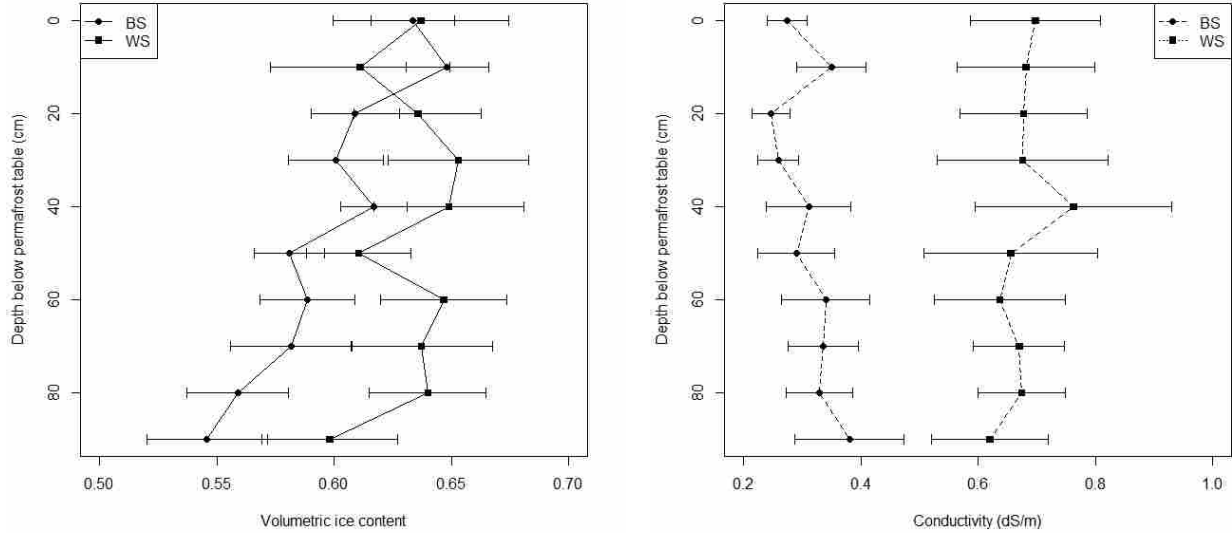
Figure 2.10. Left: Mean site volumetric ice content with standard error for each interval of depth below the permafrost table for each forest type (BS = black spruce; WS = white spruce/birch). Linear mixed effects modeling with the "lme" function of the *nlme* package (Bates et al. 2018) found a significant decrease in ice content with depth below permafrost table in black spruce forests, but no depth effect in white spruce/birch forests (t = 2.92, df = 495, p = 0.004). Right: Mean electrical conductivity with standard error for each interval of depth below the permafrost table for each forest type. Conductivity was significantly higher in white spruce/birch forests (t = 3.90, df = 18, p = 0.001) and significantly increased with depth below permafrost table (t = 2.13, df = 157, p = 0.035), but the interaction term was not significant (t = -1.76, df = 157, p = 0.080).
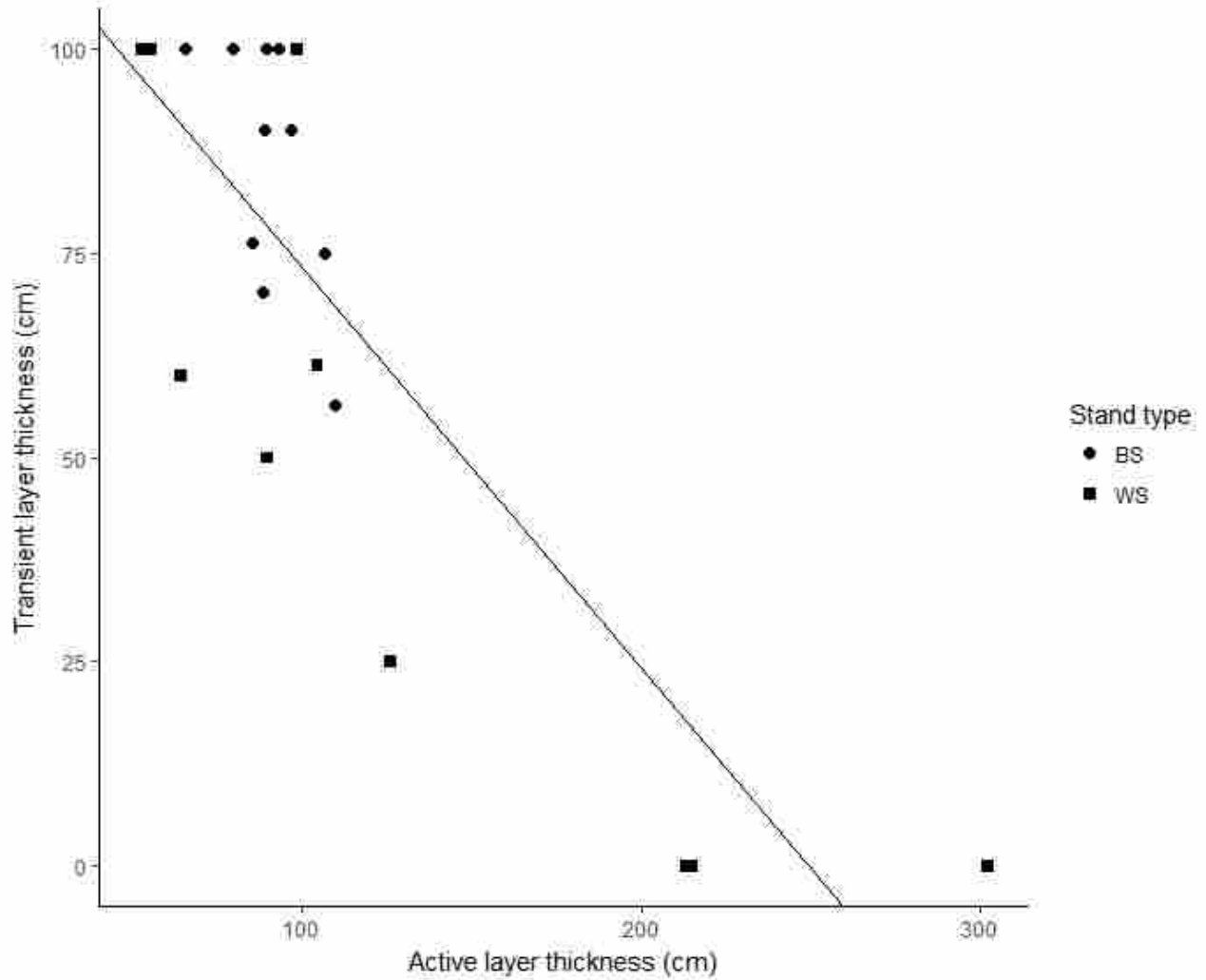
Figure 2.11. Mean transient layer thickness by mean active layer thickness at each site, from both forest types. Transient layer thickness is only measured up to 100 cm (the near-surface permafrost sampled); therefore the actual thickness may be greater. Transient layer thickness and active layer thickness were correlated with a Spearman coefficient of -0.67.

## 2.9 List of Tables

Table 2.1. Site means with standard error and range for both forest types. Two sample t-tests were performed on site means to test for differences in each characteristic between stand types, with the test statistic *t* and p-value given (df = 18) for each characteristic. Organic layer thickness, silt content, soil organic matter, and active layer thickness were log transformed to normality before testing for differences in stand means. Significant p-values at α = 0.05 are in bold.

| | Black spruce | | White spruce | | Comparing means | |
|---|---|---|---|---|---|---|
| | Mean ± SE | Range | Mean ± SE | Range | Test statistic | p-value |
| Volumetric ice content | 0.60 ± 0.02 | 0.50 – 0.73 | 0.64 ± 0.02 | 0.54 – 0.75 | -1.12 | 0.28 |
| Stand age (years) | 88 ± 10 | 55 – 138 | 73 ± 8 | 63 – 145 | 1.20 | 0.25 |
| Spruce composition (%) | 90 ± 3 | 79 – 100 | 40 ± 9 | 3 – 96 | 5.11 | **< 0.001** |
| Organic layer thickness (cm) | 18.7 ± 2.1 | 10.8 – 33.8 | 24.0 ± 4.9 | 6.7 – 63.7 | -0.63 | 0.54 |
| Silt (%) | 31.3 ± 5.7 | 13.5 – 75.1 | 29.0 ± 5.4 | 9.1 – 59.0 | 0.47 | 0.64 |
| Organic matter (%) | 2.1 ± 0.2 | 1.0 – 3.2 | 4.1 ± 0.5 | 2.7 – 7.3 | -3.85 | **0.002** |
| Active layer thickness (cm) | 90 ± 4 | 66 – 110 | 132 ± 26 | 53 – 302 | -1.11 | 0.29 |
| Transient layer thickness (cm) | 86 ± 5 | 56 – 100 | 50 ± 13 | 0 – 100 | 2.56 | **0.026** |

Table 2.2. Linear mixed effects models run with the *lme4* package in R (Bates *et al*., 2017) to test for microtopography (hummock term), core sample depth below permafrost table, and active layer thickness influences on ice content in stands of the black spruce forests. Change in AICc is from lowest AICc model. Model weight and log likelihood calculated using the "aictab" function of the *AICcmodavg* package (Mazerolle, 2017).  Random term is *borehole* nested within *site* (denoted by "R") to account for error at the borehole level and the site level. Lower AICc is a better fit model. Marginal $R^2$ represents the variance explained by fixed factors. Conditional $R^2$ represents the variance explained by both fixed and random factors. Marginal and conditional $R^2$ were calculated using the "r.squaredGLMM" function of the *MuMIn* package (Barton, 2018).

| Model | AICc | ΔAICc | Model weight | Log likelihood | Marg. $R^2$ | Cond. $R^2$ | Variance (*random*) | Variance (*residuals*) |
|---|---|---|---|---|---|---|---|---|
| VIC ~ Sample depth + AL thickness + hummock + R | -649.9 | 0 | 0.42 | 331.1 | 0.14 | 0.52 | 0.0043 | 0.0055 |
| VIC ~ Sample depth + AL thickness + R | -649.5 | 0.5 | 0.33 | 329.8 | 0.11 | 0.52 | 0.0046 | 0.0055 |
| VIC ~ Sample depth * AL thickness + R | -647.6 | 2.4 | 0.13 | 329.9 | 0.11 | 0.52 | 0.0046 | 0.0055 |
| VIC ~ Sample depth + R | -646.6 | 3.3 | 0.08 | 327.4 | 0.06 | 0.52 | 0.0054 | 0.0055 |
| VIC ~ Sample depth + hummock + R | -644.8 | 5.1 | 0.03 | 327.5 | 0.06 | 0.52 | 0.0053 | 0.0055 |
| VIC ~ AL thickness + R | -620.7 | 29.2 | 0.00 | 314.4 | 0.06 | 0.46 | 0.0046 | 0.0061 |
| VIC ~ 1 + R | -618.2 | 31.7 | 0.00 | 312.1 | 0 | 0.47 | 0.0053 | 0.0061 |

Table 2.3. Model averaged variable estimates, standard errors, and 95% confidence limits for black spruce linear mixed effects models on their relationship with volumetric ice content. Data calculated using the "modavg" function of the R package *AICcmodavg* (Mazerolle, 2017). Important variables do not contain zero between the lower and upper confidence limits (bolded). Variables are ordered in descending order of influence on volumetric ice content.

| Variable | Estimate | Standard error | Lower confidence limit | Upper confidence limit |
|---|---|---|---|---|
| Sample depth | -0.025 | 0.004 | **-0.034** | **-0.017** |
| Active layer thickness | -0.025 | 0.012 | **-0.048** | **-0.003** |
| Hummock | -0.048 | 0.036 | -0.118 | 0.022 |
| Sample depth * Active layer thickness | 0.002 | 0.005 | -0.007 | 0.011 |

Table 2.4. Linear mixed effects models run with the *lme4* package in R (Bates *et al.*, 2017) to test for core sample depth below permafrost table and active layer thickness influences on ice content in stands of the white spruce/birch forests. Change in AICc is from lowest AICc model. Model weight and log likelihood were calculated using the "aictab" function of the *AICcmodavg* package (Mazerolle, 2017). The random term is *borehole* nested within *site* (denoted by "R") to account for error at the borehole level and the site level. Lower AICc is a better fit model. Marginal $R^2$ represents the variance explained by fixed factors. Conditional $R^2$ represents the variance explained by both fixed and random factors. Marginal and conditional $R^2$ were calculated using the "r.squaredGLMM" function of the *MuMIn* package (Barton, 2018).

| Model | AICc | ΔAICc | Model weight | Log likelihood | Marg. $R^2$ | Cond. $R^2$ | Variance (random) | Variance (residuals) |
|---|---|---|---|---|---|---|---|---|
| VIC ~ Sample depth * AL thickness + R | -444.5 | 0 | 1.00 | 228.4 | 0.10 | 0.47 | 0.0053 | 0.0078 |
| VIC ~ 1 + R | -416.2 | 28.3 | 0.00 | 211.2 | 0 | 0.41 | 0.0061 | 0.0089 |
| VIC ~ AL thickness + R | -415.7 | 28.9 | 0.00 | 211.9 | 0.02 | 0.41 | 0.0058 | 0.0089 |
| VIC ~ Sample depth + R | -414.8 | 29.7 | 0.00 | 211.5 | <0.01 | 0.41 | 0.0061 | 0.0089 |
| VIC ~ AL thickness + Sample depth + R | -414.2 | 30.4 | 0.00 | 212.2 | 0.03 | 0.41 | 0.0058 | 0.0089 |

Table 2.5. Model averaged variable estimates, standard errors, and 95% confidence limits for white spruce/birch linear mixed effects models on their relationship with volumetric ice content. Data calculated using the "modavg" function of the R package *AICcmodavg* (Mazerolle, 2017). Important variables do not contain zero between the lower and upper confidence limits (bolded). Variables are ordered in descending order of influence on volumetric ice content.

| Variable | Estimate | Standard error | Lower confidence limit | Upper confidence limit |
|---|---|---|---|---|
| Sample depth | -0.005 | 0.006 | -0.017 | 0.007 |
| Active layer thickness | -0.019 | 0.016 | -0.050 | -0.011 |
| Sample depth * Active layer thickness | 0.033 | 0.006 | **0.022** | **0.044** |

# Chapter 3: Soil properties, not forest characteristics, drive transient layer permafrost ice content in fine-grained mineral soil, discontinuous permafrost

## 3.1 Abstract

Rapid high latitude climate warming is expected to drive increases in the rates of permafrost thaw. The ice-rich upper portion of permafrost that thaws and re-aggrades on multi-decadal to centennial timescales, known as the transient layer, will be the first to thaw, with implications to ecosystems and infrastructure. The role of vegetation is an important driver of the development of an ice-rich transient layer in general, but little is known of the important drivers within a particular landscape type. Here I investigate the importance of forest characteristics and soil properties on transient layer ice content in the North Slave region near Yellowknife, NWT. In addition, I investigate the influence of active layer thickness and transient layer ice content on ground cover and the ground vegetation composition. Sites were sampled from fine-grained sediments of black spruce and white spruce/birch forests – the dominant landscape type underlain by permafrost in the area. I took permafrost core samples from multiple boreholes per site and performed vegetation surveys at each site for ten sites from each forest type. These data were used to investigate drivers of ice content and ground vegetation. Soil properties (sediment grain size and soil organic matter content) were found to be the most important predictors of transient layer ice content. Ground cover and ground vegetation community composition were found to separate clearly by forest type, but were not affected by active layer thickness or transient layer ice content – an effect seen by other studies. This suggests that the important

drivers of transient layer ice content from a larger landscape view do not necessarily reflect the important drivers within one landscape type. These findings indicate that within well-drained, fine-grained mineral soil forests, areas of ice-rich permafrost may be difficult to predict using land cover and surficial site surveys without the addition of high resolution soil maps. Stand age may be useful for predicting ice content; however, the disconnect between stand age and the time since the transient layer last thawed may reduce the accuracy of these predictions. This research extends our understanding of the transient layer in this region, and information on soil properties can aid in identifying ice-rich terrain for infrastructure planning purposes or predicting ecosystem response to thaw.

## 3.2 Introduction

Climate warming is causing many environmental changes, particularly in northern regions, where warming is occurring at more than twice the mean global rate (ACIA, 2005; IPCC, 2013). Under a global mean air temperature rise of 2 °C above pre-industrial levels, equilibrium permafrost distribution is predicted to be reduced by over 40% of its current areal extent (Chadburn *et al.*, 2017). Indeed, as a result of warming ground temperatures, there have been observations of a northward shift of discontinuous permafrost (Kwong and Gan, 1994; Burn, 1998a; French and Egorov, 1998; James et al., 2013). Reduction in the areal extent of permafrost can be associated with decreased forest cover and productivity (Baltzer *et al.*, 2014; Sniderhan and Baltzer, 2016; Sniderhan *et al.*, in review), and changes in soil moisture attributable to permafrost thaw can result in compositional shifts of forest ecosystems (Schuur *et al.*, 2007; Myers-Smith *et al.*, 2008; Osterkamp *et al.*, 2009). Future changes to northern environments can be better predicted by understanding permafrost conditions, the foundation of many northern forests.

In addition to climate warming-induced thaw, disturbances that alter surface vegetation and soil properties that modify the ground thermal regime also cause permafrost thaw. In the years following such disturbances, vegetation re-establishes and contributes to ground temperature cooling and active layer thinning; during this period, the permafrost table begins to recover and aggrade upward (Burn, 1998b; Yoshikawa *et al.*, 2002; Nossov *et al.*, 2013; Brown *et al.*, 2015). This uppermost portion of the permafrost that aggrades and degrades on multi-decadal to centennial timescales (usually as a result of climatic variations or forest fire) is referred to as the "transient layer" (Shur *et al.*, 2005). The transient layer can become ice-rich as it draws water from the active layer and traps ice lenses in the aggrading permafrost. The volume

of excess ice in the transient layer dictates the amount of subsidence following disturbance, and the associated potential for landscape change (Burn, 1998b; Osterkamp *et al*., 2000; Jorgenson *et al*., 2001; Nelson *et al*., 2002). Thawing of ice-rich permafrost causes ground subsidence and can produce thermokarst terrain (Mackay, 1972), which can alter vegetation composition and structure (Schuur *et al*., 2007; Myers-Smith *et al*., 2008; Osterkamp *et al*., 2009), surface and subsurface hydrology (Xue *et al*., 2009; Quinton *et al*., 2011), energy balance (Williams, 1995), and land surface-atmosphere interactions (Hinkel *et al*., 2001). Ground subsidence is a concern for infrastructure built on ice-rich permafrost, as it can damage buildings and roads, leading to costly maintenance (Osterkamp *et al*., 1998). The transient layer plays a critical role in the stability of permafrost terrain (Shur *et al*., 2005). Most northern development involves removal of forest cover, so understanding relationships between forest cover and transient layer conditions can assist in mapping ground ice conditions for predicting ecosystem change following permafrost thaw, and for planning infrastructure development.

Biological and physical characteristics of the forest act as controls on the thermal and hydrological regimes of the ground (Morse *et al*., 2015) (Figure 3.1). Generally, characteristics that reduce thermal input (i.e., cause active layer thinning) and increase late summer soil moisture will lead to ice enrichment of the permafrost transient layer. For example, soil organic matter is porous and promotes infiltration of water from the surface towards the permafrost table (Van Cleve and Viereck, 1981; Osterkamp and Romanovsky, 1999; Johnstone *et al*., 2010). Fine-grained sediments are considered "frost susceptible" because the small pore spaces allow for a fraction of the water to remain in a liquid film around particles in warm permafrost (e.g., > -3 °C) that can result in high pore pressures during freezing, permitting water to migrate from the warmer active layer to the permafrost in late summer and aggrade ice lenses (Williams and

Smith, 1991). Canopy cover reduces insolation and modifies evapotranspirative water loss from soils in summer (Gill, 1971; Smith, 1975; Oke, 1997). The low thermal conductivity of the organic layer insulates the ground from warm summer temperatures, thus organic layer thickness is considered to be an important driver of the development of the active layer (Brown, 1965; Gill, 1971; Smith, 1975; Osterkamp *et al*., 2000). In turn, ground conditions can also affect surface vegetation through alterations to the water table. As the active layer thins, the water table rises, increasing rooting zone soil moisture through reduced drainage and decreasing rooting zone temperatures, which favours the growth of species adapted to these wet, cold conditions (Kane, 1997). An ice-rich transient layer is also more likely to occur where soil moisture is higher (Morse *et al*., 2015) and active layer has thinned due to ecological change (Gill, 1973, 1975; Smith, 1975; Pearce *et al*., 1988; Kokelj and Burn, 2003); therefore, ice content may correspond with the overlying vegetation community (Kokelj and Burn, 2005). These drivers of transient layer ice content are important controls when examined across different landscape types where a large range of these characteristics are observed (e.g., little to no organic layer in jack pine forests to metres-deep organic layer in peatlands). However, it is not known whether these drivers apply within an individual landscape type (e.g., well-drained fine-grained mineral soil forests) in the region of discontinuous permafrost near Yellowknife, Northwest Territories (NWT).

Here I aim to quantitatively evaluate the relative influence of drivers of transient layer ice content in permafrost-affected mineral soils of black spruce and white spruce/birch forests in the North Slave region near Yellowknife, NWT, located in the discontinuous permafrost zone. In addition, I examine the ground vegetation community in these forests to assess if a relationship exists between active layer thickness or transient layer ice content and the community

composition. I predict that the main controls of transient layer ice content will be consistent with the hypothesized important controls on permafrost ice content at the broader landscape scale (Figure 3.1). Hypothesis-based candidate models were created to assess the importance of different sets of predictor variables (ecological, thermal, soil properties, and disturbance history) on transient layer ice content. I also examined the role of active layer thickness and transient layer volumetric ice content on ground vegetation community composition, where shallower permafrost with higher ice content is expected to favour species adapted to cold, moist soil conditions. Understanding the links between the biological and physical components of these rapidly changing permafrost environments will allow us to anticipate future changes to land cover as climate warming drives thaw of ground ice. This data could also support the development of predictions of ground ice distribution based on land cover characteristics that can be readily mapped.

## 3.3 Methods

### 3.3.1 Study area

In the North Slave region near Yellowknife, permafrost underlies much of forested terrain, but is absent from bedrock outcrops and bodies of water (Brown, 1973; Zhang *et al*., 2014). In this region of the extensive discontinuous permafrost zone (Heginbottom *et al*., 1995) (Appendix Figure A.1), permafrost is thin and warm (Brown, 1973; Hoeve *et al*., 2004; Morse *et al*., 2015). Rapidly warming air temperatures in the Yellowknife area (IPCC, 2013) provide the potential for substantial thaw of permafrost in this region. Fine-grained sediments deposited by glacial Lake McConnell during the retreat of the Laurentide Ice Sheet provide the substrate for much of the boreal forest in this region (Smith, 1994). The study region is in the western Taiga

Shield in the High Boreal ecoregion, a heterogeneous landscape where dense to open black spruce and jack pine forests are widespread, and white spruce and white birch are present in warmer, well-drained areas (Downing *et al*., 2008) (Appendix Figure A.2).

Black spruce (*Picea mariana* (Miller) Britton, Sterns & Poggenburgh) forests make up over 37% of the Boreal Ecoclimatic Province near Yellowknife (Wolfe *et al*., 2011; Olthof *et al*., 2013). Black spruce can grow on well-drained gravels to poorly-drained, fine sediments (Viereck *et al*., 1992), with the majority of stands occurring on the latter in the Yellowknife area (Wolfe *et al*., 2011). Hummocky terrain is common in these stands, and active layers can range in thickness from 30 cm to over 100 cm (Viereck *et al*., 1992; Wolfe *et al*., 2011; Morse *et al*., 2015). Permafrost thickness can exceed 50 m in mature black spruce forests (Morse *et al*., 2015). Black spruce produces semi-serotinous cones that open through exposure to high temperatures that removes their resinous coating, resulting in black spruce seed rain on freshly burned seed bed. This typically results in stand self-replacement (Van Wagner, 1983). Common tall understory shrubs include *Rosa acicularis*, *Salix* spp., *Rhododendron groenlandicum*, and *Betula glandulosa*, and low shrubs include *Vaccinium uliginosum*, V. *vitis-idaea*, and *Linnaea borealis*. The moss layer may be continuous or patchy, and dominated by a thick layer of feather (*Hylocomium* sp.) or peat (*Sphagnum* sp.) moss depending on site drainage. Foliose lichens including *Cladina* and *Peltigera* are common on drier surfaces such as on the tops and sides of hummocks. Older stands tend to have a thicker moss layer, fewer shrubs, and a well-developed canopy (Viereck *et al*., 1992).

White birch (*Betula papyrifera* Marshall and *B. neoalaskana* Sargen) and mixed white birch - white spruce (*Picea glauca* (Moench) Voss) stands generally develop on lithalsas (mounds upraised due to ice growth in the permafrost up to 8 m high and hundreds of metres wide) in this

region, with no hummocky terrain, and have active layers usually thinner than 1 m, but can be up to 2 m (Wolfe *et al*., 2011; Morse *et al*., 2015). These forests often occur in coarser grained, better drained soils than black spruce forests, and following fire regenerate either as white birch or white birch and white spruce mixed stands – the outcome depends on seed availability and pre-fire forest composition that may lead to white birch re-sprouting. In general, white birch are relatively fast growing, and when they die out the canopy is replaced by a larger proportion of the slow growing, long-lived white spruce. Mature canopies may be entirely composed of white spruce. The understorey of a white birch dominated forest is composed of white spruce trees and a *Rosa acicularis* and *Viburnum edule* shrub layer, an herb layer of *Calamagrostis canadensis* and *Equisetum* spp., and few mosses or lichens due to the leaf litter input from the birch canopy. As the canopy progress towards a white spruce forest, leaf litter input slows, and *Alnus* spp., *Salix* spp., *Vaccinium* spp., *Rhododendron groenlandicum*, and *Empetrum nigrum* become more common in the shrub layer, and a moss layer of *Hylocomium splendens* may develop (Viereck *et al*., 1992).

*3.3.2 Study design*

Twenty study sites were selected within a 30 km radius of Yellowknife spanning a range of black spruce and white spruce forests (Appendix Figure A.1; Appendix Table A.1) to examine biophysical influences on transient layer ice content. Ten sites were chosen for both forest types and locations were constrained by access and site availability. However, only seven white spruce/birch sites were used in this study because three sites had no transient layer present. To account for potential confounding factors, sites were selected to be well-drained with little to no slope, fine-grained mineral soil, and uniform forest composition. Dominant tree species, tree size, organic layer thickness, understorey development, and microtopography were characterized

before site selection to ensure a gradient of forest developmental stages were included. Being

near a major population centre, it was not possible to include sites at an early stage of forest

development (all sites had a stand age ≥ 55 years) due to rapid forest fire suppression.

### 3.3.3 Permafrost sampling and analysis

Core samples were obtained from 3 – 4 boreholes per site, up to a depth of 100 cm below

the permafrost table. Upon retrieval of each core sample, length was measured to determine

volume, a picture was taken, visual soil and ice characteristics were described (Appendix Figure

A.6), and then the sample was sealed in a plastic bag. Core samples were determined to be from

the transient layer based on observation of uniform, lenticular segregated ice lenses as described

by Shur *et al*. (2005). The transient layer thickness was only estimated from the boreholes that

were cored to 100 cm below the permafrost table. In a laboratory setting, core samples were

analyzed for volumetric ice content, sediment grain size, and organic carbon content. Refer to

sections 2.3.3 and 2.3.4 for complete details of permafrost core sampling and analysis.

### 3.3.4 Forest structure methodology

Many aboveground components of a forest can alter the thermal or hydrological regime of

the ground to some degree. Therefore, a range of measurements were employed to characterize

the forest structure at each site. A National Forest Inventory (NFI)-style standard large tree plot

was established in each site to assess forest structure and composition (Figure 3.2). Specifically,

the diameter at breast height (DBH; 1.3 m) and species identity for all living and dead

individuals larger than 5.0 cm DBH was determined within a 400 m$^2$ circular plot. Within the

plot, basal cores were extracted from the five largest trees of the dominant species to determine

the maximum stand age. Tree cores were sanded with progressively finer grit (up to 800 grit)

until rings were clearly visible, scanned, and the rings were counted using CooRecorder 7.6 software (Cybis Elektronik & Data AB, Saltsjöbaden, Sweden).  The average of the number of rings per tree at each site was taken to get an estimate of stand age.

Ground plots (1 m$^2$ each) were set up adjacent to each borehole location to assess the shrub layer, ground cover, and the organic layer. In the shrub layer, stem counts, percent cover, and species of all woody plants (only identified to genus where different species co-existed with highly similar appearance) were determined with a visual survey at 50, 100, and 150 cm heights above the forest floor to provide information about ground vegetation vertical structure. Ground cover was assessed by estimating percent cover of bryophyte, lichen, graminoid, forb, litter, downed wood, and bare ground groups, and the dominant species of bryophytes, lichens, graminoids, and forbs were recorded. The thickness of the organic layer (litter, moss, lichen, peat, and decaying matter) was measured in each ground plot by cutting through the ground surface vertically, then recording the depth to mineral soil with a tape measure. As a measure of shading at each site, canopy cover was estimated using a densiometer centred above each ground plot, as well as at the north, east, south, west edges of the circular plot and plot centre (Figure 3.2).

### 3.3.5 Statistical analysis

All statistical tests on the data were performed using R software (version 3.4.4, R Core Team, 2018). To represent forest canopy structure, a principal components analysis (PCA) was calculated with the "prcomp" function using standardized values of site basal area, canopy cover, stem density, and proportion standing deadwood. This analysis creates new scores (principal components) determined by which canopy structure variables explain most amount of variation among the sites. Principal component 1 explained 56.7% of canopy structure variance and was

primarily driven by canopy cover, basal area, and stem density. Principal component 2 explained

16.7% of canopy structure variance and was primarily driven by the proportion of standing

deadwood. Linear mixed models were created using the *lme4* package (Bates *et al*., 2017) to

assess the influence of biophysical factors on transient layer ice content at each site in the near-

surface permafrost for both black spruce and white spruce/birch forest types. Forest types were

modeled together as there was no significant difference in transient layer ice content between the

two forest types (Chapter 2). Candidate models were created based on our hypotheses of

potential drivers to evaluate forest and soil characteristics that are most important in predicting

transient layer volumetric ice content (Table 3.1). Due to the nested nature of our sampling

(multiple boreholes per site), site was included as a random term in each model. Model 1 was

based on forest structure and included borehole-level organic layer thickness and the first two

components of the site-level canopy PCA as predictor variables. Model 2 was based on soil

properties and included site-level soil organic matter content of the permafrost and site-level

proportion silt (i.e., sediment grain size). Organic matter is the average of each 10 cm depth

interval below the permafrost table from one 1 m borehole per site and sediment grain size is the

average sediment grain size at the -10 cm, 10 cm, 40 cm, and 60 cm intervals below the

permafrost table at the same 1 m borehole per site. Model 3 was based on the disturbance cycle,

and included the site-level stand age variable (i.e., time since disturbance). Model 4 was based

on factors that influence the ground thermal regime and active layer thickness: borehole-level

organic layer thickness and site-level canopy structure principal component 1 (i.e., canopy

cover). Model 5 was the full model and included all predictor variables. Model 6 was the null

model that excluded fixed effects but retained the random term. All predictor variables were

standardized by centering and scaling then checked for collinearity using a Pearson's correlation

with a tolerance of 0.5. The model with the lowest corrected Akaike information criterion (AICc) best explains the variation in volumetric ice content, taking into account the number of parameters in the model. The AICc values were calculated using the "AICc" function of the *AICcmodavg* package (Mazerolle, 2017). Model-averaged variable estimates were calculated using "modavgShrink" from *AICcmodavg* to determine which terms were important predictors of volumetric ice content, which takes into account the prevalence of each term in the hypothetical models to reduce model selection bias (Table 3.2).

To investigate the relationship of ground cover with transient layer ice content and active layer thickness, a principal co-ordinates analysis (PCoA) was performed. A dissimilarity matrix was created from the quadrat-level (3-4 quadrats per site; adjacent to boreholes) ground cover measurements of understorey vascular plant species, bryophyte, lichen, graminoid, forb, litter, downed wood, and bare ground using the "vegdist" function of the *vegan* package (Oksanen *et al*., 2018) with the Bray-Curtis method. This matrix was then used with the "cmdscale" function to perform the PCoA. The Canberra dissimilarity matrix method produced a more uniform distribution in the analysis but explained far less of the variation of ground cover. In addition, the minor clumping observed from the Bray-Curtis method (Figure 3.3) is likely explained by the similar nature of the understorey of our white spruce/birch sites rather than an artefact of the analysis. A similar principal co-ordinates analysis was run to investigate the relationship of ground vegetation community composition with transient layer ice content and active layer thickness, with only live vegetation ground cover (e.g., vascular plant species, bryophyte, lichen, graminoid, and forb cover; excluding litter, downed wood, bare ground, and dead standing vascular plants) using the Gower method in the dissimilarity matrix. For both ground cover and ground vegetation community composition analyses, the principal co-ordinate axes were

correlated with the cover values to examine the drivers of the principal co-ordinates. A PermANOVA was performed on the ground cover and ground vegetation dissimilarity matrices using the "adonis2" function of the *vegan* package (Oksanen *et al*., 2018) with 999 permutations to test if volumetric ice content of the transient layer permafrost or the active layer thickness influenced the ground cover or ground vegetation community.

## 3.4 Results

### 3.4.1 Modeled drivers of transient layer ice content

The general rule in comparing candidate linear mixed effects models is the lowest AICc model is the best model, and the model with the fewest terms is a better model if it is within 2 AICc of the lowest AICc model. However, any model within 10 AICc of the lowest may be considered to have value (Burnham and Anderson, 2004). In our candidate model results, the highest ΔAICc is only 8.6, and the top three candidate models are within 2.8 AICc of each other. This indicates that our models are all somewhat similar in predicting transient layer volumetric ice content (Burnham and Anderson, 2002; Anderson, 2007), due to much of the variance being explained by the random terms (Table 3.1B). Nevertheless, transient layer volumetric ice content from black spruce and white spruce/birch forests was best explained by the full model (Model 5). This model had a high weight, indicating that when compared with the other candidate models it explains more variation in volumetric ice content than any other model, taking into account the number of parameters in the model (Table 3.1A). Variance in transient layer volumetric ice content was well characterized by our predictor variables (marginal $R^2 = 0.55$), and within-site variance was low (Table 3.1B), which supports that the full model had good predictive power. However, candidate model 2 (soil properties) was within 2 AICc of model 5, with four fewer

parameters, and is therefore also a good model (Table 3.1A). Model 2 included soil organic matter content and proportion of silt. As such, the two selected candidate models are the two models that include soil characteristics. These soil variables were also some of the strongest individual predictors of volumetric ice content in the averaged model (Table 3.2). Soil characteristics alone explained 28% of the variance of volumetric ice content in this model; however, in this model much greater variance was attributed to the random effects (Table 3.1B). Hypothetical model 3 (disturbance cycle), comprised of solely stand age as a proxy for time-since-disturbance, was only 2.8 AICc higher than the full model (Table 3.1A). Stand age (the fixed effect) was the third best predictor of volumetric ice content (Table 3.2). Stand age explained 15% of volumetric ice content variance, and the within-site random effect had high variance relative to variance of the residuals (Table 3.1B).

*3.4.2 Examining ground cover and ground vegetation*

When examining ground cover in black spruce and white spruce/birch forests, the Bray-Curtis dissimilarity matrix produced a PCoA with white spruce/birch quadrats separating nearly completely from black spruce quadrats on principal component 1 (Figure 3.3). Moderate grouping of white spruce/birch quadrats is likely observed due to the similar, litter-dominated nature of this forest type. Indeed, when examining the relative influence of each cover class on the PCoA scores, litter cover is strongly positively associated with this grouping. Lichen cover, *Vaccinium vitis-idaea*, *Rhododendron groenlandicum*, and understorey *Picea mariana* are strongly positively associated with quadrats from a range of black spruce sties. The first axis explained 43.17% of ground cover variation and the second axis explained 17.12%.

The PCoA for only ground vegetation cover, produced from a Gower method dissimilarity matrix, also clearly separates by forest type on the first axis with many of the white

spruce/birch quadrats clumping together (Figure 3.4). With litter no longer in this analysis, this quadrat clumping is positively associated with low shrubs *Rosa acicularis*, *Arctostaphylos uva-ursi*, *Viburnum edule*, and understorey *Picea glauca*, *Populus tremuloides*, and *Alnus* sp. Bryophyte cover was a strong driver of variation in ground vegetation on the second axis of the PCoA, and was strongly positively associated with some black spruce quadrats. *Vaccinium vitis-idaea*, lichen, and understorey *Picea mariana* were strong drivers of variation in ground vegetation along the first axis of the PCoA, and it was positively associated with some black spruce quadrats. The first axis explained 24.71% of ground vegetation variation and the second axis explained 13.36%.

The PermANOVA on all ground cover scores found no influence of transient layer volumetric ice content (F = 0.33, p = 0.60) or active layer thickness (F = 1.18, p = 0.16) on ground cover. The white spruce/birch grouping showed a mixture of thin to thick active layers, and low to high ice content (Figure 3.3). The black spruce quadrats associated with lichen cover, *Vaccinium vitis-idaea*, *Rhododendron groenlandicum* tend to have moderate ice content and thin to moderately thick active layers. Similar active layer and ice content trends were observed in quadrats associated with high bryophyte cover.

The PermANOVA on ground vegetation scores found no influence of transient layer volumetric ice content (F = 0.81, p = 0.29) or active layer thickness (F = 1.20, p = 0.37) on community composition. No apparent trends in active layer thickness or transient layer volumetric ice content gradients were visibly discerned from the PCoA (Figure 3.4).

## 3.5 Discussion

In this study, the importance of various biotic and abiotic controls on transient layer ice content was determined. In addition, the relationship of active layer thickness and ice content to ground vegetation community composition was investigated. Factors that greatly impact ground thermal and hydrological regimes, such as organic layer thickness and topography, are thought to be the most important controls in the general landscape view of transient layer ice enrichment (Zoltai and Tarnocai, 1974; Jorgenson *et al*., 2001; Shur *et al*., 2005). In the single landscape type of well-drained mineral soil black spruce and white spruce/birch forests, which represents approximately 50% of land cover in the area (Olthof *et al*., 2013; Morse *et al*., 2015), soil properties were more important controls on transient layer volumetric ice content than forest characteristics (Table 3.1A). Finer-grained sediments and higher soil organic matter contents in the permafrost were associated with higher transient layer volumetric ice content (Table 3.2). In the larger landscape scale, active layer thickness and consequently near-surface ice content is known to affect vegetation community composition by altering soil moisture of the active layer (Brown, 1965; Gill, 1973, 1975; Pearce *et al*., 1988; Walker and Walker, 1996; Kokelj and Burn, 2003). While ground cover and ground vegetation community composition was found to separate clearly by forest type, active layer thickness and transient layer volumetric ice content were not related to ground cover or ground vegetation communities in our one landscape type (Figure 3.3 and 3.4). This suggests that community composition differences within a specific land cover type cannot distinguish spatial variation in transient layer ice conditions. These results will impact ice content estimations for infrastructure planning purposes and strengthen our understanding of ecosystem responses to thaw in this landscape type of well-drained fine-grained mineral soil forests.

In our candidate models, marginal $R^2$ (variance explained by fixed effects) rapidly decreases over a relatively small AICc increase (Table 3.1AB), showing that there are large differences in the predictive power of the modeled drivers of transient layer ice content (Figure 3.5). The measured biophysical controls that most affect transient layer ice content in mineral soil black spruce and white spruce/birch forests were soil organic matter content of the permafrost and sediment grain size (Table 2; Figure 3.6). If cryoturbation, which results in redistribution of the deep active layer (former permafrost) soil is limited, these are two factors that are likely to remain unchanged following a surface disturbance such as a forest fire (Bockheim and Tarnocai, 1998; Nowinski *et al.*, 2010). Therefore, these soil properties may be instrumental in how the transient layer permafrost re-aggrades following a disturbance within this landscape type, which is characterized by low soil organic matter content (1.0 - 7.3%) and frost susceptible soils (clays and silts; silt content = 11.8 – 75.1 %). The marginal $R^2$ value of 0.28 of the soil properties candidate model indicates that these two controls are important drivers, but not sufficient to predict transient layer ice content with high accuracy. Stand age was the third best driver of transient layer volumetric ice content, suggesting that more time for ice growth leads to richer ice content in the transient layer. Stand age may be weakly tied to ice content (Figure 3.6) due to the site history of these fire-suppressed and harvested forests, and could have a stronger relationship in sites where fires burn naturally; if there is a stand-replacing fire in fire-suppressed forests, the understorey and organic layer may remain unchanged, thereby insulating the ground and preventing thaw.

Although other controls of transient layer ice content seem to be important from the perspective of broader topo-edaphic gradients (Shur and Jorgenson, 1998; Shur *et al.*, 2005), forest structure and organic layer thickness were not important predictors of ice content in our study

(Table 3.2). Forest structure and organic layer thickness may instead be correlated with other controls of permafrost ice content. For example, thick organic layers develop in peatlands due in part to the surficial water table, which slows down decomposition rates, causing organics to accumulate (Zoltai *et al*., 1988). The very high soil moisture present in these areas is then available for permafrost aggradation and associated ice accumulation. In the same way as the organic layer, forest structure often reflects the soil moisture conditions (e.g., permafrost in open peatlands likely does not have high ice content as a result of the forest structure, but rather as a result of the associated moisture conditions with this forest type). This study was constrained to a single landscape type in the discontinuous permafrost zone, in which controls of ice content may be different than between other landscape types (Morse *et al*., 2015). Additionally, this study did not cover very young (< 55 years) or very old stands (> 145 years), and therefore does not capture the full range of conditions these sites experience following disturbance.

The investigation into ground cover found that litter cover was the strongest driver of white spruce/birch sites, along principal component 1 (Figure 3.3). Leaf senescence from birch canopy was likely high enough to contribute to the lack of other ground vegetation cover observed in these sites (Figure 3.4) by reducing substrate availability (Granström, 1982), and shading bryophytes and lichen (Van Cleve and Viereck, 1981). Ground vegetation in black spruce forests was mainly driven by *V. vitis-idaea*, *R. groenlandicum*, and *P. mariana* cover along principal component 1, and bryophyte cover along principal component 2. However, although a thinner active layer was expected to be related to a shift to a high soil moisture community composition (Walker and Walker, 1996), ground cover and the ground vegetation community were not related to either active layer thickness or transient layer volumetric ice content. This may be due to an insufficient gradient of soil type and topography among the sites

studied that is necessary to create a significant change in ground vegetation community in response to active layer thickness – this then affects water table depth and permafrost ice content, which is related to soil moisture. Furthermore, the lack of young ($<$ 55 years) and very old ($>$ 145 years) sites studied neglect any relationship in community composition that may be present in early or late forest development. If our study sites were expanded to include more landscapes of varying topography, for example, it could be expected to observe a significant relationship between active layer thickness and ground vegetation community (Walker and Walker, 1996).

Our results highlight the central role of physical processes in the aggradation of transient layer ice content. Physical processes may be overriding the importance of ecological factors observed in other landscapes – in part due to warming temperatures and lower precipitation experienced in recent years (Figure 3.7). This is in contrast to other studies that have shown that the development of vegetation cover is associated with an ice-rich transient layer; vegetation protects the permafrost from warm temperatures and allows for the transport of soil moisture from the warm active layer downwards to the cold permafrost during the end of summer through a temperature-driven pressure gradient (Cheng, 1983; Mackay, 1995; Burn, 1998b; Shur *et al*., 2005). However, with warming air temperatures, the rate of permafrost aggradation may be slowing despite the development of vegetation, thus delaying the development of thinner active layers that allow for easier infiltration of soil moisture to the top of permafrost. In addition, lower precipitation at the end of summer, when permafrost can aggrade ice from the active layer, may result in the lack of moisture present for movement into the permafrost (Shur *et al*., 2005). Soil organic matter content may therefore be the best predictor of transient layer volumetric ice content in our study due to its high hydraulic conductivity and its associated role in facilitating water infiltration to the top of permafrost (Lado *et al*., 2004). However, if there is a lack of soil

moisture in the active layer, warm permafrost in this region may be subject to desiccation because there is no available late summer moisture to contribute to near-surface ice accumulation. This occurs in conjunction with the evolution of warm near-surface permafrost temperatures during the long winter season (Kokelj and Burn, 2005; Morse *et al*., 2015) – the period when the temperature-driven pressure gradient draws unfrozen water from the near-surface permafrost into the unsaturated active layer (Cheng, 1983; Burn, 1998b). If low precipitation trends continue, warm, fine-grained permafrost could gradually lose transient layer ice content through the upward movement of unfrozen water. Further studies are recommended to observe if this effect is currently taking place in this region.

## 3.6 Conclusions

The results of this study suggest that it would be difficult to use land cover or surficial site surveys to predict transient layer volumetric ice content within these forests. Stand age could be useful in this respect, but there are weaknesses to this approach – stand age may not always be reflective of ice content due to human activity in this area. In the well-drained, fine-grained mineral soils of this landscape, the importance of soil properties (generally unaffected by forest disturbances) in influencing transient layer ice content means that following a disturbance, the transient layer will aggrade ice similar to its post-fire conditions (assuming no changes in topography, climate, or forest regeneration). Our results show that the important drivers of transient layer ice content in a larger landscape view (e.g., organic layer thickness) presented in other studies do not necessarily translate to comparable gradients within a single topo-edaphic site type, and that the differences of ice content within one type are instead driven by a subset of the main controls of ice content. Moreover, ground vegetation community separated clearly by forest type, but was not affected by active layer thickness or transient layer ice content, which

has also been observed under the scope of a larger gradient of landscape types. Physical processes overriding ecological factors in this landscape may also be indicative of permafrost losing transient layer ice content as the climate warms and fall precipitation decreases. These data define the range of conditions with fine-grained mineral soil forest cover types in the discontinuous permafrost zone. Further research should consider quantitatively constraining for active layer soil moisture and investigate the important drivers of ice content in other landscapes.

## 3.7 References

ACIA. 2005. Arctic climate impact assessment. *Cambridge University Press*, Cambridge, UK.

Anderson DR. 2007. Model based inference in the life sciences: A primer on evidence. Springer New York.

Baltzer JL, Veness T, Chasmer LE, Sniderhan AE, Quinton WL. 2014. Forests on thawing permafrost: Fragmentation, edge effects, and net forest loss. *Global Change Biology*, **20**(3): 824–834. https://doi.org/10.1111/gcb.12349

Barton K. 2018. MuMIn: Multi-model inference. https://cran.r-project.org/package=MuMIn

Bates D, Maechler M, Bolker B, Walker S. 2017. lme4: Linear mixed-effects models using "eigen" and S4. https://cran.r-project.org/package=lme4

Bockheim JG, Tarnocai C. 1998. Recognition of cryoturbation for classifying permafrost-affected soils. *Geoderma*, **81**(3–4): 281–293. https://doi.org/10.1016/S0016-7061(97)00115-8

Brown DRN, Jorgenson MT, Douglas TA, Romanovsky VE, Kielland K, Hiemstra C, Euskirchen ES, Ruess RW. 2015. Interactive effects of wildfire and climate on permafrost degradation in Alaskan lowland forests. *Journal of Geophysical Research: Biogeosciences*, **120**: 1619–1637. https://doi.org/10.1002/2015JG003033

Brown RJE. 1965. Some observations on the influence of climatic and terrain features on permafrost at Norman Wells, N.W.T., Canada. *Canadian Journal of Earth Sciences*, **2**: 15–31. https://doi.org/10.1139/e65-003

Brown RJE. 1973. Influence of climatic and terrain factors on ground temperatures at three locations in the permafrost region of Canada. In *Proceedings of the Second International Conference on Permafrost* (pp. 27–34). Yakutsk, USSR: National Academy of Science, Washington, DC.

Burn CR. 1998a. Field investigations of permafrost and climatic change in northwest North America. In *Proceedings of the Seventh International Conference on Permafrost* (pp. 107–120).

Burn CR. 1998b. The response (1958-1997) of permafrost and near-surface ground temperatures to forest fire, Takhini River valley, southern Yukon Territory. *Canadian Journal of Earth Sciences*, **35**(2): 184–199. https://doi.org/10.1139/e97-105

Burnham KP, Anderson DR. 2002. Model selection and multimodel inference. A practical information-theoretic approach (2nd edn). *Springer-Verlag*, New York.

Burnham KP, Anderson DR. 2004. Multimodel inference: Understanding AIC and BIC in model selection. *Sociological Methods & Research*, **33**(2): 261–304. https://doi.org/10.1177/0049124104268644

Chadburn SE, Burke EJ, Cox PM, Friedlingstein P, Hugelius G, Westermann S. 2017. An observation-based constraint on permafrost loss as a function of global warming. *Nature*

*Climate Change*, **7**(5): 340–344. https://doi.org/10.1038/nclimate3262

Cheng G. 1983. The mechanism of repeated-segregation for the formation of thick layered ground ice. *Cold Regions Science and Technology*, **8**(1): 57–66. https://doi.org/10.1016/0165-232X(83)90017-4

Downing D, Decker R, Oosenbrug B, Tarnocai C, Chowns T, Feschuk L. 2008. Ecological regions of the Northwest Territories: Taiga Shield.

Environment Canada. 2018. Online climate data. Retrieved May 17, 2018, from http://climate.weather.gc.ca/

French HM, Egorov IE. 1998. 20th century variations in the southern limit of permafrost near Thompson, Northern Manitoba, Canada. *Permafrost - Seventh International Conference (Proceedings)*, (55): 297–304.

Gill D. 1971. Vegetation and environment in the Mackenzie River Delta, Northwest Territories. *Department of Geography, University of British Columbia*, 694.

Gill D. 1973. Ecological modifications caused by the removal of tree and shrub canopies in the Mackenzie Delta. *Arctic*, **26**(2): 95–111. https://doi.org/10.14430/arctic2904

Gill D. 1975. Influence of white spruce trees on permafrost-table microtopography, Mackenzie River Delta. *Canadian Journal of Earth Sciences*, **12**(2): 263–272. https://doi.org/10.1139/e75-023

Granström A. 1982. Seed banks in five boreal forest stands originating between 1810 and 1963. *Canadian Journal of Botany*, **60**(1974): 1815–1821. https://doi.org/10.1139/b82-228

Heginbottom JA, Dubreuil MA, Harker PA. 1995. Canada-permafrost, National Atlas of Canada, National Atlas Information Service. Natural Resources Canada.

Hinkel KM, Paetzold F, Nelson FE, Bockheim JG. 2001. Patterns of soil temperature and moisture in the active layer and upper permafrost at Barrow, Alaska: 1993-1999. *Global and Planetary Change*, **29**(3–4): 293–309. https://doi.org/10.1016/S0921-8181(01)00096-0

Hoeve TE, Seto JTC, Hayley D. 2004. Permafrost response following reconstruction of the Yellowknife Highway. In *International Conference on Cold Regions Engineering*. Edmonton, AB.

IPCC. 2013. Climate change 2013: The physical sciences basis. *University Press, Cambridge New York*.

James M, Lewkowicz AG, Smith SL, Miceli CM. 2013. Multi-decadal degradation and persistence of permafrost in the Alaska Highway corridor, northwest Canada. *Environmental Research Letters*, **8**. https://doi.org/10.1088/1748-9326/8/4/045013

Johnstone JF, Chapin III FS, Hollingsworth TN, Mack MC, Romanovsky VE, Turetsky MR. 2010. Fire, climate change, and forest resilience in interior Alaska. *Canadian Journal of Forest Research*, **40**(7): 1302–1312. https://doi.org/10.1139/X10-061

Jorgenson MT, Racine CH, Walters JC, Osterkamp TE. 2001. Permafrost degradation and ecological changes associated with a warming climate in central Alaska. *Climatic Change*,

**48**: 551–579. https://doi.org/10.1023/A:1005667424292

Kane DL. 1997. The impact of hydrologic perturbations on arctic ecosystems induced by climate change. In *Global Change and Arctic Terrestrial Ecosystems* (pp. 63–81). New York, NY: Springer New York. https://doi.org/10.1007/978-1-4612-2240-8_4

Kokelj SV, Burn CR. 2003. Ground ice and soluble cations in near-surface permafrost, Inuvik, Northwest Territories, Canada. *Permafrost and Periglacial Processes*, **14**(3): 275–289. https://doi.org/10.1002/ppp.458

Kokelj SV, Burn CR. 2005. Near-surface ground ice in sediments of the Mackenzie Delta, Northwest Territories, Canada. *Permafrost and Periglacial Processes*, **16**(3): 291–303. https://doi.org/10.1002/ppp.537

Kwong Y, Gan T. 1994. Northward migration of permafrost along the Mackenzie Highway and climatic warming. *Climatic Change*, **26**: 399–419. https://doi.org/10.1007/bf01094404

Lado M, Paz A, Ben-Hur M. 2004. Organic matter and aggregate-size interactions in saturated hydraulic conductivity. *Soil Science Society of America Journal*, **68**(1): 234. https://doi.org/10.2136/sssaj2004.2340

Mackay JR. 1972. The world of underground ice. *Annals of the Association of American Geographers*, **62**(1): 1–22. https://doi.org/10.1111/j.1467-8306.1972.tb00839.x

Mackay JR. 1995. Active layer changes (1968 to 1993) following the forest-tundra fire near Inuvik, N.W.T., Canada. *Arctic and Alpine Research*, **27**(4): 323–336. https://doi.org/10.1657/1523-0430(06-026)

Mazerolle M. 2017. AICcmodavg: Model selection and multimodel inference based on (Q)AIC(c). https://cran.r-project.org/package=AICcmodavg

Morse PD, Wolfe SA, Kokelj SV, Gaanderse AJR. 2015. The occurrence and thermal disequilibrium state of permafrost in forest ecotopes of the Great Slave Region, Northwest Territories, Canada. *Permafrost and Periglacial Processes*, (June). https://doi.org/10.1002/ppp.1858

Myers-Smith IH, Harden JW, Wilmking M, Fuller CC, McGuire AA, Chapin III FS. 2008. Wetland succession in a permafrost collapse: Interactions between fire and thermokarst. *Biogeosciences*, **5**(5): 1273–1286. https://doi.org/10.5194/bg-5-1273-2008

Nelson FE, Anisimov OA, Shiklomanov NI. 2002. Climate change and hazard zonation in the circum-Arctic permafrost regions. *Natural Hazards*, **26**: 203–225. https://doi.org/10.1023/A:1015612918401

Nossov DR, Jorgenson MT, Kielland K, Kanevskiy MZ. 2013. Edaphic and microclimatic controls over permafrost response to fire in interior Alaska. *Environmental Research Letters*, **8**: 035013. https://doi.org/10.1088/1748-9326/8/3/035013

Nowinski NS, Taneva L, Trumbore SE, Welker JM. 2010. Decomposition of old organic matter as a result of deeper active layers in a snow depth manipulation experiment. *Oecologia*, **4**(163): 785–792. https://doi.org/10.1007/s00442-009-1556-x

Oke TR. 1997. Surface climate processes. In *The surface climates of Canada* (pp. 21–43). *McGill-Queen's University Press*, Montreal & Kingston, Canada.

Oksanen J, Blanchet FG, Friendly M, Kindt R, Legendre P, McGlinn D, Minchin PR, O'Hara RB et al. 2018. vegan: Community ecology package. https://cran.r-project.org/package=vegan

Olthof I, Latifovic R, Pouliot D. 2013. Medium resolution land cover map of Canada from SPOT 4/5 data. In *34th Canadian Symposium on Remote Sensing*. Victoria, BC.

Osterkamp TE, Esch DC, Romanovsky VE. 1998. Permafrost. In *Implications of Global Change in Alaska and the Bering Sea Region* (pp. 115–127). Center for Global Change and Arctic System Research, University of Alaska.

Osterkamp TE, Jorgenson MT, Schuur EAG, Shur YL, Kanevskiy MZ, Vogel JG. 2009. Physical and ecological changes associated with warming permafrost and thermokarst in interior Alaska. *Permafrost and Periglacial Processes*, **256**: 235–256. https://doi.org/10.1002/ppp

Osterkamp TE, Romanovsky VE. 1999. Evidence for warming and thawing of discontinuous permafrost in Alaska. *Permafrost and Periglacial Processes*, **10**(1): 17–37. https://doi.org/10.1002/(SICI)1099-1530(199901/03)10:1<17::AID-PPP303>3.0.CO;2-4

Osterkamp TE, Viereck LA, Shur YL. 2000. Observations of thermokarst and its impact on boreal forests in Alaska, USA. *Arctic, Antarctic, and Alpine Research*, **32**(3): 303–315. https://doi.org/10.1080/15230430.2000.12003368

Pearce C, Mclennan D, Cordes L. 1988. The evolution and maintenance of white spruce woodlands on the Mackenzie Delta, NWT, Canada. *Holarctic Ecology*, **11**(4): 248–258. https://doi.org/10.1111/j.1600-0587.1988.tb00807.x

Quinton WL, Hayashi M, Chasmer LE. 2011. Permafrost-thaw-induced land-cover change in the Canadian subarctic: Implications for water resources. *Hydrological Processes*, **25**(May 2010): 152–158. https://doi.org/10.1002/hyp.7894

R Core Team. 2018. R: A language and environment for statistical computing. Vienna, Austria. http://www.R-project.org/

Schuur EAG, Crummer KG, Vogel JG, Mack MC. 2007. Plant species composition and productivity following permafrost thaw and thermokarst in Alaskan tundra. *Ecosystems*, 280–292. https://doi.org/10.1007/s10021-007-9024-0

Shur YL, Hinkel KM, Nelson FE. 2005. The transient layer: implications for geocryology and climate-change science. *Permafrost and Periglacial Processes*, **16**(1): 5–17. https://doi.org/10.1002/ppp.518

Shur YL, Jorgenson MT. 1998. Cryostructure development on the floodplain of the Colville River Delta, Northern Alaska. In *Proceedings of the Seventh International Conference on Permafrost* (pp. 993–999).

Smith DG. 1994. Glacial Lake McConnell: paleogeography, age, duration, and associated river deltas, Mackenzie River basin, western Canada. *Quaternary Science Reviews*, **13**(1987): 829–843. https://doi.org/10.1016/0277-3791(94)90004-3

Smith MW. 1975. Microclimatic influences on ground temperatures and permafrost distribution, Mackenzie Delta, Northwest Territories. *Canadian Journal of Earth Sciences*, **12**(8): 1421–1438. https://doi.org/10.1139/e75-129

Sniderhan AE, Baltzer JL. 2016. Growth dynamics of black spruce (*Picea mariana*) in a rapidly thawing discontinuous permafrost peatland. *Journal of Geophysical Research: Biogeosciences*, **121**(12): 2988–3000. https://doi.org/10.1002/2016JG003528

Sniderhan AE, Mamet SD, Baltzer JL. In review. Treeline to treeline: non-uniform growth dynamics of a dominant boreal tree species in the face of rapid climate change. Submitted to *Environmental Research Letters*.

Van Cleve K, Viereck LA. 1981. Forest succession in relation to nutrient cycling in the boreal forest of Alaska. *Forest Succession, Concepts and Application*, 184–211. https://doi.org/10.1007/978-1-4612-5950-3_13

Van Wagner CE. 1983. Fire behaviour in northern conifer forests and shrublands. In *The role of fire in northern circumpolar ecosystems* (pp. 65–80). *John Wiley & Sons*, Chichester, UK.

Viereck LA, Dyrness CT, Batten AR. 1992. The Alaska vegetation classification. *USDA General Technial Report*, 142.

Walker DA, Walker MD. 1996. Terrain and vegetation of the imnavait creek watershed. *Landscape function and disturbance in Arctic tundra. Ecological Studies (Analysis and Synthesis)*, **120** (pp. 73–108). https://doi.org/10.1007/978-3-662-01145-4_4

Wickham H, Chang W. 2016. ggplot2: Create elegant data visualisations using the grammar of graphics. https://cran.r-project.org/package=ggplot2

Williams PJ. 1995. Permafrost and climate change: Geotechnical implications. *Philosophical Transactions: Physical Sciences and Engineering*, **352**(1699): 347–358. https://doi.org/10.1098/rsta.1995.0075

Williams PJ, Smith MW. 1991. The frozen earth fundamentals of geocryology. *Cambridge University Press*, New York.

Wolfe SA, Duchesne C, Gaanderse AJR, Houben AJ, D'Onofrio RE, Kokelj SV, Stevens CW. 2011. Report on 2010-11 permafrost investigations in the Yellowknife area, Northwest Territories. *Geological Survey Canada*. https://doi.org/10.4095/289596

Xue X, Guo J, Han B, Sun Q, Liu L. 2009. The effect of climate warming and permafrost thaw on desertification in the Qing-Tibetan Plateau. *Geomorphology*, **108**(3–4): 182–190. https://doi.org/10.1016/j.geomorph.2009.01.004

Yoshikawa K, Bolton WR, Romanovsky VE, Fukuda M, Hinzman LD. 2002. Impacts of wildfire on the permafrost in the boreal forests of Interior Alaska. *Journal of Geophysical Research*, **108**(D1): 8148. https://doi.org/10.1029/2001JD000438

Zhang Y, Olthof I, Fraser RH, Wolfe SA. 2014. A new approach to mapping permafrost and change incorporating uncertainties in ground conditions and climate projections. *Cryosphere*, **8**: 2177–2194. https://doi.org/10.5194/tc-8-2177-2014

Zoltai SC, Tarnocai C. 1974. Soil and vegetation of hummocky terrain. *Information Canada*.

Zoltai SC, Taylor S, Jeglum JK, Mills GF, Johnson JD, others. 1988. Wetlands of boreal Canada. In *Wetlands of Canada by National Wetlands Working Group, Canada Committee on Ecological Classification* (pp. 97–154). Polyscience Publications Inc., Montreal, Canada.

## 3.8 List of Figures
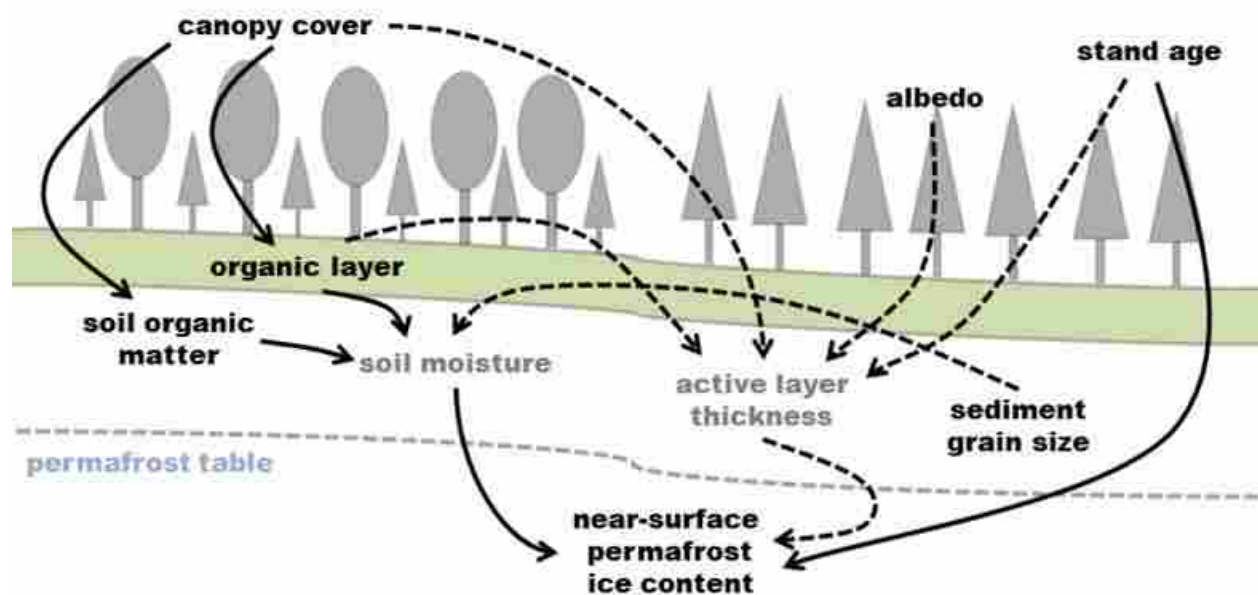


Figure 3.1. Proposed important biotic and abiotic drivers of near-surface ice content in this study. Solid line arrows indicate a positive relationship between the terms, and dashed line arrows are negative relationships. Any control that acts to increase soil moisture will increase the water available for ice growth in the near-surface permafrost. Any control that acts to thicken the active layer will make it more difficult for water to reach the bottom of the active layer and get drawn into the permafrost for ice growth via a thermally-driven pressure gradient. Soil moisture and active layer thickness are grey because they are not included in the models.
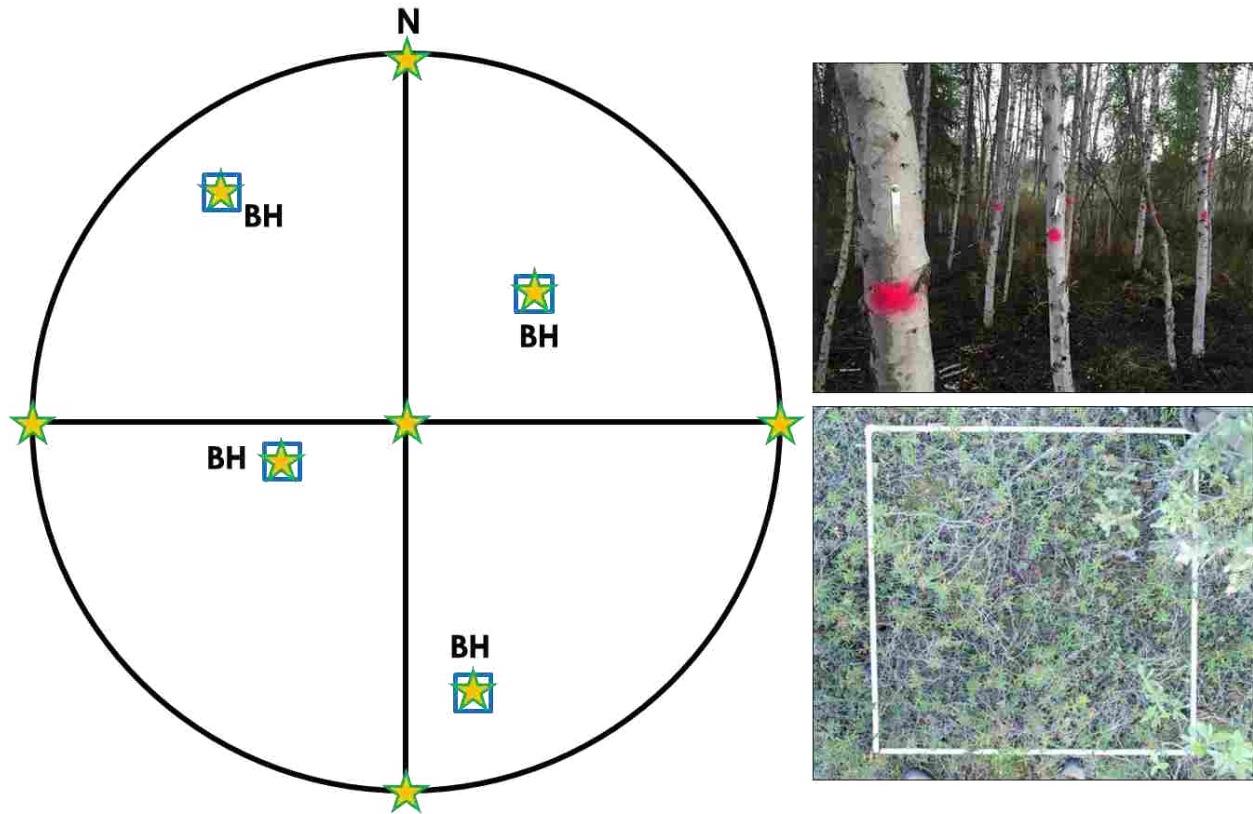
Figure 3.2. Left: A circular National Forest Inventory-style large tree plot (400 m$^2$). All trees ≥ 5.0 cm diameter at breast height (DBH) were identified to species level and their DBH was recorded. BH indicates possible locations of boreholes at the site, with ground plots (blue squares) set up adjacent to the borehole. Yellow stars mark the locations of canopy cover measurements. Top right: Mixed white spruce/birch forest site after trees in the NFI plot were measured and recorded. Bottom right: 1 m$^2$ ground plot in an inter-hummock trough at black spruce forest site. Shrub layer is dominated by Labrador tea (*Rhododendron groenlandicum*), and ground cover is a mixture of moss (*Dicranum* sp. And *Hylocomium* sp.), lichen (*Peltigera* sp.), and litter.
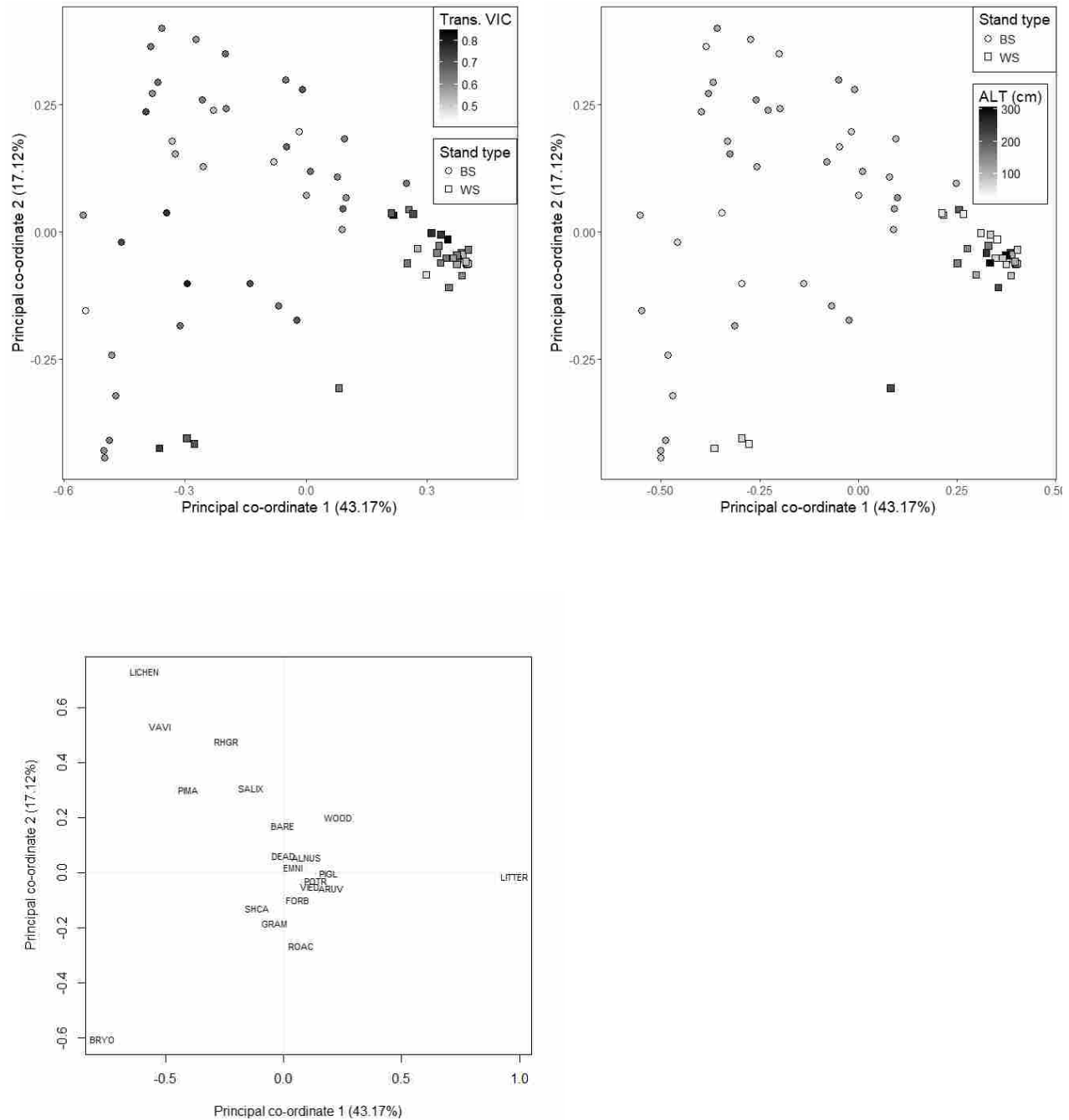
Figure 3.3. Top: Principal co-ordinates analysis for all ground cover measurements including non-living cover, performed with the Bray-Curtis method to calculate the dissimilarity matrix. Quadrats are marked by stand type and shaded by transient layer volumetric ice content (left) and active layer thickness (right). Bottom: Cover values were correlated with the principal co-ordinate scores and plotted to show the relationship of each cover variable in the above PCoA. Codes for each cover variable are: ALNUS: *Alnus* sp.; ARUV: *Arctostaphylos uva-ursi*; BARE: bareground; BRYO: bryophyte; DEAD: dead standing vascular plant; EMNI: *Empetrum nigrum*; FORB: forb; GRAM: graminoid; LICHEN: lichen; LITTER: litter; PIGL: *Picea glauca*; PIMA: *Picea mariana*; POTR: *Populus tremuloides*; RHGR: *Rhododendron groenlandicum*; ROAC:

111

*Rosa acicularis*; SALIX: *Salix* sp.; SHCA: *Shepherdia canadensis*; VAVI: *Vaccinium vitis-idaea*; VIED: *Viburnum edule*; WOOD: downed wood.
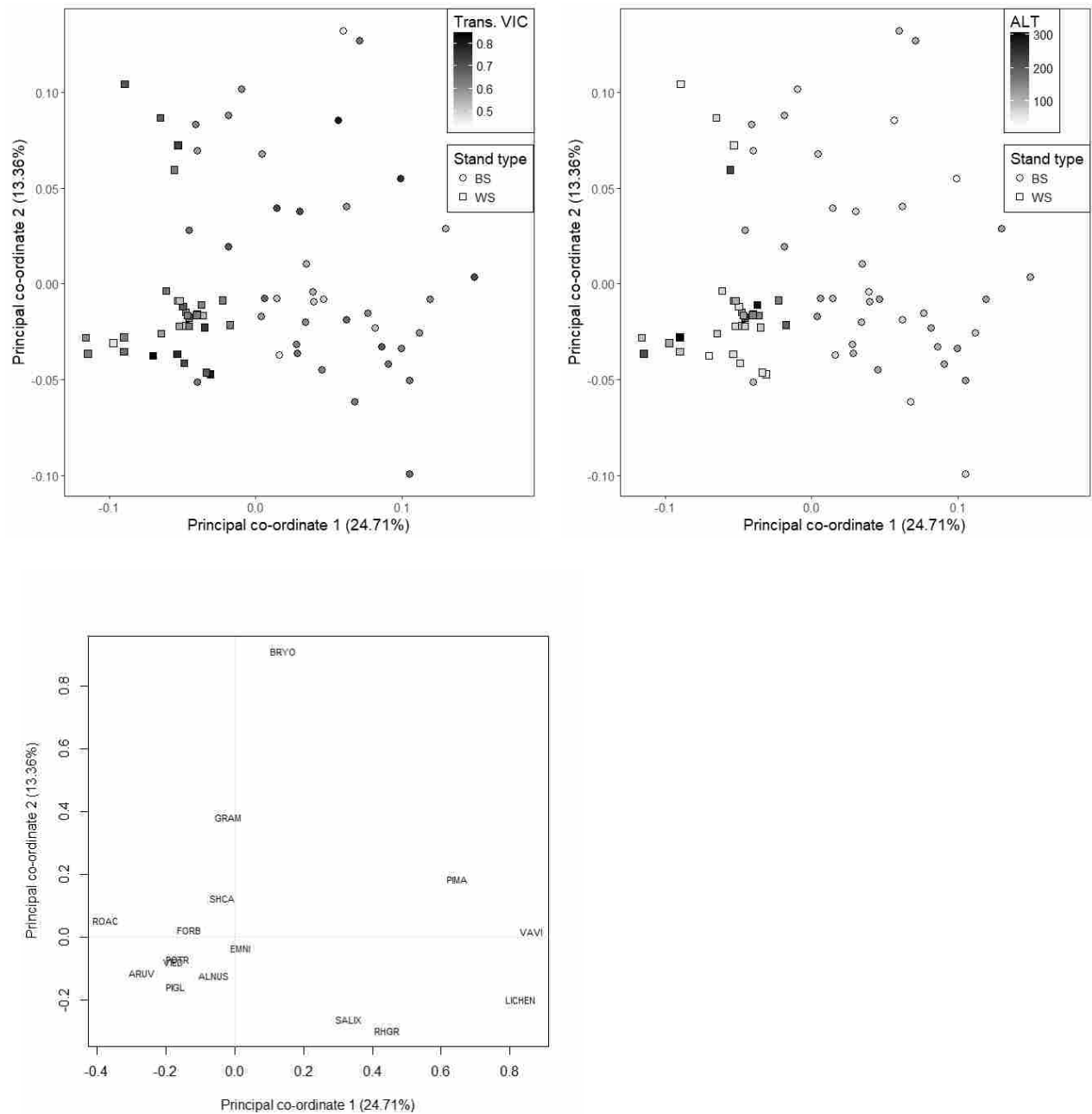
Figure 3.4. Top: Principal co-ordinates analysis for ground vegetation cover measurements excluding non-living cover, performed with the Gower method to calculate the dissimilarity matrix. Quadrats are marked by stand type and shaded by transient layer volumetric ice content (left) and active layer thickness (right). Bottom: Cover values were correlated with the principal co-ordinate scores and plotted to show the relationship of each cover variable in the above PCoA. Codes for each cover variable are: ALNUS: *Alnus* sp.; ARUV: *Arctostaphylos uva-ursi*; BRYO: bryophyte; EMNI: *Empetrum nigrum*; FORB: forb; GRAM: graminoid; LICHEN: lichen; PIGL: *Picea glauca*; PIMA: *Picea mariana*; POTR: *Populus tremuloides*; RHGR: *Rhododendron groenlandicum*; ROAC: *Rosa acicularis*; SALIX: *Salix* sp.; SHCA: *Shepherdia canadensis*; VAVI: *Vaccinium vitis-idaea*; VIED: *Viburnum edule*.

113
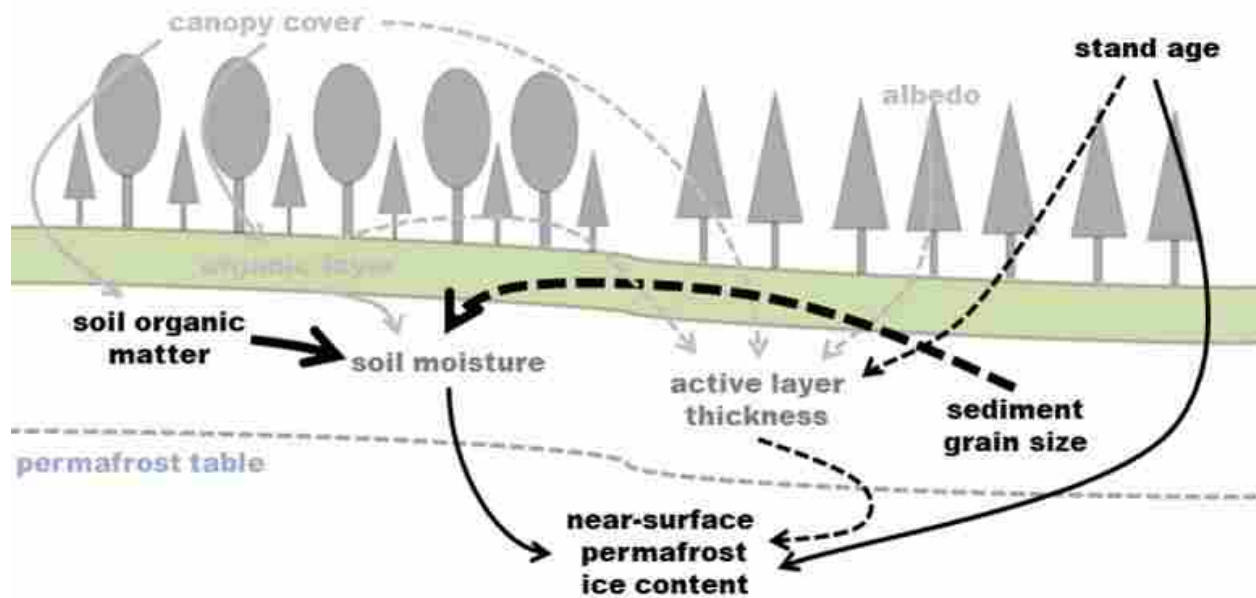
Figure 3.5. Effects of transient layer permafrost ice content from the results of the hypothesis-driven candidate models, highlighting the most important model-averaged variables (black text and arrows). Solid line arrows indicate a positive relationship between the terms; dashed line arrows are negative relationships; larger arrows have a stronger effect on ice content.
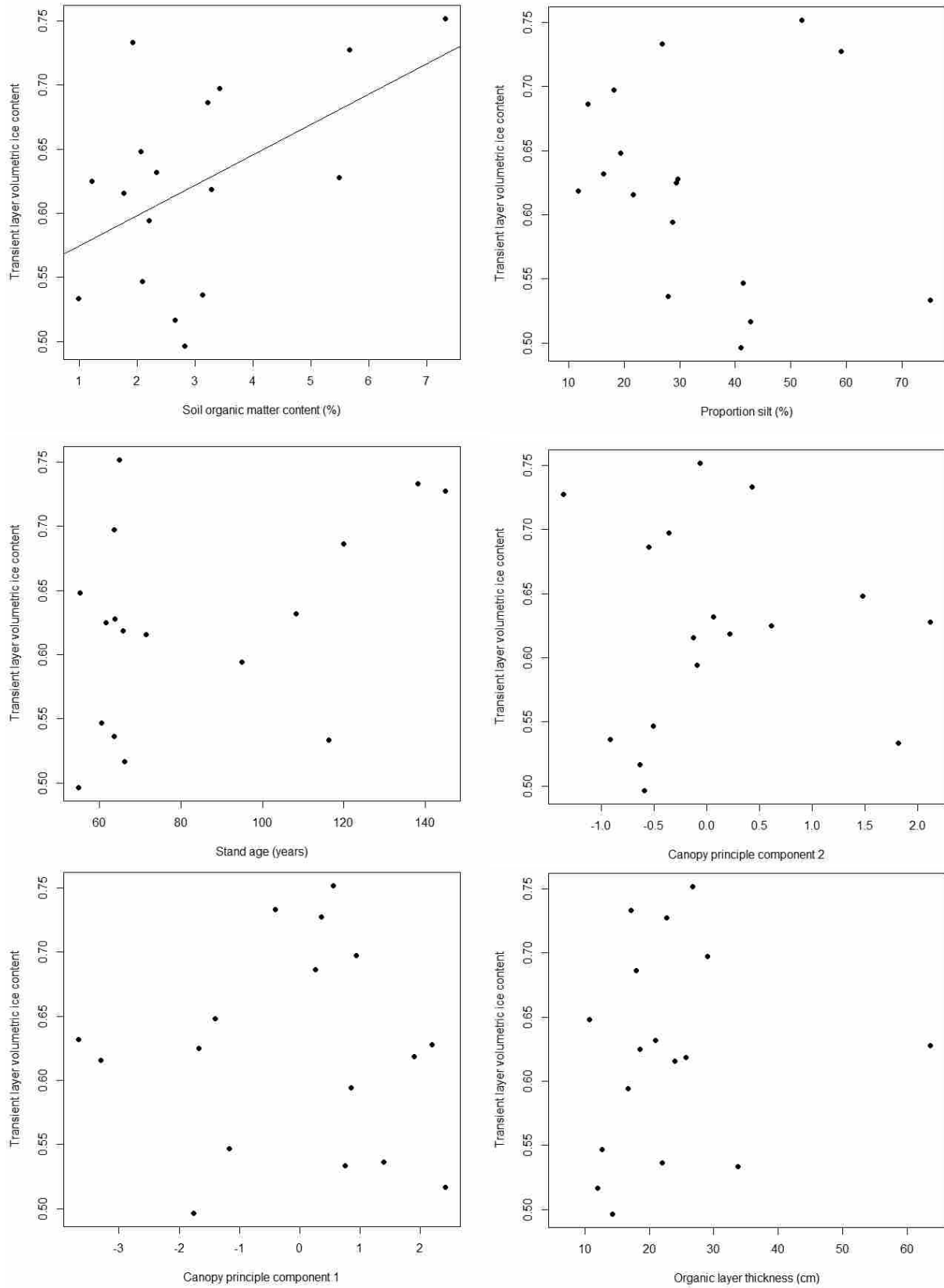
Figure 3.6. Transient layer volumetric ice content mean site values from both black spruce (10 sites) and white spruce/birch (7 sites) forests for each fixed effect in the candidate models (Table

2). Through linear modeling, site-mean permafrost soil organic matter content is significantly positively related to transient layer volumetric ice content (t = 2.26, p = 0.039), but no significant relationship was observed in the site means when ice content was plotted against proportion silt (t = -0.74, p = 0.47), stand age (t = 1.79, p = 0.094), canopy principal component 2 (t = -0.05, p = 0.96), canopy principal component 1 (t = -0.09, p = 0.93), or organic layer thickness (t = 0.54, p = 0.60).
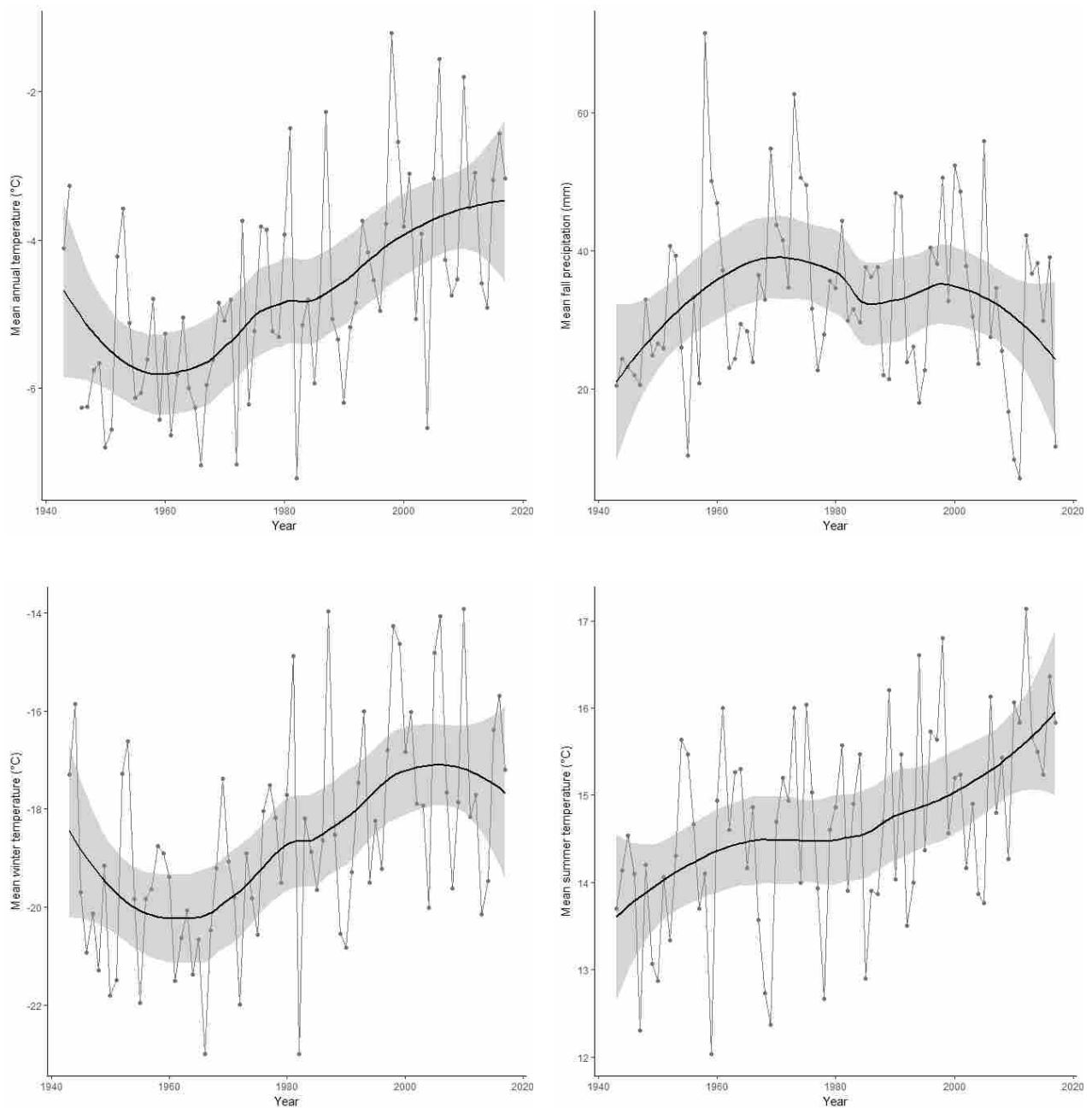
Figure 3.7. Mean annual air temperature (top left), mean fall precipitation (August to October; top right), mean winter temperature (November to March; bottom left), and mean summer temperature (June to August; bottom right) from 1943 – 2017 in Yellowknife, NWT represented by dots connected by grey lines. Smooth black line fits a locally weighted polynomial regression (LOESS) at each value, with the 95% confidence limits shown by the shaded area. Smooth line was calculated using a smoothness span of 0.6, which uses 60% of the points nearest to each value for the LOESS calculation. Fit and plotted using the ggplot2 package (Wickham and Chang, 2016). Data from Environment Canada (2018).

## 3.9 List of Tables

Table 3.1A. Hypothesis-driven linear mixed effects models tested to determine the effect of forest and soil characteristics on transient layer volumetric ice content. The random term, *site*, in each model is to account for variability of parameters measured at borehole-level (organic layer thickness and volumetric ice content). All other parameters are site-level. Soil organic matter is the average soil organic matter content of the permafrost from a borehole 1 m below the permafrost table. Proportion silt is the average silt content from the same borehole, at the intervals -10, 10, 40, and 60 cm below the permafrost table. Stand age is the average age from the 5 largest diameter trees at each site. VIC is the average volumetric ice content of permafrost samples within the transient layer of each borehole. Models are listed from lowest corrected Akaike information criterion (AICc) to highest, with lower AICc being a better fit. AICc calculated using the "AICc" function of the *AICcmodavg* package (Mazerolle, 2017).

| Model name | Model | AICc | ΔAICc | Model weight | Log likelihood |
|---|---|---|---|---|---|
| Full (5) | VIC ~ Canopy PC1 + Canopy PC2 + Organic layer thickness + Soil organic matter content + Proportion silt + Stand age + *site* | -166.3 | 0 | 0.536 | 93.9 |
| Soil Properties (2) | VIC ~ Soil organic matter content + Proportion silt + *site* | -164.7 | 1.6 | 0.243 | 87.9 |
| Disturbance (3) | VIC ~ Stand age + *site* | -163.4 | 2.8 | 0.131 | 86.1 |
| Null (6) | VIC ~ 1 + *site* | -162.4 | 3.9 | 0.077 | 84.4 |
| Thermal (4) | VIC ~ Organic layer thickness + Canopy PC1 + *site* | -158.2 | 8.0 | 0.010 | 84.7 |
| Forest (1) | VIC ~ Organic layer thickness + Canopy PC1 + Canopy PC2 + *site* | -157.8 | 8.6 | 0.003 | 84.7 |

Table 3.1B. Marginal and conditional $R^2$ values, with variance explained by random effect term *site* and residuals from the linear mixed effects models of Table 1A. Marginal $R^2$ represents the variance explained by fixed factors. Conditional $R^2$ represents the variance explained by both fixed and random factors. $R^2$ values were calculated using the "r.squaredGLMM" function of the *MuMIn* package (Barton, 2018). High site variance indicates variation between boreholes is more important than the fixed effects in the model.

| Model name | Model | Marg. $R^2$ | Cond. $R^2$ | Variance (*site*) | Variance (residuals) |
|---|---|---|---|---|---|
| Full (5) | VIC ~ Canopy PC1 + Canopy PC2 + Organic layer thickness + Soil organic matter content + Proportion silt + Stand age + *site* | 0.55 | 0.72 | 0.0013 | 0.0021 |
| Soil Properties (2) | VIC ~ Soil organic matter content + Proportion silt + *site* | 0.28 | 0.73 | 0.0033 | 0.0020 |
| Disturbance (3) | VIC ~ Stand age + *site* | 0.15 | 0.73 | 0.0042 | 0.0020 |
| Null (6) | VIC ~ 1 + *site* | 0 | 0.72 | 0.0053 | 0.0020 |
| Thermal (4) | VIC ~ Organic layer thickness + Canopy PC1 + *site* | 0.01 | 0.72 | 0.0052 | 0.0020 |
| Forest (1) | VIC ~ Organic layer thickness + Canopy PC1 + Canopy PC2 + *site* | 0.01 | 0.72 | 0.0052 | 0.0020 |

Table  3.2. Model-averaged variable estimates calculated using "modavgShrink" from the *AICcmodavg* R package (Mazerolle, 2017) to determine which terms were important predictors of transient layer volumetric ice content, which takes into account the prevalence of each term in the hypothetical models (Table 3.1AB) to reduce model selection bias. Variables are ordered in descending order of importance of predicting transient layer volumetric ice content. Variables that do not contain zero between their lower and upper confidence limits are considered important.

| Variable | Estimate | Standard error | Lower confidence limit | Upper confidence limit |
|---|---|---|---|---|
| Soil organic matter content | 0.039 | 0.024 | -0.008 | 0.086 |
| Proportion silt | -0.022 | 0.017 | -0.055 | 0.011 |
| Stand age | 0.026 | 0.021 | -0.015 | 0.068 |
| Canopy PC2 | 0.009 | 0.012 | -0.014 | 0.033 |
| Canopy PC1 | -0.009 | 0.011 | -0.031 | 0.014 |
| Organic layer thickness | -0.001 | 0.006 | -0.014 | 0.011 |

# Chapter 4: General discussion

## 4.1 Summary

Northern regions are experiencing enhanced rates of climate warming and, consequently, accelerating rates of permafrost thaw. Thawing of ice-rich terrain causes ground subsidence, which can drastically alter ecosystems and damage infrastructure. In the discontinuous permafrost zone of the North Slave region near Yellowknife, NWT, understanding near-surface ice conditions and the factors that affect ice content are relevant to managing the continued development and industrial pressures in the area. As climate warming continues, there is increased potential for alterations to ecosystem structure and function and the associated services provided. Here I described near-surface ground ice stratigraphy, examined the controls of near-surface ground ice content, and assessed whether active layer thickness or ice content are related to ground vegetation communities in predictable ways.

### 4.1.1 Chapter 2 summary

a. Linear models found higher mean volumetric ice content was related to smaller mean sediment grain size in black spruce forests, and white spruce/birch forests had higher mean volumetric ice content related to higher mean soil organic matter content.

b. The transient layer was inferred based on cryostructures and thickness of segregated ice, and was found to be inversely associated with active layer thickness. Transient layer cryostructures (ataxitic and lenticular) were observed in all black spruce sites, but were absent in several white spruce/birch sites. Sites

without discernable transient layer cryostructures had thicker active layers and more variable ice content in permafrost.

c.     Local variability of ground ice content in black spruce forests was not found to differ as a function of microtopography.

d.     Core sample depth below permafrost and active layer thickness were both important predictors of volumetric ice content in black spruce forests, with higher ice content occurring near the top of permafrost at sites with thin active layers, consistent with the model of transient layer development described by Shur *et al*. (2005).

e.     In white spruce/birch forests, active layer thickness mediated the relationship between core sample depth below permafrost table and volumetric ice content such that for samples associated with shallow active layers, volumetric ice content decreased with sample depth. As with the black spruce forests this suggests the presence of a thick transient layer. The opposite was true for white spruce/birch sites with thick active layers, suggesting the absence of a transient layer and that active layer development had truncated formational ice preserved since the initial establishment of permafrost in these deposits.

*4.1.2 Chapter 3 summary*

a.     In the well-drained mineral soil sites with black spruce or white spruce/birch forest cover, soil properties (soil organic matter content and sediment grain size) were more important controls on transient layer volumetric ice content than forest characteristics (organic layer thickness and canopy structure). Finer grained

sediments and higher soil organic matter contents were associated with higher transient layer volumetric ice content.

**b.** Ground cover and ground vegetation communities separated clearly by forest type, but active layer thickness and transient layer volumetric ice content did not influence ground cover or ground vegetation community composition.

### 4.1.3 Overall

**a.** Ground ice profiles in black spruce forests showed decreasing ice content with depth into the permafrost and horizontal, lenticular cryostructures; this is consistent with what is expected from the transient layer of permafrost. In these forests, higher ice content in association with thinner active layers likely relates to transient layer ice enrichment as permafrost aggradation slows with forest development. Electrical conductivity of permafrost pore water increased with depth in both stands, supporting the transient layer model.

**b.** Evidence of a transient layer was absent from thicker active layer white spruce/birch forests at sites where deep thaw truncated formational ice at depth. The transient layer is unlikely to re-form at these sites unless ecosystem change causes ground temperatures to decrease, allowing permafrost to aggrade. However, most white spruce/birch sites (seven out of ten) had a transient layer present.

**c.** In this landscape type of well-drained, fine-grained mineral soils, the importance of soil properties (generally unaffected by forest disturbances) in influencing transient layer ice content means that following a disturbance, the transient layer

will aggrade ice similar to its post-fire conditions, assuming no changes in topography, climate, or forest regeneration.

**d.**     Our results show that the important drivers of transient layer ice content in a larger landscape view (e.g., organic layer thickness) evident in other studies are not evident within a single topo-edaphic site type, and that the differences of ice content within one type are instead driven by a subset of the main physical controls of ice content. This may be influenced by the stand ages available to be sampled in this region; in more northern environments where stand-replacing fires are less common, multi-centennial stands are more common.

*4.1.4 Significance*

These results indicate that within well-drained, fine-grained mineral soil forests, land cover and surficial site surveys may not be able to be used to distinguish areas of ice-rich permafrost. Stand age could be useful in this respect, but it may not be reflective of ice content since it does not necessarily indicate the time since the transient layer last thawed. Higher resolution soils maps may be used to help predict ice content if they are sufficiently detailed on sediment grain size and organic matter content. This will impact ice content estimations for infrastructure planning purposes and strengthen our understanding of the effect of the transient layer on forest characteristics.

## 4.2 Contributions

Ecologists, hydrologists, and permafrost scientists alike may be interested in this research due to the close relationships these fields form in this study. Implications from the findings may also be of interest to climatologists looking to better characterize ice content of permafrost to

improve modeled projections of permafrost thaw and subsequent permafrost carbon release as a positive feedback to climate warming. This research complements work done by Morse *et al.* (2015) performed in the same region, which measured 1 metre ground temperatures over 3 years and examined gravimetric moisture content up to 3 metres below the ground surface, snow depth, active layer thickness, and leaf area index. Their work was performed in black spruce, white birch, and peatland ecosystems to determine the thermal equilibrium state of the near-surface permafrost in the North Slave region.

The study area of this thesis is near the most populated area in the NWT, which has well-developed road infrastructure and expanding industrial activities. In some cases, infrastructure development on lithalsas involves the removal of the top layer of soil to flatten the ground surface. This research shows that depending on site conditions, this process may result in the destabilization of formerly thaw-stable ground, which can damage infrastructure. This destabilization is caused by effectively moving ice-rich formational permafrost at depth closer to the ground surface. Ground subsidence will then occur as the near-surface ice-rich permafrost thaws due to the surface disturbance. Data from this thesis will be made available in an Open Report with the Northwest Territories Geological Survey to assist in geotechnical planning for infrastructure expansion in this region.

### 4.2.1 Contributions from Chapter 2

Characterization of near-surface ice content and structure in the discontinuous permafrost of the North Slave region near Yellowknife has been advanced with this research. In terms of ice structure and the development of the transient layer, the results from black spruce forests in Chapter 2 strengthen the conceptual model of ice growth in near-surface permafrost summarized in Chapter 1 and identified by Shur and Jorgenson (2007). However, white spruce/birch forests

may have a site history and near-surface ground ice which does not follow the conceptual model, depending on a variety of surface and soil characteristics including soil moisture, topography, and ground thermal regime. The study also suggests that development of a transient layer may not be ubiquitous in fine-grained permafrost settings, particularly where near-surface permafrost is very warm. Insight gained of near-surface ground ice structure and distribution will help to characterize the potential for landscape change under a continually warming climate.

### 4.2.2 Contributions from Chapter 3

Previous studies have separately examined the roles of physical and biotic factors on permafrost and its ice content, but this study statistically analyzes the relative influence of a multitude of biophysical controls on ground ice content, with implications for the aggradation of ice content in the transient layer. Chapter 3 highlighted the disconnect between forest characteristics and transient layer ice content that was expected from the literature, and found instead only an influence of physical factors affecting transient layer ice content. Although other studies found active layer thickness was influential in structuring vegetation communities across a large gradient of landscape types, no influence of active layer thickness with ground vegetation community was found. Together this indicates that the important factors influencing feedbacks across a large landscape gradient are not necessarily the same factors within one type of landscape.

## 4.3 Integrative approach

The multi-disciplinary nature of this thesis fulfills the integrative aspect of the M.Sc. Integrative Biology program foremost by applying elements from both forest ecology (biology) and permafrost sciences (physical geography). Methods from both fields were used in this

research for forest surveys and permafrost core sample extraction and analysis. These two fields are represented by the two supervisors of this thesis, the first being an ecologist in the department of biology at Wilfrid Laurier University, and the second being a permafrost scientist at the Northwest Territories Geological Survey. The unique perspectives provided by each have formed this thesis into research that can be valuable to both fields, rather than being a study from one specific viewpoint.

In addition to biology and geography, this research also draws from the fields of hydrology, thermodynamics, soil science, and climatology to understand the processes that lead to ice accumulation and growth in the transient layer as permafrost aggrades. Without the integration of all these fields, the context of this thesis would not be fully comprehensible. In the larger view of Earth's major "spheres," this thesis involves interactions between the biosphere (plants), atmosphere, lithosphere (soils), and cryosphere (permafrost).

## 4.4 Future research

To improve upon this research, more sites of each forest type should be selected, expanding the gradient in stand age to properly assess the role of stand development. Due to local factors, forests may develop at varying rates; therefore, sampling a larger number of sites would help to isolate site characteristics for their effects on near-surface permafrost ice content. Soil moisture is an important factor with effects on both forest and permafrost, so further research would need to take good measures of soil moisture such that it can be included as a factor in statistical modeling and be used to help explain forest and ice structures. Information of ground thermal conditions could also aid in interpreting results of transient layer thickness, or lack thereof.

Future research can apply similar methods to examine the relationship of transient layer permafrost ice content within other forest types in the region, namely peatlands. In addition to a myriad of differences in forest characteristics, these sites also grow on different substrates, with peatlands growing on a thick layer of partially decomposed organic material. As a result, it is likely the case that similar quantitative analyses of how characteristics at these sites affect transient layer permafrost ice content will show differing results from the findings of this thesis, but in combination would identify important controls over ground ice accumulation both within and across land cover types.

Some of our research results imply that ground ice loss from warm permafrost may be a gradual process that could proceed under periods of dry conditions and while the ground remains cryotic during winter. An investigation is recommended into the potential for ice loss from the near-surface permafrost in fine-grained sediments of the North Slave region. If the permafrost is indeed slowly losing ice to the active layer above, subsidence potential of thawing permafrost from surface disturbance is decreased, and the rate of permafrost thaw from a warming climate may be increased. Concerted measurements of soil moisture and temperature profiles, combined with data on climate trends may be used to gain insight on the rate of moisture exchange between the bottom of the active layer and the top of permafrost. Alternatively, an experimental setup simulating conditions of this region may be able to quantify the net movement of moisture over the simulated course of a year.

## 4.5 References

Morse PD, Wolfe SA, Kokelj SV, Gaanderse AJR. 2015. The occurrence and thermal disequilibrium state of permafrost in forest ecotopes of the Great Slave Region, Northwest Territories, Canada. *Permafrost and Periglacial Processes*, (June). https://doi.org/10.1002/ppp.1858

Shur YL, Hinkel KM, Nelson FE. 2005. The transient layer: implications for geocryology and climate-change science. *Permafrost and Periglacial Processes*, **16**(1): 5–17. https://doi.org/10.1002/ppp.518

Shur YL, Jorgenson MT. 2007. Patterns of permafrost formation and degradation in relation to climate and ecosystems. *Permafrost and Periglacial Processes*, **19**: 7–19. https://doi.org/10.1002/ppp

# Appendix



Figure A.1. Permafrost extent in the Northwest Territories. Yellowknife is represented by the yellow star. Study site locations near Yellowknife are shown in the inset with black spruce sites marked by red circles and white spruce/birch sites marked by blue triangles. Sites of the same forest type near each other are grouped together as a larger marker with the number indicating the number of study sites in that area.

Figure A.2. Aerial photograph of the heterogeneous landscape of the Great Slave Lowlands, North Slave region at Boundary Creek by Highway 3 taken in June 2016. **A**: black spruce; **B**: mixed white birch and white spruce; **C**: white birch; **D**: bedrock. Permafrost is generally present under the forested terrain, and warmer in white birch stands than black spruce stands. No permafrost is present in exposed bedrock or beneath bodies of water. Photograph courtesy of Peter Morse.

Figure A.3. Photograph of (A) a dense black spruce site on the younger end of the age gradient of selected sites (71 years); (B) a drunken black spruce site on the older end of the age gradient of selected sites (138 years); (C) a white birch site on the younger end of the age gradient of selected sites (64 years); and (D) a white spruce site on the older end of the age gradient of selected sites (145 years).
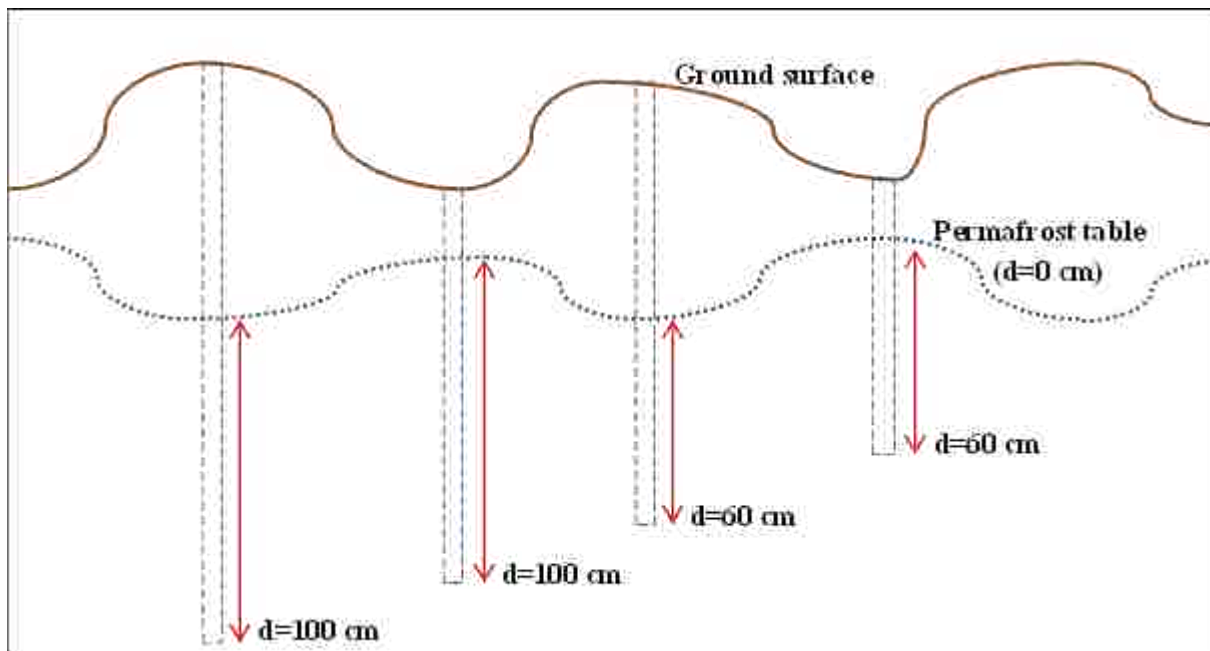
Figure A.4. Schematic diagram of borehole drilling at a hummocky site. Four boreholes are drilled; two boreholes 100 cm into the permafrost, two boreholes 60 cm into the permafrost, with one of each in a hummock top and one of each in an inter-hummock trough.
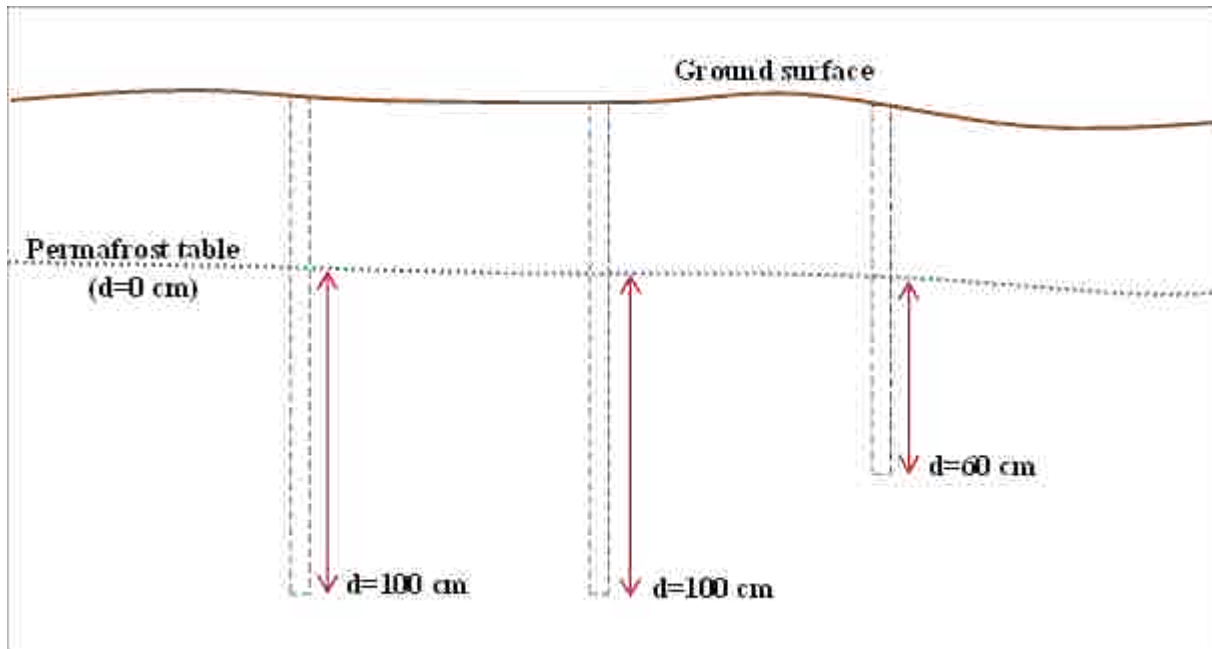
Figure A.5. Schematic diagram of borehole drilling at a site with no hummocks. Three boreholes are drilled; two boreholes 100 cm into the permafrost, one borehole 60 cm into the permafrost.

Sample:                                          Field mass (g):


Interval (cm):                                   Volume (g):
Depth (cm):                                      Bulk density (g/cm³):
Length (cm):                                     Dry mass (g):
Pic #:

**ICE NOT VISIBLE**

| SYMBOL | SUBGROUP DESCRIPTION | |
|--------|---------------------|---|
| Nf | Poorly-bonded or friable | |
| Nbn | No excess ice, well-bonded | |
| Nbe | Excess ice, well-bonded | |

**VISIBLE ICE LESS THAN 50% BY VOLUME**

| SYMBOL | SUBGROUP DESCRIPTION | |
|--------|---------------------|---|
| Vx | Individual ice crystals or inclusions | |
| Vc | Ice coatings on particles | |
| Vr | Random or irregularly oriented ice formations | |
| Vs | Stratified or distinctly oriented ice formations | |

**LEGEND:**   Soil ☐   Ice ■
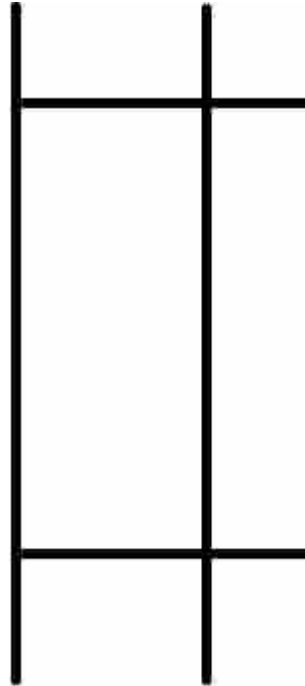
Visible ice (%):
Ice lensing
  Thickness (mm):
  Direction:  Sub-Horiz.  Sub-Vert.
Diag.
  Type:  Uniform  Increasing  Decreasing
       Non-uniform    Reticulate
Ataxitic


Munsell:
Colour:  Grey     Red      Green
         Orange specks
Type:  Uniform     Mottled     Stratified
Soil:  Clay  Silty clay  Clayey silt  Silt
       Sandy silt  Organic    Charcoal
Notes:

Figure A.6. Example of a data sheet used in defining core sample characteristics in the field.
Centre diagram is used to define specific depths and depictions of core features.
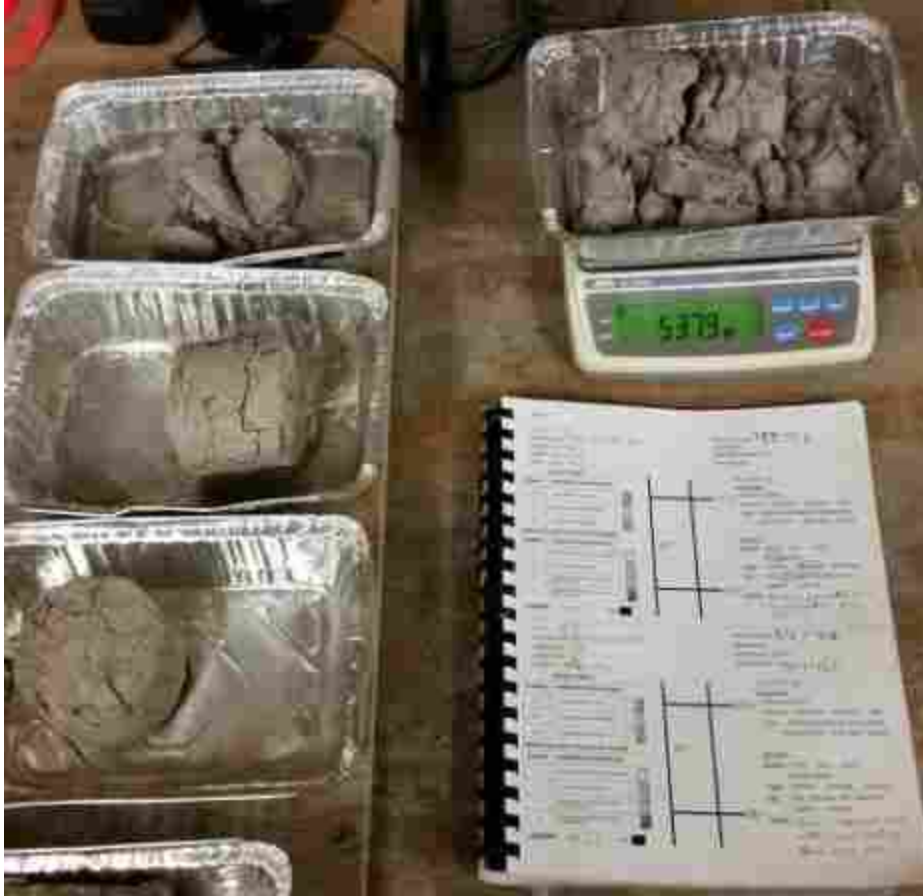
Figure A.7. Permafrost core samples in their trays being gravimetrically weighed after drying in the oven at 105 °C.

Black spruce
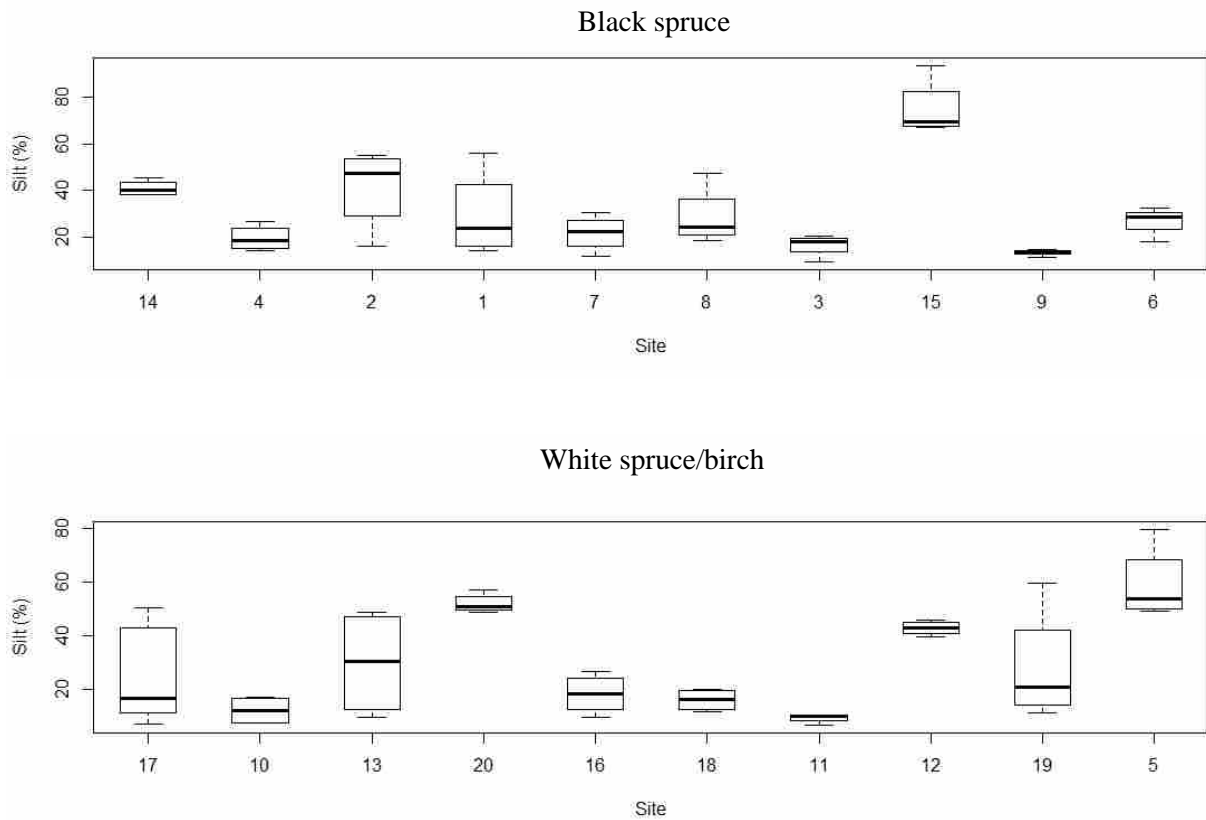


White spruce/birch



Figure A.8. Proportional silt content (%) at each site of black spruce stands, arranged by site from youngest to oldest stand age (top) and white spruce/birch stands, arranged by site from lowest to highest composition white spruce (bottom).

Table A.1. Study site locations and descriptions.

| Site | Year drilled | Latitude | Longitude | Stand type | Microtopography | Bore-holes drilled |
|------|--------------|----------|-----------|------------|-----------------|--------------------|
| 1 | 2014 | 62.4958 | -114.2885 | Black spruce | Earth hummocks | 4 |
| 2 | 2014 | 62.4981 | -114.2896 | Black spruce | Earth hummocks | 4 |
| 3 | 2014 | 62.5247 | -114.3257 | Black spruce | Earth hummocks | 4 |
| 4 | 2014 | 62.5776 | -114.0567 | Black spruce | Earth hummocks | 4 |
| 5 | 2014 | 62.6030 | -114.1159 | White spruce/birch | Large mounds (2 m tall, 10 m diameter) | 4 |
| 6 | 2014 | 62.6030 | -114.1173 | Black spruce | Earth hummocks | 4 |
| 7 | 2014 | 62.6023 | -114.1153 | Black spruce | Earth hummocks | 4 |
| 8 | 2015 | 62.5082 | -114.2251 | Black spruce | Earth hummocks | 4 |
| 9 | 2015 | 62.5274 | -114.3126 | Black spruce | Earth hummocks | 4 |
| 10 | 2015 | 62.5422 | -114.9861 | White spruce/birch | Absent | 3 |
| 11 | 2015 | 62.5350 | -114.9750 | White spruce/birch | Absent | 3 |
| 12 | 2015 | 62.5300 | -114.9654 | White spruce/birch | Mostly absent, but some small, collapsed hummocks (< 20 cm tall) | 3 |
| 13 | 2015 | 62.5270 | -114.9605 | White spruce/birch | Absent | 3 |
| 14 | 2015 | 62.5977 | -114.1268 | Black spruce | Earth hummocks | 4 |
| 15 | 2015 | 62.5957 | -114.1164 | Black spruce | Earth hummocks | 4 |
| 16 | 2015 | 62.5539 | -115.0116 | White spruce/birch | Mostly absent, but a couple depressions present (1 m deep, 4 m diameter) | 3 |
| 17 | 2015 | 62.4713 | -114.3074 | White spruce/birch | Absent | 2 |
| 18 | 2015 | 62.4981 | -114.3133 | White spruce/birch | Absent | 3 |
| 19 | 2015 | 62.5337 | -114.9705 | White spruce/birch | Absent | 3 |
| 20 | 2015 | 62.5186 | -114.8904 | White spruce/birch | Earth hummocks | 4 |

Table A.2. Site-level characteristics for black spruce forest type with sites arranged by increasing stand age. Volumetric ice content standard error is calculated from the borehole average (n = 4).

| Site | Stand age ± SE (years) | Black spruce (%) | White birch (%) | Organic layer ± SE (cm) | Organic matter ± SE (%) | Proportion silt ± SE (%) | Volumetric ice content ± SE | Active layer thickness ± SE (cm) | Transient layer thickness ± SE (cm) |
|---|---|---|---|---|---|---|---|---|---|
| 14 | 55 ± 2 | 85.8 | 14.2 | 14 ± 4 | 2.8 ± 0.2 | 40.9 ± 1.7 | 0.50 ± 0.01 | 93 ± 10 | 100 ± 0 |
| 4 | 55 ± 2 | 79.4 | 20.6 | 11 ± 6 | 2.1 ± 0.1 | 19.4 ± 2.8 | 0.65 ± 0.01 | 80 ± 12 | 100 ± 0 |
| 2 | 60 ± 2 | 75.4 | 20.5 | 13 ± 6 | 2.1 ± 0.1 | 41.5 ± 8.9 | 0.55 ± 0.01 | 97 ± 15 | 95 ± 5 |
| 1 | 62 ± 2 | 80.3 | 19.7 | 18 ± 8 | 1.2 ± 0.2 | 29.5 ± 9.5 | 0.59 ± 0.03 | 110 ± 9 | 75 ± 12 |
| 7 | 71 ± 2 | 100 | 0 | 24 ± 10 | 1.8 ± 0.1 | 21.6 ± 3.9 | 0.60 ± 0.01 | 107 ± 9 | 88 ± 12 |
| 8 | 95 ± 8 | 79.9 | 2.0 | 17 ± 2 | 2.2 ± 0.1 | 28.7 ± 6.5 | 0.55 ± 0.03 | 86 ± 7 | 85 ± 8 |
| 3 | 108 ± 17 | 91.8 | 8.2 | 21 ± 4 | 2.3 ± 0.1 | 16.4 ± 2.4 | 0.62 ± 0.01 | 89 ± 8 | 95 ± 5 |
| 15 | 116 ± 5 | 96.3 | 2.7 | 34 ± 3 | 1.0 ± 0.1 | 75.1 ± 6.3 | 0.53 ± 0.03 | 90 ± 12 | 100 ± 0 |
| 9 | 120 ± 3 | 83.6 | 6.1 | 18 ± 4 | 3.2 ± 0.05 | 13.5 ± 0.7 | 0.69 ± 0.02 | 88 ± 11 | 85 ± 11 |
| 6 | 138 ± 5 | 91.4 | 0.6 | 17 ± 3 | 1.9 ± 0.05 | 26.8 ± 3.1 | 0.73 ± 0.04 | 66 ± 21 | 100 ± 0 |

Table A.3. Site-level characteristics for the white spruce forest trajectory, with sites arranged by increasing white spruce composition. Volumetric ice content standard error is calculated from the borehole average (sites 5 and 20, n = 4; sites 17 and 18, n = 2; remaining sites, n = 3).

| Site | Stand age ± SE (years) | White spruce (%) | White birch (%) | Organic layer ± SE (cm) | Organic matter ± SE (%) | Proportion silt ± SE (%) | Volumetric ice content ± SE | Active layer thickness ± SE (cm) | Transient layer thickness ± SE (cm) |
|---|---|---|---|---|---|---|---|---|---|
| 17 | 67 ± 3 | 2.8 | 87.8 | 13 ± 3 | 3.1 ± 0.1 | 24.0 ± 7.4 | 0.69 ± 0.06 | 302 ± 3 | |
| 10 | 66 ± 1 | 9.1 | 59.0 | 26 ± 7 | 3.3 ± 0.03 | 11.8 ± 2.6 | 0.62 ± 0.01 | 104 ± 14 | 74 ± 14 |
| 13 | 64 ± 2 | 10.5 | 89.5 | 64 ± 3 | 5.5 ± 1.2 | 29.6 ± 10.1 | 0.60 ± 0.04 | 64 ± 5 | 73 ± 27 |
| 20 | 65 ± 3 | 29.6 | 61.8 | 27 ± 2 | 7.3 ± 0.5 | 51.9 ± 1.9 | 0.75 ± 0.03 | 52 ± 5 | 100 ± 0 |
| 16 | 64 ± 2 | 31.6 | 68.4 | 29 ± 2 | 3.4 ± 0.1 | 18.1 ± 3.7 | 0.67 ± 0.05 | 90 ± 15 | 57 ± 30 |
| 18 | 67 ± 6 | 40.0 | 60.0 | 18 ± 4 | 3.1 ± 0.1 | 15.8 ± 2.1 | 0.64 ± 0.06 | 213 ± 3 | |
| 11 | 63 ± 2 | 55.5 | 35.0 | 7 ± 0.3 | 3.7 ± 0.1 | 9.1 ± 0.9 | 0.61 ± 0.01 | 215 ± 16 | |
| 12 | 66 ± 2 | 58.6 | 25.1 | 12 ± 3 | 2.7 ± 0.1 | 42.8 ± 1.4 | 0.54 ± 0.01 | 126 ± 12 | 33 ± 12 |
| 19 | 64 ± 1 | 69.1 | 28.7 | 22 ± 4 | 3.1 ± 0.1 | 28.0 ± 10.9 | 0.54 ± 0.02 | 98 ± 9 | 100 ± 0 |
| 5 | 145 ± 2 | 96.0 | 4.0 | 23 ± 4 | 5.7 ± 0.1 | 59.0 ± 7.1 | 0.73 ± 0.03 | 55 ± 6 | 100 ± 0 |

Table A.4. Results of woody plants and ground cover by functional group from 1 m$^2$ ground plot surveys adjacent to each borehole for black spruce sites (n = 4). Dominant understorey species listed if present in ≥ 75% of ground plots. Dominant ground cover listed if dominant by percent cover relative to its functional group. Understorey species codes: Picmar = *Picea mariana*, Rhogro = *Rhododendron groenlandicum*, Vacvit = *Vaccinium vitis-idaea*.

| Site | Shrub cover ± SE (%) | Dominant understorey species | Bryophyte ± SE (%) | Dominant bryophyte | Lichen ± SE (%) | Dominant lichen |
|------|------|------|------|------|------|------|
| 1 | 75.8 ± 6.1 | Rhogro, Vacvit | 17.5 ± 5.2 | *Hylocomium* sp. | 35.0 ± 12.4 | *Cladina* sp. *Cladonia* sp. |
| 2 | 57.8 ± 5.4 | Rhogro, Vacvit, *Salix*, Picmar | 21.2 ± 2.4 | *Hylocomium* sp. | 18.8 ± 10.5 | *Cladina* sp. *Cladonia* sp. |
| 3 | 51.2 ± 8.0 | Rhogro, Vacvit, Picmar | 35.0 ± 20.3 | *Hylocomium* sp. | 23.2 ± 9.8 | *Cladina* sp. *Peltigera* sp. |
| 4 | 77.5 ± 12.3 | Rhogro, Vacvit | 6.2 ± 3.8 | *Hylocomium* sp. | 48.8 ± 15.2 | *Cladina* sp. *Peltigera* sp. |
| 6 | 47.8 ± 8.5 | Rhogro, Vacvit, Picmar | 51.2 ± 15.3 | *Hylocomium* sp. | 58.8 ± 11.8 | *Cladina* sp. *Peltigera* sp. |
| 7 | 40.0 ± 6.8 | Vacvit, *Salix*, Picmar | 11.5 ± 5.4 | *Hylocomium* sp. *Dicranum* sp. | 63.8 ± 16.8 | *Peltigera* sp. |
| 8 | 19.0 ± 6.0 | Vacvit, Rosaci | 96.8 ± 1.0 | *Hylocomium* sp. | 4.0 ± 1.3 | *Peltigera* sp. *Cladina* sp. |
| 9 | 30.8 ± 5.3 | Vacvit | 55.0 ± 7.1 | *Hylocomium* sp. | 16.2 ± 9.0 | *Peltigera* sp. |
| 14 | 39.5 ± 5.2 | Rhogro, Vacvit | 25.0 ± 3.5 | *Dicranum* sp. *Hylocomium* sp. | 38.8 ± 4.3 | *Peltigera* sp. |
| 15 | 36.2 ± 10.8 | Rhogro, Vacvit, Picmar | 71.2 ± 14.2 | *Hylocomium* sp. *Polytrichum* sp. | 32.8 ± 14.8 | *Peltigera* sp. |

Table A.4 continued… Forb species codes: Chaang = *Chamerion angustifolium*, Geoliv = *Geocaulon lividum*.

| Site | Graminoid ± SE (%) | Dominant graminoid | Forb ± SE (%) | Dominant forb | Downed wood ± SE (%) | Litter ± SE (%) | Bare ground ± SE (%) | Organic layer ± SE (cm) |
|---|---|---|---|---|---|---|---|---|
| 1 | 1.2 ± 1.2 | *Calamagrostis* sp. | 2.2 ± 1.7 | *Equisetum* sp. | 0.5 ± 0.5 | 63.8 ± 9.0 | | 22.8 ± 4.5 |
| 2 | 1.5 ± 0.9 | *Calamagrostis* sp. | | | 2.0 ± 0.4 | 67.5 ± 11.6 | 1.8 ± 1.8 | 25.7 ± 7.1 |
| 3 | 1.5 ± 1.2 | *Calamagrostis* sp. | 2.0 ± 1.0 | *Equisetum* sp. | 6.8 ± 3.0 | 52.5 ± 9.2 | | 6.7 ± 0.3 |
| 4 | 0.2 ± 0.2 | *Calamagrostis* sp. | 0.8 ± 0.2 | *Equisetum* sp., *Pyrola* sp. | 3.8 ± 1.5 | 47.5 ± 18.1 | 6.2 ± 6.2 | 12.0 ± 3.0 |
| 6 | 1.5 ± 1.2 | *Calamagrostis* sp. | 13.5 ± 5.5 | *Equisetum* sp., Geoliv | 2.5 ± 1.0 | 26.2 ± 8.0 | | 63.7 ± 3.2 |
| 7 | 2.0 ± 1.1 | *Calamagrostis* sp. | 5.8 ± 2.5 | *Equisetum* sp., Geoliv | 6.0 ± 3.1 | 26.2 ± 14.8 | | 29.0 ± 2.1 |
| 8 | 0.8 ± 0.2 | *Calamagrostis* sp. | 1.0 ± 0.7 | *Pyrola* sp. | 1.2 ± 0.6 | 4.2 ± 1.6 | | 13.3 ± 3.3 |
| 9 | | | 4.2 ± 2.1 | *Pyrola* sp., Geoliv, Chaang | 2.5 ± 1.0 | 46.2 ± 10.5 | | 18.3 ± 4.4 |
| 14 | | | 3.8 ± 1.5 | *Pyrola* sp. | 5.5 ± 1.8 | 42.5 ± 10.3 | | 22.0 ± 4.0 |
| 15 | 4.5 ± 3.5 | *Calamagrostis* sp. | 7.8 ± 5.9 | *Equisetum* sp. | 0.5 ± 0.3 | 8.0 ± 7.3 | 0.5 ± 0.3 | 26.8 ± 1.9 |

Table A.5. Results of woody plants and ground cover by functional group from 1 m$^2$ ground plot surveys adjacent to each borehole for white spruce/birch sites (n = 3, except for sites 5 and 20 where n = 4). Dominant understorey species listed if present in ≥ 67% of ground plots. Dominant ground cover listed if dominant by percent cover relative to its functional group. Understorey species codes: Arcuva = *Arctastaphylos uva-ursi*, Picgla = *Picea glauca*, Rhogro = *Rhododendron groenlandicum*, Rosaci = *Rosa acicularis*, Vacvit = *Vaccinium vitis-idaea*.

| Site | Shrub cover ± SE (%) | Dominant understorey species | Bryophyte ± SE (%) | Dominant bryophyte | Lichen ± SE (%) | Dominant lichen |
|---|---|---|---|---|---|---|
| 5 | 31.0 ± 18.5 | Rosaci | 73.8 ± 21.2 | *Hylocomium* sp. | 0.2 ± 0.1 | |
| 10 | 6.0 ± 5.0 | Arcuva, Rosaci | 0.3 ± 0.3 | *Dicranum* sp. | 0.3 ± 0.3 | *Cladonia* sp. |
| 11 | 2.3 ± 1.9 | Rosaci | 3.7 ± 1.3 | *Hylocomium* sp., *Dicranum* sp. | 6.7 ± 4.4 | *Peltigera* sp. |
| 12 | 6.7 ± 4.7 | Rosaci | 6.7 ± 3.3 | *Hylocomium* sp. | 2.3 ± 1.3 | *Cladonia* sp., *Cladina* sp., *Peltigera* sp. |
| 13 | 0.7 ± 0.3 | | 0.7 ± 0.3 | *Hylocomium* sp. | | |
| 16 | 4.7 ± 3.3 | Rhogro | 1.0 ± 0.6 | *Hylocomium* sp., *Dicranum* sp. | 0.3 ± 0.3 | *Cladonia* sp. |
| 17 | 6.3 ± 2.3 | Vacvit | 1.0 ± 0.6 | *Hylocomium* sp. | | |
| 18 | 40.7 ± 15.3 | Rosaci | 23.3 ± 18.6 | *Hylocomium* sp., *Dicranum* sp. | | |
| 19 | 0.7 ± 0.3 | Rosaci | 0.3 ± 0.3 | *Dicranum* sp. | | |
| 20 | 25.8 ± 10.3 | Rhogro, Vacvit, Picgla | 3.5 ± 2.3 | *Hylocomium* sp. | 0.2 ± 0.2 | *Cladonia* sp. |

Table A.5 continued… Forb species codes: Chaang = *Chamerion angustifolium*, Geoliv = *Geocaulon lividum*, Rubcha = *Rubus chamaemorus*.

| Site | Graminoid ± SE (%) | Dominant graminoid | Forb ± SE (%) | Dominant forb | Downed wood ± SE (%) | Litter ± SE (%) | Organic layer ± SE (cm) |
|---|---|---|---|---|---|---|---|
| 5 | 1.2 ± 0.6 | *Calamagrostis* sp. | 11.2 ± 6.6 | *Equisetum* sp., Geoliv | 3.2 ± 0.6 | 40.0 ± 18.5 | 22.8 ± 4.5 |
| 10 | 2.0 ± 0.6 | *Calamagrostis* sp. | 1.3 ± 0.9 | Chaang | 4.3 ± 1.8 | 100 ± 0 | 25.7 ± 7.1 |
| 11 | 0.7 ± 0.3 | *Calamagrostis* sp. | 0.7 ± 0.3 | Chaang, *Pyrola* sp. | 3.0 ± 2.1 | 93.3 ± 1.7 | 6.7 ± 0.3 |
| 12 | | | 1.3 ± 0.9 | *Pyrola* sp. | 10.0 ± 0.0 | 93.3 ± 3.3 | 12.0 ± 3.0 |
| 13 | 1.0 ± 1.0 | *Calamagrostis* sp. | 8.0 ± 6.0 | Chaang, *Pyrola* sp. | 5.0 ± 2.9 | 99.3 ± 0.3 | 63.7 ± 3.2 |
| 16 | 3.7 ± 3.2 | *Calamagrostis* sp. | 5.0 ± 2.9 | Chaang | 2.0 ± 1.0 | 100 ± 0 | 29.0 ± 2.1 |
| 17 | 2.3 ± 0.3 | *Calamagrostis* sp. | 8.7 ± 0.9 | Chaang | 3.3 ± 3.3 | 99.3 ± 0.7 | 13.3 ± 3.3 |
| 18 | 1.7 ± 1.7 | *Calamagrostis* sp. | 31.7 ± 7.3 | *Equisetum* sp., Geoliv | | 95.0 ± 2.9 | 18.3 ± 4.4 |
| 19 | 3.3 ± 1.7 | *Calamagrostis* sp. | 10.0 ± 10.0 | *Pyrola* sp. | 8.0 ± 6.0 | 100 ± 0 | 22.0 ± 4.0 |
| 20 | 1.0 ± 0.0 | *Calamagrostis* sp. | 10.2 ± 8.3 | *Equisetum* sp., Rubcha | 9.0 ± 3.5 | 98.8 ± 1.2 | 26.8 ± 1.9 |